**NTNU – Trondheim**
Norwegian University of
Science and Technology

# History matching of the Norne Field using the Ensemble based Reservoir Tool (EnKF/ES)

## Daniel Aleksander Solheim

NORWEGIAN UNIVERSITY OF SCIENCE AND
TECHNOLOGY

# History matching of the Norne Field using the Ensemble based Reservoir Tool (EnKF/ES)

by

Daniel Aleksander Solheim

A thesis submitted in partial fulfillment for the
degree of Master of Science

in the
The Faculty of Engineering Science and Technology
Department of Petroleum Engineering and Applied Geophysics

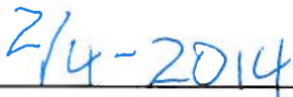April 2, 2014

# Declaration of Authorship

I, Daniel Aleksander Solheim, declare that this thesis titled, History matching of the Norne Field using the Ensemble Reservoir Tool (EnKF/ES), and the work presented in it are my own. I confirm that:

- This work was done wholly or mainly while in candidature for a research degree at NTNU.

- Where any part of this thesis has previously been submitted for a degree or any other qualification at NTNU or any other institution, this has been clearly stated.

- Where I have consulted the published work of others, this is always clearly attributed.

- Where I have quoted from the work of others, the source is always given. With the exception of such quotations, this thesis is entirely my own work.

- I have acknowledged all main sources of help.

- Where the thesis is based on work done by myself jointly with others, I have made clear exactly what was done by others and what I have contributed myself.

Signed:

Date: 2/4-2014

NORWEGIAN UNIVERSITY OF SCIENCE AND TECHNOLOGY

# *Abstract*

The Faculty of Engineering Science and Technology
Department of Petroleum Engineering and Applied Geophysics

Master of Science

## History matching of the Norne Field using the Ensemble based Reservoir Tool (EnKF/ES)

by Daniel Aleksander Solheim

In this thesis two stochastic algorithms, the Ensemble Smoother (ES) and the Ensemble Kalman Filter (EnKF), have been utilized as automatic history matching methods through the Statoil developed program the Ensemble based Reservoir Tool. Statoil, through the IO Center at NTNU, provided real historical production and pressure data. These data was used to condition on a parametrized ECLIPSE reservoir model of the Norne field. Parameters conditioned on includes the field parameters porosity, i-permeability, net-to-gross, and z-direction transmissibility multiplier, as well as fault multipliers, region transmissibility multipliers, minimum pore volumes and relative permeability endscaling options. The E-segment model and the Full-field model were both studied.

With an ensemble size of 120 realizations for the E-Segment model and 80 realizations for the Full-field model, both algorithms performed well. In most of the results an initial high uncertainty in the prior provided the necessary coverage of the historical observed data. Overall the EnKF performed better than the ES, which is natural comparing time and computational power required. Some spurious correlations and one particular ensemble collapse were experienced. The EnKF-analysed ensemble production rates provides a lot less uncertainty than the initial ensemble, and for most plots a slightly better match than the reference case. The EnKF-algorithm is shown to be vulnerable to small ensemble sizes versus large amounts of conditioning parameters, as well as highly correlated historical observations.

NORGES TEKNISK-NATURVITENSKAPELIGE UNIVERSITET

# Sammendrag

Fakultet for ingeniørvitenskap og teknologi

Institutt for petroleumsteknologi og anvendt geofysikk

Master of Science

### Historietilpasning av Nornefeltet ved bruk av the Ensemble based Reservoir Tool (EnKF/ES)

av Daniel Aleksander Solheim

I denne oppgaven ble to stokastiske algoritmer, the Ensemble Smoother (ES) og the Ensemble Kalman Filter (EnKF), benyttet til historietilpasning. Algoritmene ble brukt gjennom det eksternt utviklede programmet the Ensemble based Reservoir Tool. Sanne produksjons- og trykkdata, gjort tilgjengelig av Statoil og IO Senteret på NTNU, ble brukt for å kondisjonere på en parametrisert ECLIPSE reservoir model av Norne-feltet. Kondisjoneringsparametere inkluderer feltparameterne porøsitet, i-permabilitet, net-to-gross og z-retning-transmissibilitetsmultiplikator, samt også forkastningsmultiplikatorer, region-transmissibilitetsmultiplikatorer, minimum porevolumer og relativ permeabilitetsskaleringsinnstillinger. Både E-segment-modellen og Fullfelts-modellen ble studert.

Med en ensemblestørrelse på 120 realisasjoner for E-segment-modellen og 80 realisasjoner for Fullfelts-modellen produserte begge algoritmene gode resultater. Størstedelen av resultatplottene inneholder en ensembleprognose med en god dekning av de historiske observerte dataene. Overordnet produserte EnKF bedre resultater enn ES, noe som er logisk forskjellene i tidsbruk og nødvendig regnekraft tatt i betraktning. En del mindre gode korrelasjoner, samt én spesielt grov ensemblekollaps ble observert. De EnKF-analyserte ensemble-produksjonsratene har generelt en mye mindre usikkerhet enn ensembleprognosen, og for størstedelen av resultatplottene viser de EnKF-analyserte ensemble-produksjonsratene et bedre resultatet enn referansemodellen. EnKF-algoritmen viser seg å være sensitiv for små ensemblestørrelser sett i forhold til store mengder kondisjoneringsparametere, samt høyt korrelerte historiske observasjoner.

# *Acknowledgements*

First of all I would like to thank my supervisor Professor Jon Kleppe, as well as co-supervisor Richard Rwechungura, for valuable inputs and discussions during this thesis work. Professor Jon Kleppe also gave me time and patience when I needed to get rid of a quarrelsome tendinitis in my underarms at the start of my master thesis, and naturally were not able to have much progress.

Further, a special thanks is given to Jon Sætrom and Joakim Hove at Statoil for putting up with the countless emails about the ERT and in their best effort explaining and fixing smaller and larger questions and issues I had. Jon Sætrom was the one who introduced me to ERT the summer of 2013, so without him this thesis would have looked very different.

For technical support with the installation and maintenance of the ERT at both the Department of Petroleum Engineering and Applied Geophysics and the NTNU HPC Group I owe Erlend Våtevik, IT IPT, and Egil Holvik, IT NTNU HPC, a great deal of thanks. Their continuous effort and lightning fast response to problems made it possible for me to work on a new platform (Linux) with a new software without too much banging of heads against walls.

I would also like to thank Statoil (operator of the Norne field) and its license partners ENI and Petoro for the release of the Norne data. I acknowledge the IO Center at NTNU for cooperation and coordination of the Norne Cases.

Finally, large appreciations goes out to my to friends Dag Morten Stensholt and Johan Skot-Hansen for keeping spirits high and the mood even higher at my study place, and last, but not at least, to my girlfriend Marie Birkeland whom has kept me up in dark times and pushed me forward in lazy weeks, a very special thanks is given.

# Contents

# List of Figures

# List of Tables

# Abbreviations

| | |
|---|---|
| **D** | Darcy, permeabiliy unit |
| **HM** | History Matching |
| **AHM** | Automatic History Matching |
| **GOR** | Gas Oil Ratio |
| **NTG** | Net To Gross |
| **STOIIP** | Stock Tank Oil Initially In Place |
| **pdf** | probability density function |
| **ERT** | Ensemble based Reservoir Tool |
| **EKF** | Extended Kalman Filter |
| **ES** | Ensemble Smoother |
| **EnKS** | Ensemble Kalman Smoother |
| **EnKF** | Ensemble Kalman Filter |
| **RML** | Randomized Maximum Likelihood |
| **WWPRH** | Well Water Production Rate History |
| **WGPRH** | Well Gas Production Rate History |
| **WOPRH** | Well Oil Production Rate History |
| **WBHPH** | Well Bottom Hole Pressure History |
| **WTHPH** | Well Tubing Head Pressure History |
| **WWIRH** | Well Water Injection Rate History |
| **WGIRH** | Well Gas Injection Rate History |

# Nomenclature

| | |
|---|---|
| $C_{\psi\psi}$ | Covariance of a scalar state |
| $d$ | True historical observation |
| $d^o$ | Measured historical observation ($d^o = d + \epsilon_d$) |
| $f(\psi)$ | Probability density function, where $\psi$ is a vector or a vector of fields |
| $f(\phi)$ | Probability density function, where $\phi$ is a vector or a vector of fields |
| $T$ | Final time of assimilation period |
| $\alpha$ | Poorly known model parameter to be estimated |
| $\psi$ | State variable, either in scalar or vector form |
| $\Delta$ | Real number representing the difference between observed and predicted data |
| $W_D$ | Diagonal data weighting matrix |
| $\beta$ | Weighing factor (belief in the initial model) |
| $m_1$ | Model |
| $m_0$ | Prior model |
| $C_d$ | Data covariance matrix |
| $C_m$ | Model parameters covariance matrix |
| $\mathbf{x}$ | Vector describing ensemble members |
| $n_e$ | Ensemble size |
| $n_d$ | Number of historical observations |
| $\mathbf{X}^T$ | A transposed vector $\mathbf{X}$ |
| Tr | Trace value |
| Var | Variance |
| Cov | Covariance |

Gaussian  Functions named after Carl Friedrich Gauss describing normal distributions

ECLIPSE  Black-oil, 3D, 3-phase reservoir simulator owned, maintained and developed by SIS, a division of Schlumberger

IO Center  Center for Integrated Operations in the Petroleum Industry

WCONHIST  ECLIPSE keyword for observed rates for history matching production wells

WCONINJH  ECLIPSE keyword for observed rates for history matching injection wells

# Chapter 1

# Introduction

## 1.1 Aim and Objective

The aim of this thesis is to perform computer-assisted (semi-automatic) history matching of the Norne Field, both the E-segment and the Full-field model. Two separate algorithms will be used and comparative notes will be taken regarding the two. Further discussion around the parametrization of a reservoir model and conditioning done by pressure and production history will be thoroughly weighted. The objective of this thesis is to better understand the task of computer-assisted history matching, improve the behaviour and exactness of the Norne reservoir model and lay grounds for future research in this area at NTNU.

## 1.2 Methodology

Various methodologies have long existed for better developing and improving reservoir models used for predictions of future field behavior. Uncertainty quantification of these predictions have always been the major obstacle. The first research done on what we now know as computer-assisted, or automatic, history matching (AHM) was probably done by Kruger around 1960. He pointed out the obvious fact that for a model to resemble a real life problem, the calculated and observed

pressure data should be in agreement (Kruger, 1961). Kruger also saw it beneficial to utilize these "electronic computers" for solving the non-unique inverse problem that history matching is in an automated way. In the mid 1970s, optimal control theory was heavily applied in obtaining history matched models (Chavent et al., 1975), while in the early 1990s the simulated annealing technique as a global optimization algorithm was introduced. Without the use of gradients, this technique was different from most of the earlier methods (Ouenes and Saad, 1993).

From the middle of the 1990s a change was seen in the how the industry wanted history matched reservoir models. From the search for a single global solution there was now a desire for several local minima which made it easier to quantify and control the uncertainty of the predictions. [It has been shown that the search for a single true solution (global minimum) may in certain circumstances produce very weak results compared to several local minima (Tavassoli et al., 2004)]. With the explosive growth and accessibility of computational power, new AHM methods were developed quickly. Stochastic methods were now favoured, and the simulated annealing technique, evolutionary strategies and genetic algorithms were some of the first stochastic HM methods (Romero et al., 2000, Schulze-Riegert et al., 2002, Sen et al., 1995). The following years saw new methods emerge, such as the Mesh Adaptive Direct Search (MADS), the Particle Swarm Optimization (PSO) and the Generalized Pattern Search (GPS). The latest and most popular algorithms within the stochastic methods has been the Ant Colony Optimization and Differential Evolution (Hajizadeh et al., 2010).

Stochastic and derivative-free methods are often impractical in large or even medium-scale history matching problems due to the large amount of simulator responses required. The use of the adjoint method for calculating gradients was introduced already in the mid-1970s (Chen and Seinfeld, 1975), but it was not until 2003 the adjoint method was successfully extended to a 3D, three-phase flow problem (Li et al., 2003). This breakthrough gave the gradient-based methods much renewed interest and it is still an area subject to extensive research today (Kahrobaei et al., 2013).

The Ensemble Kalman Filter, introduced by Evensen in 1994 (Evensen, 1994) and based on the Kalman filter (Kalman, 1960), laid foundations for a new category of history matching methods, namely data assimilation. The 3DVAR, 4DVAR and the Randomized Maximum Likelihood (RML) are other methods in this category. These are derivative-free methods, however based on recursive Bayesian estimation and probability distributions, they differ from other stochastic methods. Several reports and papers over the last years discuss these types of AHM methods.

Seemingly, the discipline of history matching has gradually evolved into heavy computerized tasks utilizing intricate mathematical and statistical algorithms. As a result, this thesis will focus on automatic history matching of the Norne Field with the use of the Ensemble Smoother and the Ensemble Kalman Filter. These are made available through the Ensemble based Reservoir Tool (ERT) developed at Statoil (Statoil and NCC, 2013). Conditioning will be performed with the use of historical pressure and production rate data made available by Statoil through the Norne Benchmark Case. The Norne reservoir model is originally created by Statoil, however through the Norne Benchmark Case created in a collaborable effort by Statoil and NTNU, the reservoir model are continually being improved (IO Center, 2010). The computer load will be shared by the NTNU HPC Group's Kongull cluster, which is a CentOS 5.3 Linux cluster running Rocks on HP servers with 2 AMD Opteron model 2431 6-core (Istanbul) processors per node.

## 1.3 Reservoir Simulation

Reservoir simulation is one of the most important performing tasks in the discipline of reservoir engineering. It refers to the construction and operation of a model where the behavior resembles the appearance of actual reservoir behavior (Coats, 1987). The main purpose when performing reservoir simulation is to acquire a continuous prediction of future reservoir performance, creating a base for future field decisions. This decision-making refer to decisions concerning e.g. future production and injection schemes and economical investments in various reservoir

projects. Important results of future field performance include, but are not limited to, oil and gas recovery rates and economical outcome.

Reservoir simulation can only take place after the construction of an initial reservoir model from a geological model. The geological model is built with the use of reservoir data, i.e., seismic data, well bore logging, core data, and with probabilistic methods like Kriging populating a predefined grid with the given data. To transform the geological model to a simulation model, the detailed geological model must be upscaled so that the amount of grid cells is within the computational limit of existing software and hardware, or the reservoir engineer's work capability. Ideally, the reservoir simulation model is kept continuously up to date with the geological reservoir description, i.e. as close as possible to how the geophysicists and reservoir engineers conceive the true state of the reservoir at all times (Rwechungura, 2012). This is very hard to achieve with continuous changes in the reservoir models due to production, injection and natural changes, i.e. compaction, fracturing, cementation, etc. Reservoir models can consist of several hundred thousands, and even millions, of grid blocks. Although simplified from the actual heterogeneity and upscaled from the much more detailed geological model, useful reservoir models are seldom homogenous. This makes model updating a very computationally expensive task.

## 1.4 Inverse Theory

Inverse theory is a general framework that is used to convert observed measurements into information about a physical object or system. All our physical theories allow us to make predictions - given a complete description of a physical system, the outcome of some measurement can be predicted. This is called a forward problem (Tarantola, 2005). The other way around, using the actual results of some measurements to infer the values of the parameters that characterize the system, is a so-called inverse problem (see Figure 1.1. Thus, the forward problem

has one unique solution, while the inverse problem does not. As an example, consider measurements of the gravity field around the Earth. Given the distribution of mass inside the Earth, we can, by using physical laws and theories, uniquely predict what the gravity field around the Earth looks like (forward problem). On the other hand, there are different distributions of mass that give exactly the same gravity field, therefore an inverse problem with multiple solutions would be to infer the mass distribution inside the Earth from observations of the gravity field.

Simply stated, an inverse problem can be described as a problem in which the answer is known but the question is not. As a result of this, for an inverse problem, one needs to make explicitly available any a priori information on the model parameters and take care of representing the data uncertainties in a good way. A priori information (or prior information) means information that is obtained independently of the results of measurements. For example, a well-designed geophysical inverse problem should use the concepts of geostatistics and probability densities to formulate the inverse problem (Tarantola, 2005).
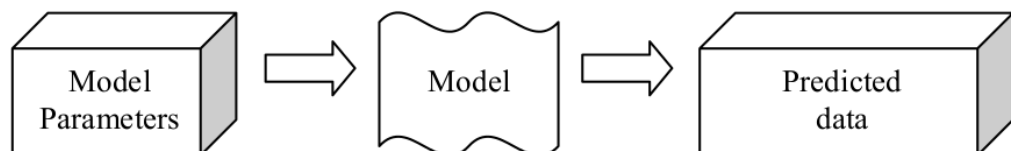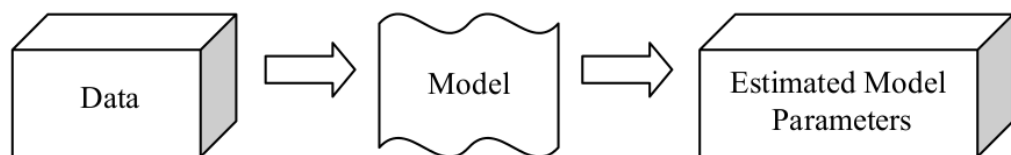


FIGURE 1.1: Schematic difference of a Inverse and Forward Problem (Dadashpour, 2009)

## 1.4.1 Optimization

Used in most fields of science, the task of optimizing is to select the best element (with regard to some criteria) from some set of available alternatives. More specifically, an optimization problem would be to find the best available values of some objective function, i.e. either maximizing or minimizing the function, given a defined domain. This is exactly what is sought after in history matching. Here the objective function is defined as the difference between simulated and observed data, and the purpose is to minimize this mismatch. Looking at an objective function in economics, the purpose would be to maximize the profit.

The most important general approach to optimization is based on numerical methods. In these, iterative numerical procedures are used to generate a series of progressively improved solutions to the optimization problem, starting with an initial estimate of the solution (Antoniou and Lu, 2007). What algorithm to use depends on the objective function at hand, the possible constraints and the smoothness of the function. Some algorithms make use of the first and second derivative of the objective functions, while others are only able to find the local minimum/maximum. Time and computational power are also important factors when choosing which algorithm to use.

Regardless of the specifics, all good algorithms should possess the following properties (Nocedal and Wright, 2006):

- **Robustness:** They should perform well over a wide variety of problems in their class for all reasonable choices of the initial variables.

- **Efficiency:** They should not require too much computer time or storage.

- **Accuracy:** They should be able to identify a solution with precision without being overly sensitive to errors in the data, or to the arithmetic rounding errors that occur when the algorithm is implemented on a computer.

## 1.5   General history matching

History matching is the process of adjusting a reservoir model until it closely reproduces the same behavior as observed and measured petroleum data. The accuracy of the HM depends on the quality of the reservoir model and both the quality and quantity of all available historical reservoir data, i.e. production rates, pressure measurements and 4D seismic data.

When an adequate reservoir model is constructed, reservoir simulation can begin. Then the reservoir model, in an iterative process, is adjusted until the simulated data matches the historical recorded data. This is achieved through the task of optimization. When a desired criteria is reached, the model is ready to simulate future reservoir performance. As more historical data is recorded, the simulation model is continually updated. This makes it a continuous process often repeated and enhanced throughout the lifetime of the petroleum field in question.

HM usually requires numerous iterations making it a very costly operation based on time spent and computational power used. It is a non-unique inverse problem creating non-unique solutions, thus making future predictions of business decisions non-unique (Dadashpour, 2009). These decisions can be critical and costly investments like facility upgrades, workover schedules, stimulation of wells, water flooding, development drilling and new EOR-methods. Information leading to such a decision must be as exact as possible, as it is a well known fact in the oil industry that the quality of a business decision depends largely on the quality of the history matching.

We differ between manual HM and the more lately used semi-automatic HM (here AHM) (see Figure 1.2). Manual HM requires experienced reservoir engineers who analyze the difference between the simulated and observed value, and manually change one or two parameters at a time to improve the match. Such trial and error evaluation is seldom reliable for long periods of time, and is always associated with large uncertainties. This is due to the engineers available time and the hundreds of thousands of grid blocks in a simulation model, each with separate

values which ideally should be re-calculated and updated. However, with the use of AHM, computers and optimization techniques are utilized to speed up the process. This gives the advantage of a much quicker convergence towards an acceptable difference between model performance and reservoir performance. Optimization methods frequently used in the past decades include gradient-based-, derivative free-, stochastic search- and probabilistic methods. Common procedure for all the methods is to estimate parameters, iteratively reduce an objective function, and finally re-calculate estimated parameters.
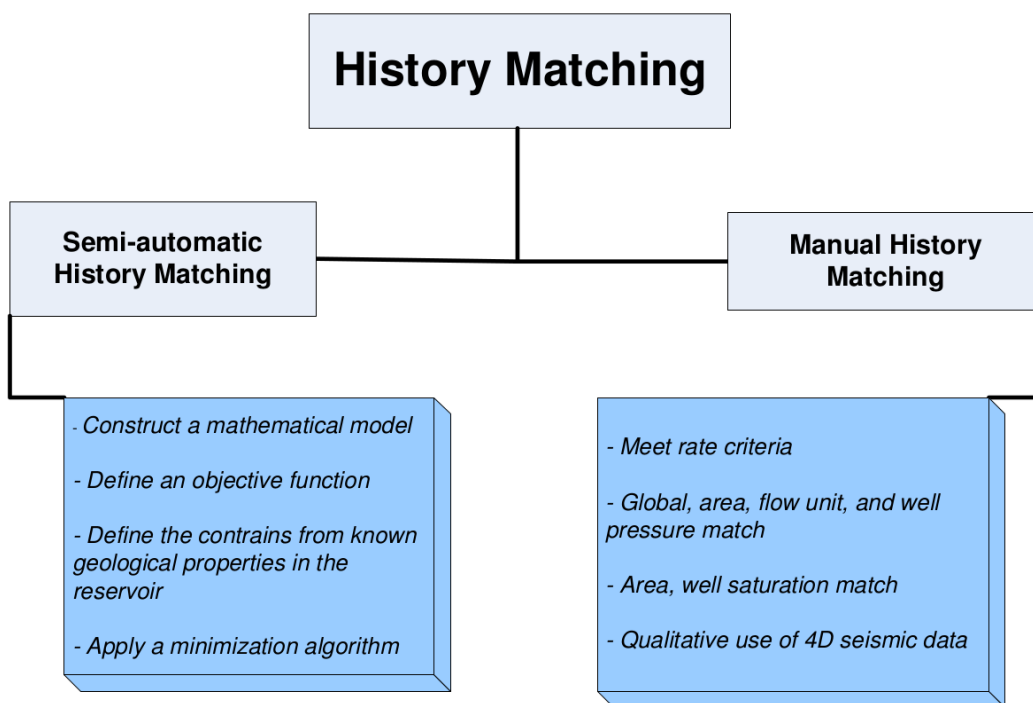


FIGURE 1.2: Semi-Automatic HM vs. Manual HM (Rwechungura, 2012)

## 1.5.1 Objective Function

The definition of an objective function depends on the task at hand and it is in most cases either a cost function or a utility function. In computer-assisted HM cases cost functions are used to map values of variables onto a real number (here, $\Delta$) representing the difference between observed data and the response of the system, as predicted by the forward modelling [$\Delta = d_{obs} - d_{cal}$]. These variables can in HM cases be e.g. porosity, permeability, reservoir structure, fault systems,

aquifers, and degree of homogeneity. The three most commonly used methods for quantifying objective functions are the least square method, the weighted least square method and the generalized least square method (Equation 1.1, 1.2 and 1.3, respectively).

$$F = \Delta^T \Delta \tag{1.1}$$

$$F = \Delta^T W_D \Delta \tag{1.2}$$

$$F = \frac{1}{2}(1 - \beta)\Delta^T C_d^{-1}\Delta + \frac{1}{2}\beta[m_1 - m_0]^T C_m^{-1}[m_1 - m_0] \tag{1.3}$$

where $W_D$ is a diagonal matrix that assigns individual weights to each measurements. The weights for each data types are assigned as a function of the number of available data points in a set, and on the uncertainty associated with each type of measurement. The $\beta$ factor is a weighting factor which expresses the relative strength of the belief in the initial model, while $C_d$ is the covariance matrix of the data providing information about the correlation among the data. $C_m$ is the covariance matrix of the parameters of the mathematical model (Dadashpour, 2009).

## 1.5.2   Mathematical Model

Equations like the Newton's second law and the relativity theory is a result of the human longing of understanding everything around us. Physical laws were established, describing naturally occurring phenomenons. Put together and included certain parameters, mathematical models describing and reproducing the behavior of actual physical systems in numbers are created. Such a model is, as earlier stated, a forward model and forward modelling for systems dealing with parameters that are only implicitly available, as in earth sciences, creates more difficult problems (Rwechungura, 2012).

The main purpose of the mathematical model (our forward model) is to predict the behavior of the system with a reasonable accuracy under various conditions. The following fundamental laws are relevant to the fluid dynamics in the reservoir

and are put together creating an appropriate mathematical model (Dadashpour, 2009);

- Mass Conservation Law

- Darcy's Law

- The Equation of State

- Relative Permeability and Capillary Pressure Relationships

## 1.6   Optimization Methods

There are hundreds of different methods and algorithms for optimizing or minimizing cost- or objective functions. Optimization is even a specific branch in applied mathematics and continuous work is done to improve old algorithms and to invent new ones.

A recent way of classifying HM methods is in terms of how the particular methods explore the parameter space vs. exploit the local regions of the parameter space to find a minimum value of the objective function (Streamsim Technologies, Inc., 2011). Figure 1.3 gives an overview of some algorithms. Exploration refers to the search of different areas in the parameter space while exploitation is the refinement of the previously visited regions to find better answers. In the earlier days of AHM most of the focus was on single solution methods (exploitation), although development has shown that exploration of the parameter space using stochastic- and data assimilation optimization methods has become increasingly popular. Multiple combinations of reservoir properties can provide good matches to observed field behavior. In order to realistically quantify the uncertainty of predictions, multiple history-matched reservoir models are desired (Hajizadeh et al., 2010).
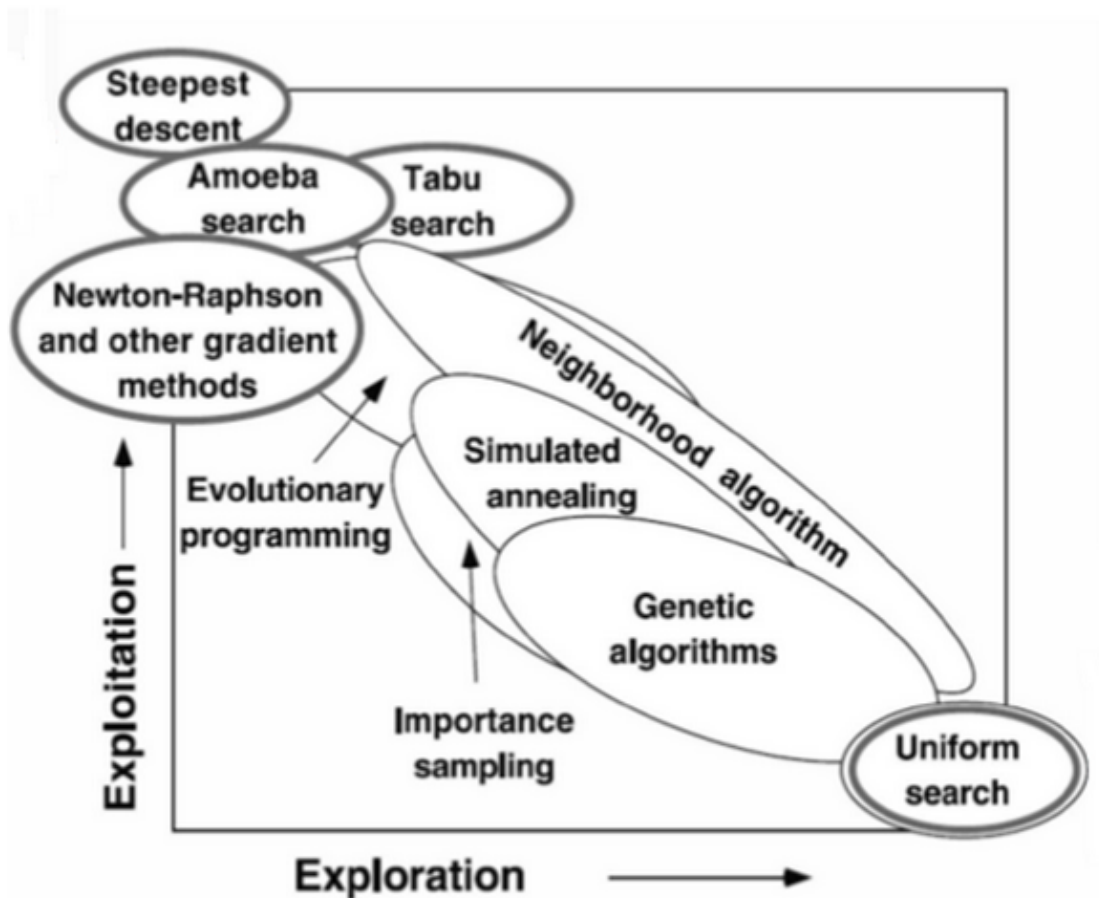
FIGURE 1.3: Schematic showing the difference of exploration vs. exploitation optimization methods (Streamsim Technologies, Inc., 2011).

Algorithms for minimizing objective functions in HM can generally be divided into three groups:

- Gradient-based Methods

- Stochastic/Non-gradient-based Methods

- Data Assimilation

Gradient-based methods are based on calculating local gradients to angle the parameter choice towards a location that minimizes some of the discrepancy between observed and simulated values. Some of these methods only need to calculate the first (Jacobian) derivative, while others also make use of the second (Hessian) derivative which in many cases can be very tiresome to calculate. The gradients are

most often approximated by finite difference approximation (Dadashpour, 2009). Emphasise is here on robustness, quickness and local minima, which has the disadvantage of not likely finding the global minima and henceforth not the best history match. Typically utilized gradient-based optimization methods are the steepest decent method, the Gauss-Newton method, the conjugate gradient method and the sequential quadratic method. Some of the latest and most promising developments and results in AHM has been seen with the use of gradient-based methods coupled with the adjoint method for calculating the gradients (Kahrobaei et al., 2013). In simplified terms the adjoint method introduces more variables to the problem at hand, thus avoiding certain parts of the difficult gradient calculation. The adjoint method is however not intuitively understood and requires intimate knowledge and modifications of the simulator code itself, making it very difficult to utilize in certain cases.

Stochastic optimization methods and derivative-free methods search for global solutions and are normally able to avoid local minima. They include, but are not limited to, genetic algorithms, evolutionary algorithms, the simulated annealing technique, Tabu Search, particle swarm intelligence algorithms, Hooke-Jeeves Direct Search. All of these methods treat the simulator like a "black box", where the optimization loop does not require intimate knowledge of how the reservoir model response is obtained (Streamsim Technologies, Inc., 2011). This can often be attractive for reservoir engineers without a deep understanding of the mathematics supporting the optimization method. As one can extensively control the behavior of these algorithms, they provide the opportunity to balance the exploration and exploitation while searching for optimal solutions (Hajizadeh et al., 2010). These methods have been thoroughly studied, and proven robust and easy to adapt for different problems. In the last 10-15 years, new stochastic algorithms like the neighborhood algorithm, the ant colony optimization method and differential evolution have been developed, tested and proven promising (Hajizadeh et al., 2010, Mohamed et al., 2009, Schulze-Riegert et al., 2002). All this however comes at a high computational cost as these methods may require hundreds or thousands of

evaluations of the reservoir model response, which can virtually be impossible for CPU-intensive reservoir models.

Data assimilation is an analysis technique in which the observed information is accumulated into the model state by taking advantage of consistency constraints with laws of time evolution and physical properties (Lorenc, 1986). Background information in the form of an a priori estimate of the reservoir model state is necessary to turn the under-determined analysis problem into a well-posed one. Better yet, a set of different model states based on some assumptions of the reservoir model (from physical laws and geological constraints to well logs, seismic data, etc) makes an ensemble in which the observed data either can undergo sequentially or non-sequentially, intermittent or continuous in time assimilation. The Ensemble Kalman Filter (EnKF) introduced in 1994 has been the subject of massive attention the last 20 years (Evensen, 1994), and is probably the most used data assimilation method to date.

# Chapter 2

# The Norne Field

The Norne Field is situated 80 km north of the Heidrun field and compromises the license blocks 6608/10 and 6508/1 on the Norwegian Continental Shelf. This is approximately 200 km offshore, about midway between Trondheim and Mo i Rana, with a water depth of 370 to 390 meters. The field was discovered in December 1991, and the discovery well contained a total hydrocarbon column of 135 m - a 110 meter oil column with an overlying gas cap. Two more wells was drilled in the northern and eastern part of the structure in early 1993 and early 1994. These confirmed the results from the discovery well, as well as giving an estimate of the extension of the field to the north and east. Especially the eastern well hit a structure with high potential, and the results from this well were important for optimum sizing of the process facility (Steffensen and Karstad, 1996).

Oil production started November 6$^{\text{th}}$ 1997 with Statoil as operator and Eni Norge AS and Petoro AS as partners. The field has been development with a production and storage vessel, the "Norne FPSO", connected to seven subsea wellhead templates named B, C, D, E, F and K (see Figure 2.1). Flexible risers carry the wellstream to the ship, which rotates around a cylindrical turret moored to the seabed. Risers and umbilicals are also connected to the turret. Gas export started in 2001 after being re-injected into the formation in the earlier production years , and the gas is now transported through a dedicated pipeline to Åsgard and from there through the Åsgard Transport Pipeline to Kårstø (NPD, 2012).
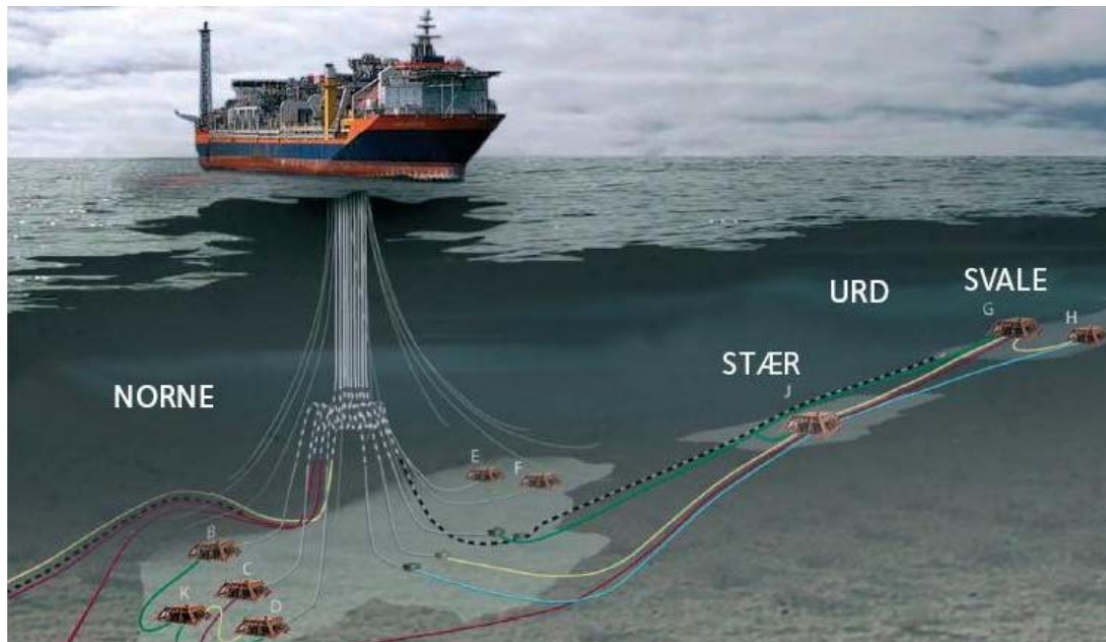
FIGURE 2.1: Development of the Norne Field (Statoil, 2006).

Today (2012) Norne produces approximately 18.000 bbl oil, 0.16 billion $Sm^3$ gas and 0.02 million tonnes NGL per day. Production from the Norne Field has, despite the production decrease later years (see Figure 2.2), been a huge success, and it is one of the fields in the North Sea with the highest recovery rate at above 60 %.

TABLE 2.1: Recoverable reserves from the Norne Field (NPD, 2012)

| **Recoverable Reserves** | *Original in place* | *Remaining as of 31.12.2011* |
|---|---|---|
| Oil | 90.8 million $Sm^3$ | 4.6 million $Sm^3$ |
| Gas | 11.8 billion $Sm^3$ | 5.4 billion $Sm^3$ |
| NGL | 11.8 million tonnes | 1.0 million tonnes |
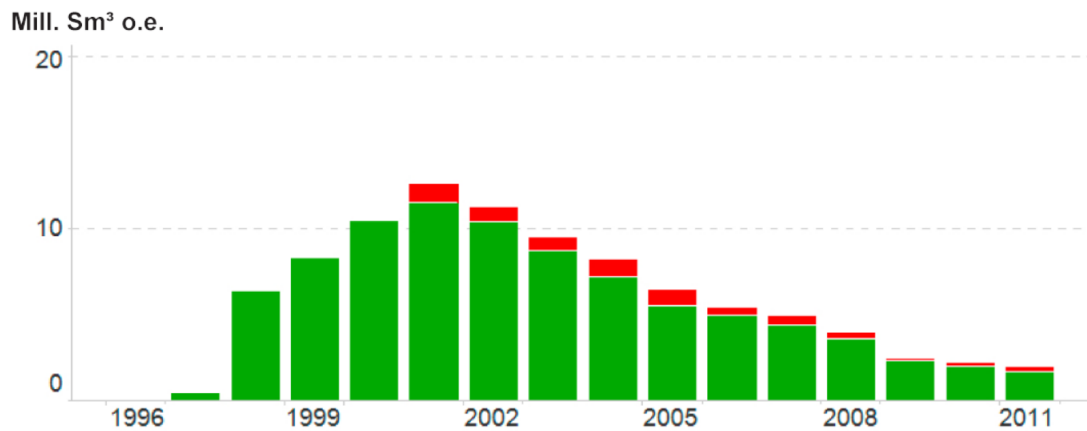
FIGURE 2.2: Cumulative oil production per year of the Norne Field. Green and red color representing "Oil, condensate and NGL production" and "Gas production", respectively (NPD, 2012).

## 2.1 Geology

The Norne Field is situated on a horst block measuring approximately 9 km x 3 km, consisting of two separate oil components, the Norne main structure (C-, D- and E-segment) and the Northeast segment (G-segment) as seen in Figure 2.3. The reservoir is subdivided into four different formations from top to base; Garn, Ile, Tofte and Tilje. 98 % of oil in place is situated in the Norne main structure, and approximetely 80 % of this oil is located in The Ile and Tofte formation while gas is found in the Garn formation (see Figure 2.4).
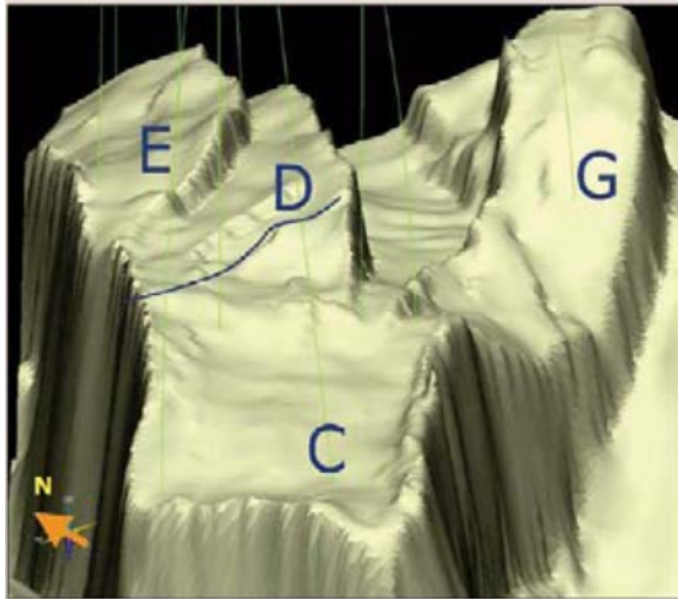
FIGURE 2.3: Top reservoir map showing Norne horst block with the four segments (Morell, 2010).

The reservoir is found at a depth of 2500-2700 m, and the reservoir sandstones are dominated by fine-grained and well to very vell stored sub-arkosic arenites (a sedimentary clastic rock with sand grain size of 0.0625-2.0 mm). Despite ongoing diagenetic processes affecting the sandstones quality, most of the sandstones are good reservoir rocks with porosity in the range of 25-30 % and permeability varying from 20 to 2500 mD. The source rocks are believed to be the Spekk Formation from Late Jurassic and coal bedded Åre Formation from Early Jurassic. The cap rock, sealing the reservoir and keeping the oil and gas in place, is the Melke Formation. The Not Formation also behaves as a cap rock, preventing communication between the Garn and Ile Formations (Rwechungura et al., 2010).
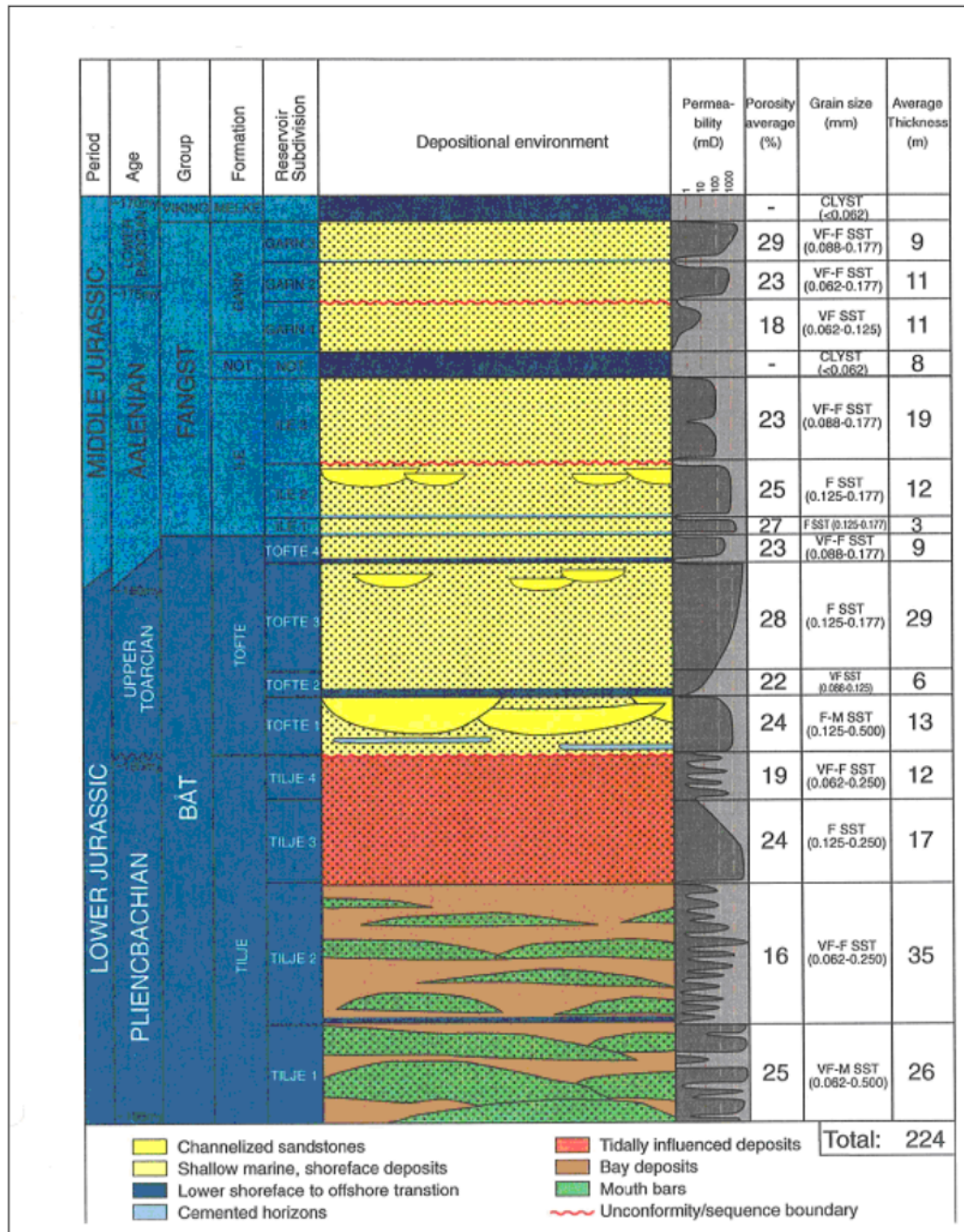
FIGURE 2.4: Stratigraphical sub-division of the Norne reservoir (Statoil, 2001).

## 2.1.1 Zonation

The present [2006] geological model consists of 17 reservoir zones (Verlo and Het-land, 2008). Today's reservoir zonation is slightly altered from earlier subdivisions.

The main differences is that the Ile and Tofte zones have been further subdivided, the Tilje zones have been simplified and the Garn zones has changed name to numbered Not zones (see Figure 2.5). The zonation from 2001 was made to correspond as good as possible to the lithology changes seen in the reservoir, thus zones were chosen with basis in sequence boundaries, maximum flooding surfaces or distinct breaks in porosity or permeability correlating across the field as seen in Figure 2.4 (Statoil, 2001).

| NORNE 2002 | | NORNE 2006 | | |
| --- | --- | --- | --- | --- |
| Lower Melke | | Not 3 | Upper Not Shale | |
| Garn 3 | | Not 2 | Not 2.3 | Not Sst |
| Garn 2 | | | Not 2.2 | |
| Garn 1 | | | Not 2.1 | |
| Not | | Not 1 | Lower Not Shale | |
| Ile 2 | Ile 2.2 | Ile 2 | Ile 2.2 | Ile 2.2.2 |
| | | | | Ile 2.2.1 |
| | Ile 2.1 | | Ile 2.1 | |
| Ile 1 | Ile 1.3 | Ile 1 | Ile 1.3 | |
| | Ile 1.2 | | Ile 1.2 | |
| | Ile 1.1 | | Ile 1.1 | |
| Tofte 2 | Tofte 2.2 | Tofte 2 | Tofte 2.2 | |
| | Tofte 2.1 | | Tofte 2.1 | |
| Tofte 1 | Tofte 1.2 | Tofte 1 | Tofte 1.2 | |
| | Tofte 1.1 | | Tofte 1.1 | |

FIGURE 2.5: Old and present zonation (Verlo and Hetland, 2008).

### 2.1.2 Reservoir Communication

**Faults**

Compartmentalization is a major factor in the Norne Field. One of reason for this is the field location on a horst, resulting in many faults criss-crossing the reservoir. Major faults can be discovered by studying seismic data, which together

with known history of the area, contributes to confirm the positions of the faults. Figure 2.6 illustrates cross sections through the Norne Field with fluid contacts and major faults. A significant amount of lineaments are discovered from ESP data including dip and azimuth maps generated at the Top Garn level. These lineaments trend NNW-SSE and SW-NE parallell to the two main fault strike directions on the field. Some of the lineaments are identified as small faults in the seismic data, which lead to a more faulted field than shown in the structural maps (Verlo and Hetland, 2008). The displacement of these faults is probably between 5 and 20 m (Statoil, 2001). Figure 2.14 shows how these faults are modelled in the 2004 reservoir model.
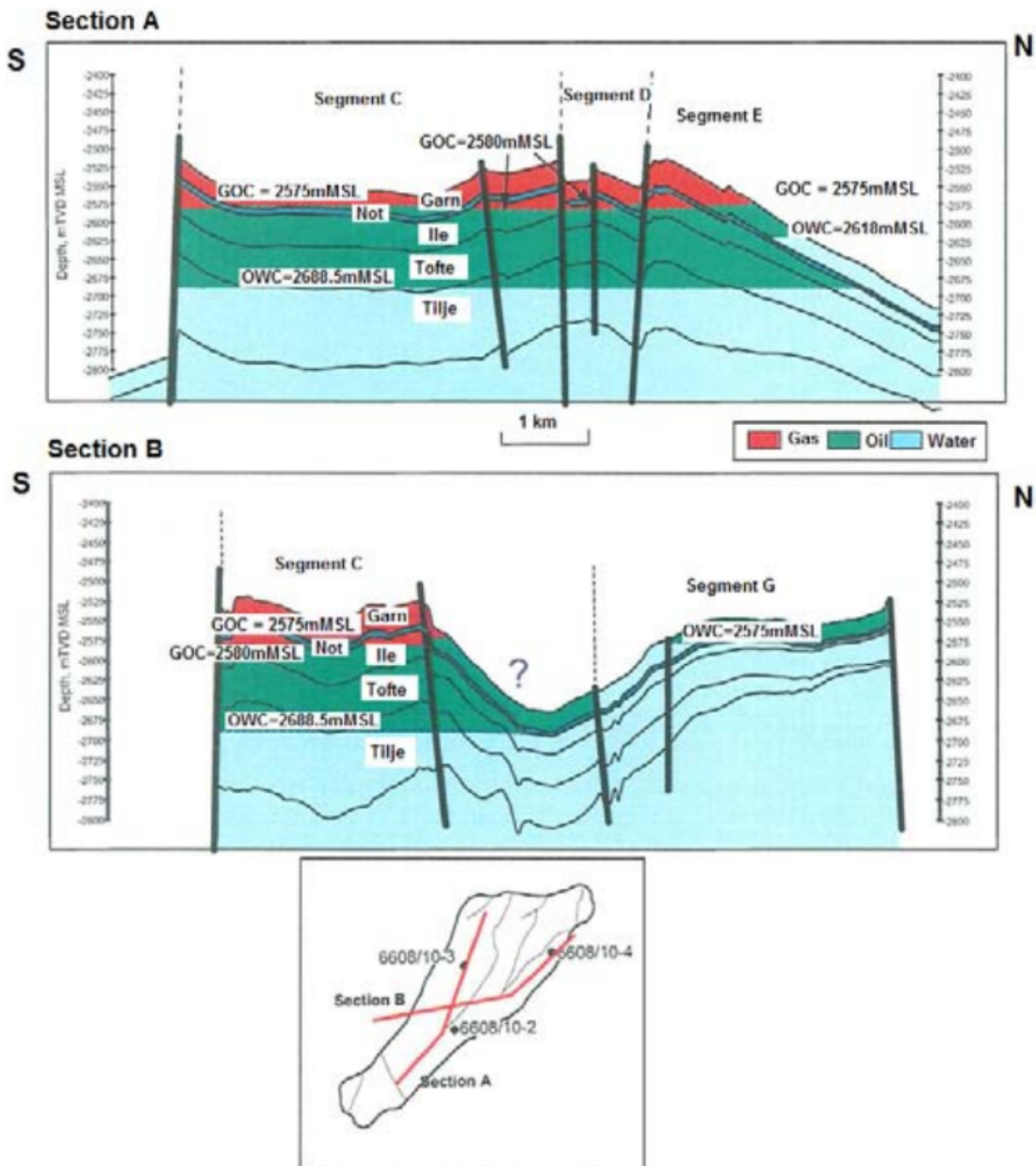
FIGURE 2.6: Structural cross-sections through the Norne Field with fluid contacts (Statoil, 2001).

### Stratigraphical barriers

Several stratigraphic barriers are present in the field. Continuous intervals which restrict the vertical flow within the Norne Field are listed in table 2.2.

Table 2.2: Intervals restricting the flow within the Norne Field [names corresponding to the zonation from Norne 2002 (see Figure 2.4)]

| Formation | Comments |
|---|---|
| The Melke Formation | Claystone formation, upper seal |
| Garn 3/ Garn 2 | Carbonate cemented top layer at Garn 2 |
| The Not Formation | Claystone formation |
| Ile 3/Ile 2 | Carbonate cementations and increased clay content at base Ile 3 |
| Ile 2/Ile 1 | Carbonate cemented layers at base Ile 2 |
| Ile 1/Tofte 4 | Carbonate cemented layers at top Tofte 4 |
| Tofte 2/Tofte 1 | Significant grain size contrast |
| Tilje 3/Tilje 2 | Claystone formation |

Pressure development in field clearly indicated what influence the stratigraphic barriers have on the flow within the reservoir. The barriers affecting the flow most distinctively are the Not Formation, the carbonate cemented layers which separate the Ile 1 and the Tofte 4 formations, as well as the the claystone separating the Tilje 3 and Tilje 2 formations (Statoil, 2001).

Further see (Verlo and Hetland, 2008) for an extensive geological description of the Norne Field.

## 2.2 Wells

The Norne Field has 4 templates for production and 2 templates for injection. Each template has 4 well slots available - 3 for production and 1 for injection/production. Currently the field is exclusively developed with horizontal producers (NPD, 2012). The following principles was decisive for the wellbore locations;

- Water injectors located at the flanks of the reservoir

- Gas injectors located at the structural heights of the reservoir

- Oil producers located between gas and water injectors for delaying gas and water breakthrough

To avoid gas inflow oil producers are located at some distance from major faults. Wellbore locations were after initial placement optimized (branches, new perforation/shut-ins or completely new drilling locations) with regards to gas and water breakthrough by the use of reservoir simulation studies. The wells are completed in different formations depending on the current drainage strategy in use (see Figure 2.7). The total number of active wells in December 2006 was 17; 11 being oil producers, 3 water injectors and 3 gas injectors, and a detail overview of the active periods of each and every production well can be seen in Table 2.3.

TABLE 2.3: Overview producing wells. The active period is based on the observed historical data, while the plugged date is based on (Verlo and Hetland, 2008).

| Wells | Active (Open - No production) | Plugged |
|---|---|---|
| **B-1H** | | October 2005 |
| Gas | April 1999 - October 2005 | |
| Oil | April 1999 - October 2005 | |
| Water | August 2002 - October 2005 | |
| **B-1BH** | | N/A |
| Gas | January 2006 - N/A | |
| Oil | January 2006 - N/A | |
| Water | May 2006 - N/A | |
| **B-2H** | | N/A |
| Gas | December 1998 - N/A | |
| Oil | December 1998 - N/A | |
| Water | January 2001 - N/A | |
| **B-3H** | | N/A |
| Gas | July 1999 - N/A | |
| Oil | July 1999 - N/A | |
| Water | August 2001 - N/A | |
| **B-4H** | | May 2001 |
| Gas | April 1998 - Varying production from May 1999 | |
| Oil | April 1998 - Varying production from May 1999 | |
| Water | No water production | |
| **B-4BH** | | September 2003 |
| Gas | August 2001 - December 2002 | |
| Oil | August 2001 - December 2002 | |
| Water | September 2001 - December 2002 | |
| **B-4DH** | | N/A |
| Gas | July 2004 - N/A | |

| | | |
|---|---|---|
| Oil | July 2004 - N/A | |
| Water | December 2004 - N/A | |
| **D-1H** | | September 2002 |
| Gas | November 1997 - August 2001 | |
| Oil | November 1997 - August 2001 | |
| Water | September 2000 - August 2001 | |
| **D-1CH** | | N/A |
| Gas | November 2003 - N/A | |
| Oil | November 2003 - N/A | |
| Water | January 2005 - N/A | |
| **D-2H** | | N/A |
| Gas | December 1997 - N/A | |
| Oil | December 1997 - N/A | |
| Water | November 2004 - N/A | |
| **D-3AH** | | June 2005 |
| Gas | August 2000 - June 2005 | |
| Oil | August 2000 - June 2005 | |
| Water | July 2002 - June 2005 | |
| **D-3BH** | | N/A |
| Gas | February 2006 - N/A | |
| Oil | February 2006 - N/A | |
| Water | August 2006 - N/A | |
| **D-4H** | | November 2002 |
| Gas | June 1998 - April 2002 (on-off from Aug 00) | |
| Oil | June 1998 - April 2002 (on-off from Aug 00) | |
| Water | April 2000 - April 2002 (on-off from Aug 00) | |
| **D-4AH** | | N/A |
| Gas | June 2003 - July 2006 | |
| Oil | June 2003 - July 2006 | |
| Water | January 2004 - October 2005 | |
| **E-1H** | | N/A |
| Gas | September 1999 - N/A | |
| Oil | September 1999 - N/A | |
| Water | April 2002 - N/A | |
| **E-2H** | | N/A |
| Gas | November 1999 - July 2005 | |
| Oil | November 1999 - July 2005 | |
| Water | January 2002 - July 2005 | |
| **E-2AH** | | N/A |
| Gas | August 2005 (no prod. Nov 05-Oct 06) - N/A | |
| Oil | August 2005 (no prod. Nov 05-Oct 06) - N/A | |
| Water | October 2006 - N/A | |
| **E-3H** | | May 2000 |
| Gas | September 1998 - April 2000 | |
| Oil | September 1998 - April 2000 | |
| Water | November 1998 - April 2000 | |
| **E-3AH** | | January 2005 |

| | | |
|---|---|---|
| Gas | Dec 2000 (no prod. May 01-Jan 02) - Jan 2005 | |
| Oil | Dec 2000 (no prod. May 01-Jan 02) - Jan 2005 | |
| Water | May 2002 - January 2005 | |
| **E-3CH** | | N/A |
| Gas | May 2005 - N/A | |
| Oil | May 2005 - N/A | |
| Water | July 2005 - N/A | |
| **E-4AH** | | N/A |
| Gas | June 2000 (no prod. Jun 01-Aug 02) - July 2005 | |
| Oil | June 2000 (no prod. Jun 01-Aug 02) - July 2005 | |
| Water | March 2004 - July 2005 | |
| **K-3H** | | N/A |
| Gas | October 2006 - N/A | |
| Oil | October 2006 - N/A | |
| Water | October 2006 - N/A | |
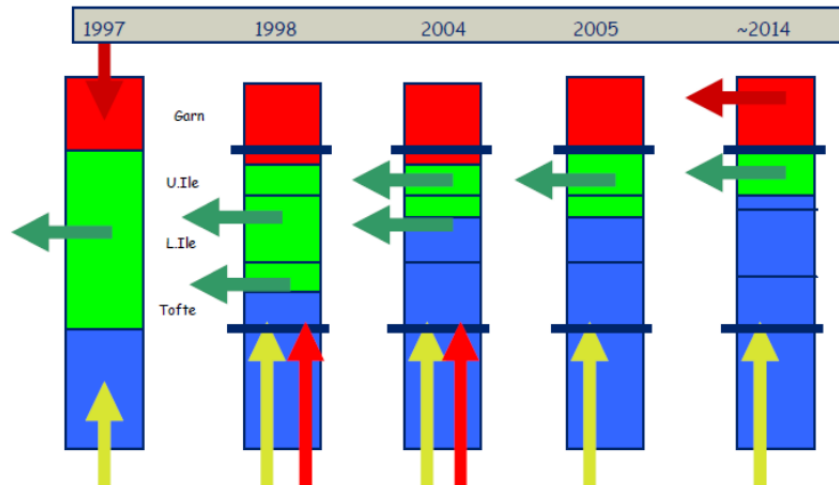


FIGURE 2.7: Drainage strategy for the Norne Field. Vertical arrows = injection streams, horizontal arrows = production streams. Blue fill = water, green fill = oil, red fill = gas (Statoil, 2006).

## 2.2.1 Injection strategy

The water injection strategy is based on the following issues

- As good as possible areal distribution of the water injectors to maintain a steady rise of the water level and hence good areal sweep.

- Since the vertical communication in the Norne reservoir is poor, it was necessary to convert the drainage strategy from vertical- to flank sweep. This objective was obtained by placing the water injectors towards the flanks.

- The water injectors are conventional wells that inject water into the water zone and lower part of the oil zone from Tilje 3 up to Ile 3. Tilje 1 is considered to consist of unconsolidated sand, and is located below the tight, laterally extensive shale in Tilje 2, and is not considered to be suited for water injection.

- Three of the four water injectors are located in the Norne C-segment (see Figure 2.3) which accounts for 60 % the STOIIP.

The initial strategy to maintain reservoir pressure was to re-inject produced gas into the gas cap and water into the water zone (Steffensen and Karstad, 1996). Since the gas cap had high pressure and was sealed off by the Not formation, the gas injection was changed to the water zone and the lower part of the oil zone. This change in strategy was successful, although making the prediction of gas flow in the reservoir more complicated and uncertain. A higher GOR than expected caused the production to be restricted by gas handling capacity. Gas export was started in 2001 in order to obtain a balanced gas- and water injection strategy, and prevent further increase in GOR. The deep gas injection ceased in 2005, and the initial strategy was again partially implemented – in 2006 gas from the C-wells started to inject into the gas cap to prevent pressure depletion (Morell, 2010).

Further see (Morell, 2010) for extended information about the well history of the Norne Field.

## 2.3 Reservoir Model

The Norne field has been simulated by four different ECLIPSE-models:

- The PDO Model - this model has grid dimensions 40x70x16 and is based on a 1994 interpretation of the 3D seismic survey ST9203

- The 1998 Model - this model has grid dimensions 56x124x24 and is based on a 1998 interpretation of the 3D seismic survey ST9203

- The 2004 Model - this model has grid dimensions 46x112x22 and is based on a 2004 interpretation of the 4D seismic surveys ST0103, ST0305, ST0409

- The 2006 Model - this model has grid dimensions 55x136x32 and is based on a 2006 interpretation of the 4D seismic surveys ST0103, ST0305, ST0409 and ST0603
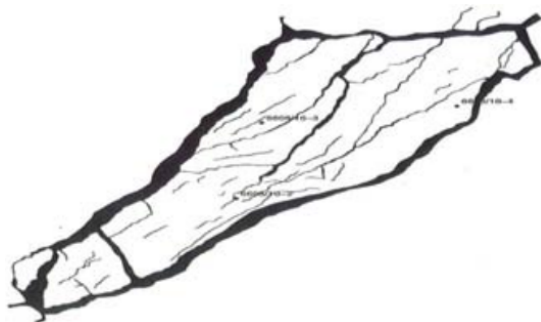


FIGURE 2.8: Fault zonation PDO model



FIGURE 2.9: Fault zonation 1998 model



FIGURE 2.10: Fault zonation 2004 model
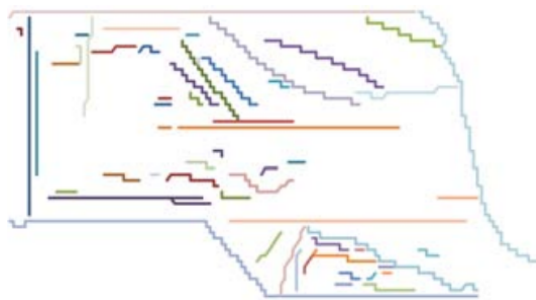


FIGURE 2.11: Fault zonation 2006 model

All of these models are created and further developed by Statoil, and where made available for NTNU through the Norne Benchmark Case (IO Center, 2010). The fault zonation for each model can be seen in Figure 2.8, 2.9, 2.10 and 2.11.

The ECLIPSE-model applied in this thesis is a modified version of the 2004-model. Structurally the models are similar, but issues with the relative permeability scaling, hysteresis and the rock functions have been addressed (Cheng, 2012).

### 2.3.1  Reservoir Model Specifics

The Norne Reservoir Simulation Model is three-phase, 3D, black-oil ECLIPSE 100 model. The modified 2004-model applied in this thesis is discretized by a 46x112x22 grid and is physically divided into two sections by the Not Shale Formation. The upper and lower sections consists of 3 and 18 stratigraphical layers respectively.

**E-segment model**

The Norne Benchmark Case first made available a model focusing only on the E-segment of the Norne Field [2011], coarsening and using multipliers for the rest of the field so that the E-segment could be simulated as a stand-alone reservoir model. Attempts was first made to build a separated E-segment model with flux boundaries, but results showed that a coarsened model had fewer limitations with regards to handling EOR applications, polymers, tracers and other special features (Rwechungura et al., 2010). Therefore the coarsened model (see Figure 2.12) was used for the first Norne Comparative Case Study.
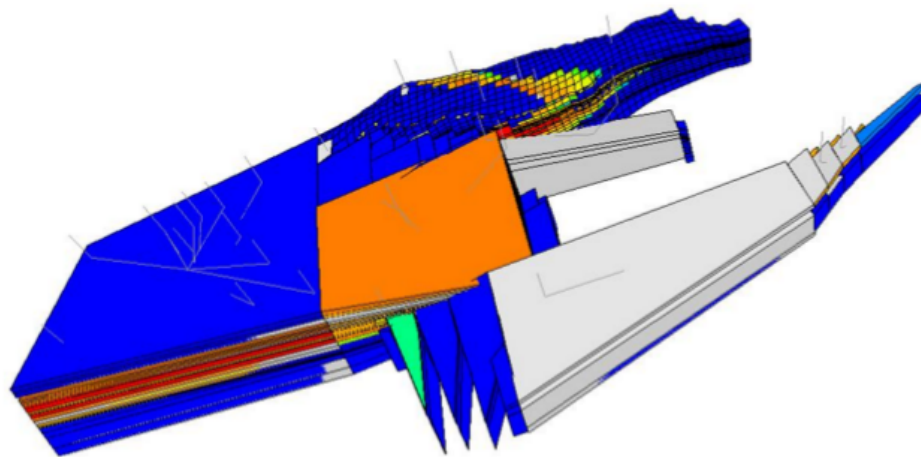


FIGURE 2.12:  The coarsened Norne E-segment Model (Rwechungura et al., 2010).

The Norne E-segment model consists of 8733 active cells with an average cell blocks size of 80 to 100m in the horizontal direction.

**Full-field model**

The Norne Full-field model was released by the Norne Benchmark Case in 2013 compromising a full reservoir model of the Norne Field with 44431 active cells and 32 wells with accompanying information.
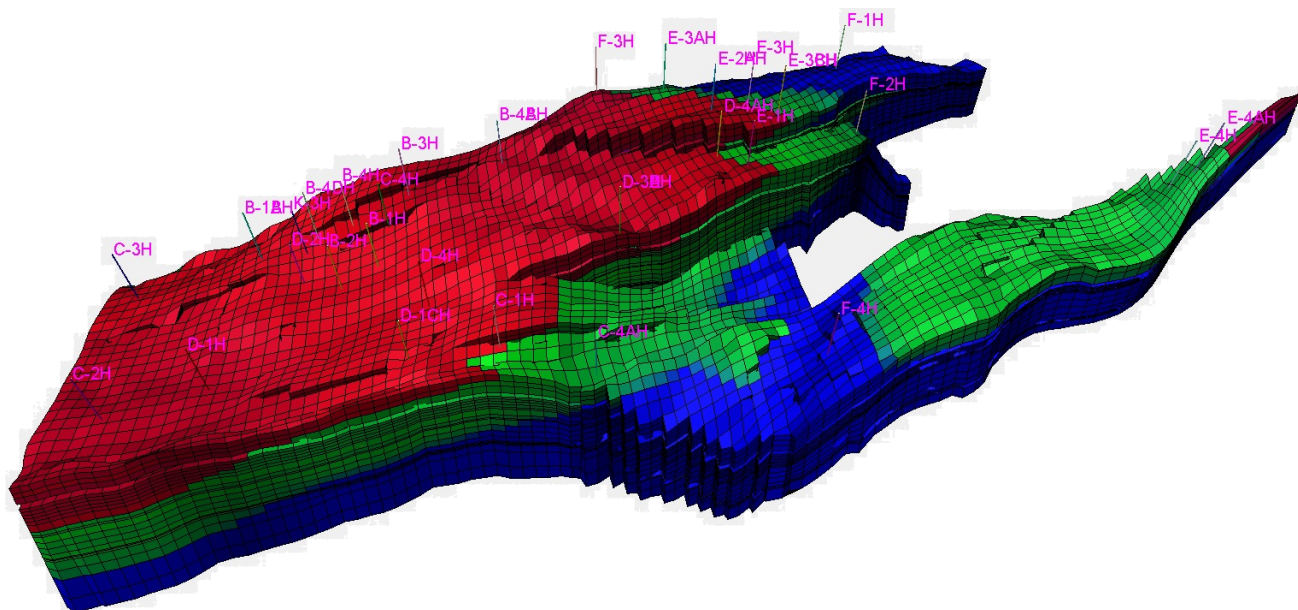


FIGURE 2.13: The Norne Full-field model including all drilled wells.

The most important properties of the oil and gas in the Norne Field is listed in Table 2.4, and schematics showing the reservoir model interpretation of the faults criss-crossing the Norne Field can be seen in Figure 2.14.

Table 2.4: Existing Norne oil and gas properties modelled in the reservoir model

| **Property** | *Value* |
| --- | --- |
| Initial Pressure | 273 bar at 2639 m TVD |
| Reservoir Temperature | 98 °C |
| Oil Density | 859.5 kg/m$^3$ (API=32.7°) |
| Gas Density | 0.854 kg/m$^3$ |
| Water Density | 1033 kg/m$^3$ |
| $B_o$ | 1.32 |
| $B_g$ | 0.0047 |
| Rock Wettability | Mixed |
| Pore Compressibility | $4.84 \times 10^{-5}$ bar$^{-1}$ at 277 bar |
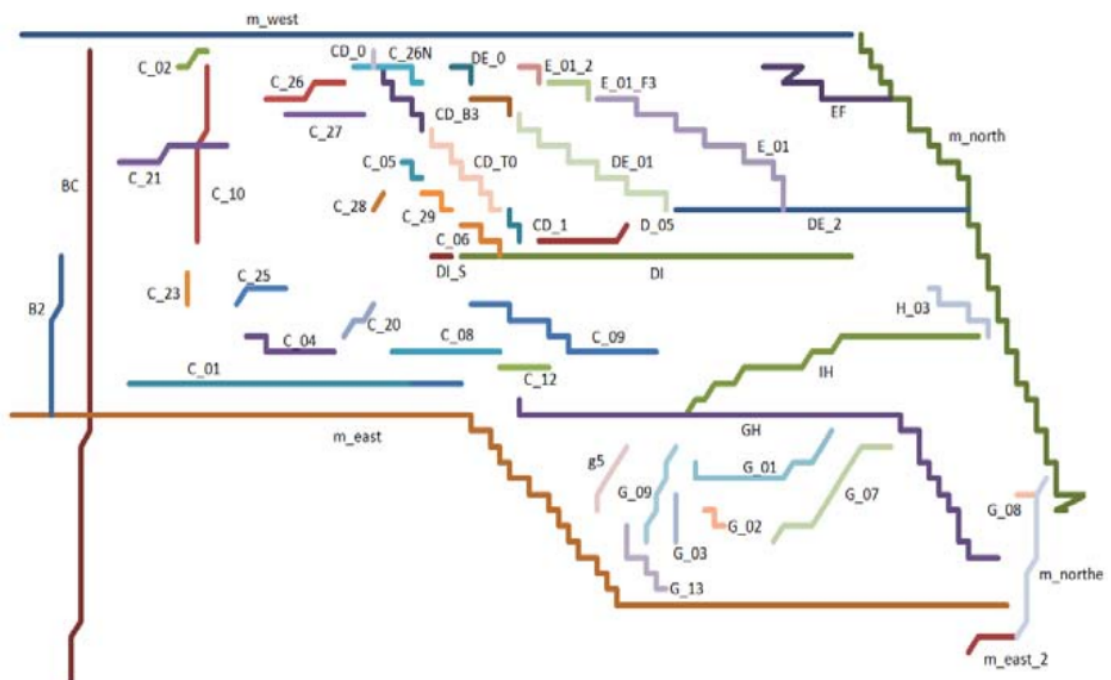


Figure 2.14: Schematics showing the interpretations of faults in the applied ECLIPSE-model (Morell, 2010).

# Chapter 3

# The Ensemble Kalman Filter and the Ensemble Smoother

## 3.1 Background

R.E. Kalman, together with other developers, published several papers in and around 1960 establishing the mathematical foundations of the Kalman type filters. This is a type of optimization algorithms using series of measurements, taking into account random variations and other inaccuracies, to produce estimates of unknown variables more precise than those based on a single measurement alone. Modified versions of the original Kalman filter algorithms has applications in numerous fields of technology, despite originally formulated only for linear system models (Kalman, 1960) and most systems in engineering being nonlinear. The Extended Kalman Filter, which is a series of algorithms concerning different ways of treating the state and observation models, is probably the modification of the Kalman filter most used.

In the Extended Kalman Filter (EKF) there is not a requirement of linear functions, but the state transition- and observation models must be differentiable. Approximations of the covariance evolution by multivariate Taylor Series expansion and the discarding of higher orders, results in a linearization of the non-linear

function around the current estimate. Thus, the usefulness of the EKF depends on the properties of the model dynamics.

The Ensemble Smoother (ES), the Ensemble Kalman Smoother (EnKS) and the Ensemble Kalman Filter (EnKF) are different from the EKF in that the system model is only represented by a set of models based on a probability distribution of certain critical parameters - an ensemble. These algorithms belong to a class of particle methods which use a Monte Carlo or ensemble representation for the probability distribution function (pdf), an ensemble integration using stochastic models to model the time evolution of the pdfs, and different schemes for conditioning the predicted pdf given the observations (Evensen, 2007). The assumption of a Gaussian pdf for the model prediction makes it possible to represent the pdf for the model prediction using only the mean and covariance of the pdf, resulting in a linear update equation.

**Ensemble** An idealization consisting of a large number of virtual copies of a system, each of which represents a possible state that the real system might be in. In other words, here a statistical ensemble is a probability distribution for the state of the system (Gibbs, 1902).

**Monte-Carlo Methods** A broad class of problem solving algorithms used to approximate the probability of certain outcomes by running multiple simulations using random variables in order to calculate those same probabilities heuristically.

**Particle Filters** Algorithms making use of sequential Monte Carlo algorithms for calculating posteriors in partially observable controllable Markov chains with discrete time (Thrun, 2002).

The EnKF was introduced in 1994 (Evensen, 1994), however it was first adapted to the problem of estimating reservoir variables or parameters (permeability and porosity field) in 2003 (Vefring et al., 2003). Since its infancy EnKF has been investigated thoroughly in reservoir characterization settings as well as for HM

problems (Fahimuddin et al., 2010, Gao et al., 2006, Han et al., 2013), and although the major consensus is that EnKF is a well-established and excellent method for performing AHM, it may however produce biased results if not handled with care. It has been shown that for strongly nonlinear problems EnKF can fail to achieve an acceptable data match at certain times in the assimilation process (Li and Reynolds, 2007). With a sufficiently large initial ensemble however, Li and Reynolds stated that "each ensemble member of model parameters obtained at each step of the EnKF is a linear combination of the initial ensemble". In other words, with a large enough initial ensemble of a not too nonlinear problem, the EnKF algorithm performs mostly very well.

## 3.2   Technical Description

Both the ES and the EnKF are Monte Carlo implementations of the Bayesian update problem. Given a probability density function (pdf) of the state of the modeled system (the prior, often called the forecast) and the data likelihood, the Bayes theorem

$$f(\psi|\phi) = \frac{f(\psi)f(\phi|\psi)}{f(\phi)} \tag{3.1}$$

is used to obtain the pdf after the data likelihood has been taken into account (the posterior, often called the analysis). The Bayesian update equation

$$
\begin{aligned}
f(\psi_1, \ldots, \psi_k, \alpha, \psi_0, \psi_b | d) &\propto \\
f(\alpha) f(\psi_0) f(\psi_b) &\prod_{i=1}^{k} f(\psi_i | \{\psi_{l \neq i}\}, \alpha) \prod_{j=1}^{J} f(d_j | \psi_i(j), \alpha)
\end{aligned} \tag{3.2}
$$

comes from formulating the combined parameter and state estimation problem using Bayesian statistics. It can be shown that under the condition of measurement error being independent in time and the dynamical model being a Markov process, a recursive formulation can be used for Bayes' theorem where measurements are processed sequentially in time (Evensen, 2007).

The Bayesian update equation (3.2) is further combined with advancing the model in time, updating the model with measurement data from time to time - possibly due to the recursive formulation of Bayes' theorem. The original Kalman Filter keeps track of the change of the mean and the covariance matrix by the Bayesian update, and advances the covariance matrix in time provided the system is linear, although maintaining the covariance matrix is not feasible computationally for high-dimensional systems. This is where ES and EnKF makes use of the ensemble, and replace the covariance matrix with the sample covariance

$$C_{\psi\psi} = \overline{(\psi - \overline{\psi})(\psi - \overline{\psi})^T} \tag{3.3}$$

computed from the ensemble. The ensemble mean $\overline{\psi}$ is regarded as the best-guess estimate, while the ensemble spread defines the error variance. The covariance (now 3.3) is now determined by the smoothness of the ensemble members (Evensen, 2007).

The difference between ES and EnKF can be found in how the measurement driven updates are implemented in the system (see Figure 3.1 and 3.2). Where ES gathers all the observed measurements into one large update of the predictions, the EnKF updates the whole model every time new observed updates are implemented into the system.
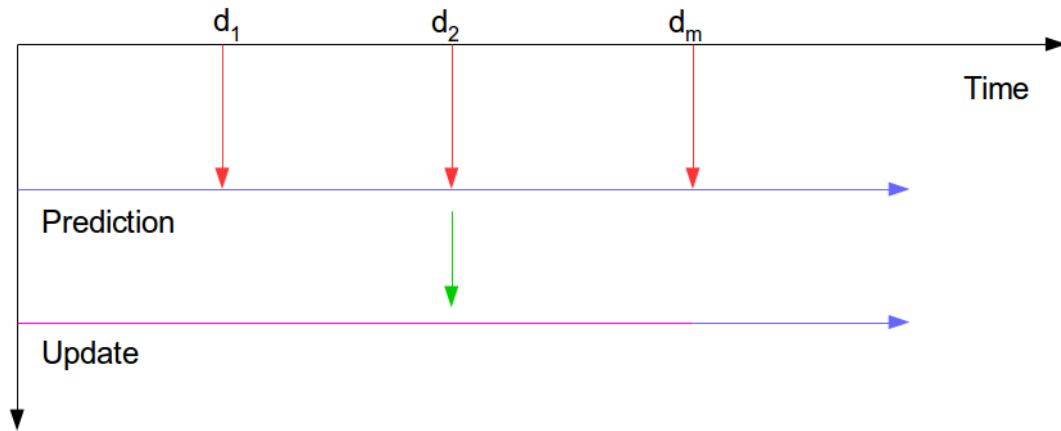
FIGURE 3.1: Illustration of the update procedure used in the ES. The horizontal axis is time and the measurements are indicated at regular intervals. The vertical axis indicates the number of updates with measurements.The blue arrows represent the forward ensemble integration, the red arrows are the introduction of measurements, while the green arrow denotes the updating procedure from ES. The purple line represents the updated model until the end of observed measurements. Adapted from (Evensen, 2007).
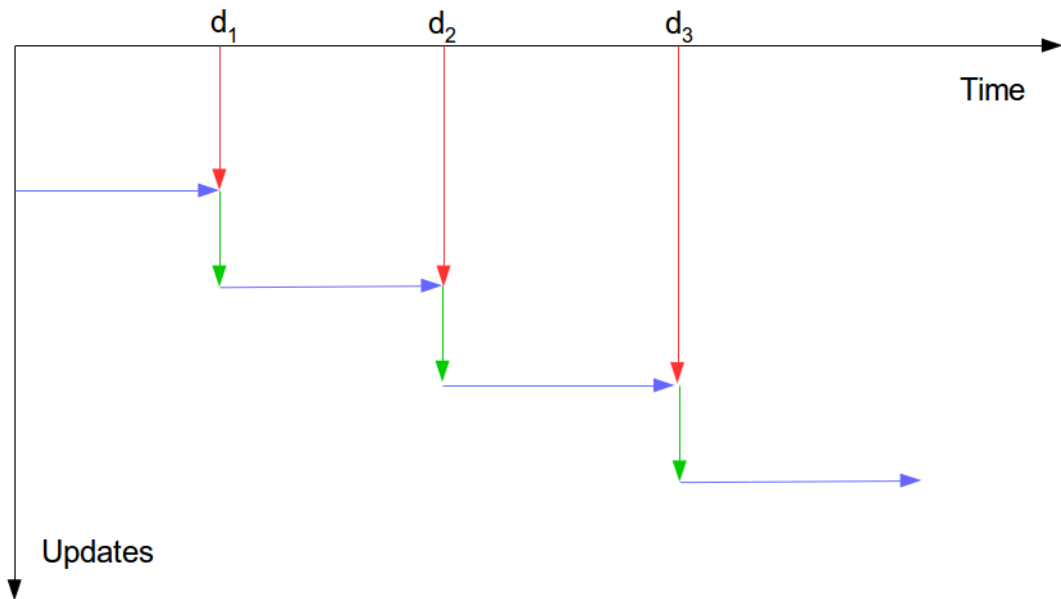


FIGURE 3.2: Illustration of the update procedure used in the EnKF. The blue arrows represent the forward ensemble integration, the red arrows are the introduction of measurements, while the green arrows is the EnKF update algorithm. Thus, the blue arrows indicate the EnKF solution as a function of time, which is updated every time measurements are available. Adapted from (Evensen, 2007).

## 3.3 The Ensemble based Reservoir Tool

The Ensemble based Reservoir Tool (ERT) is a software developed by Statoil for handling many ECLIPSE simulations at the same time, both for sensitivity analysis and AHM purposes (Statoil and NCC, 2013). The ERT incorporates both the EnKF, ES and the RML-EnKF algorithms, as well as tools for analysis, ranking and plotting of results. The full ERT software is quite Linux (Posix) specific, and although the support libraries for working with ECLIPSE files have been successfully ported to Windows, this thesis has exclusively made use of the ERT on a Linux-based platform. The ERT has a text user interface (TUI) (see Figure 3.3) and is executed directly in the system bash with a configuration file as only argument (see Subsection 3.3.1). The code is distributed under the GPL[1] licence. The source code is located on GitHub[2] and the daily management of the code is a cooperation between the Norwegian Computing Center (NCC) and Statoil.

### 3.3.1 Setup

Some preparatory steps must be taken to be able to use an ECLIPSE reservoir model with the ERT, as well as creating a configuration and observation file. In essence, the ECLIPSE data file needs to be modified so that it can be started from any point in the file system, a non-unified restart and summary file must be written at each report step and the layout of the grid can not change between realizations (Statoil and NCC, 2013).The following modifications and additions are obligatory to be able to use an ECLIPSE reservoir model with the ERT;

**Use global INCLUDE and IMPORT statements** The ERT does not run ECLIPSE simulations in the folder where the original ECLIPSE files resides. Thus, it is necessary that all paths to files in INCLUDE and IMPORT statements

---

[1]GNU General Public License. URL: http://www.gnu.org/licenses/gpl.html
[2]Build software better, together. URL: https://github.com/

(expect for those files that will be generated by the ERT) in the original ECLIPSE data file are global.

**Initialization** The SOLUTION section in the ECLIPSE data file is used to specify initial conditions for the ECLIPSE run or restart. In the case of an new ECLIPSE run, initial conditions are either calculated from equilibrium conditions using the EQUIL (and potentially SWATINIT) keyword, or given explicitly using e.g. SWAT, SGAS, PRESSURE etc. If dealing with an ECLIPSE restart, initial conditions are read from an ECLIPSE restart file given with the RESTART keyword. As EnKF is sequential in its design and starts and stops the simulation repeatedly when conditioning to observed data, the ERT is originally meant to modify a large part of the SOLUTION section automatically to make ECLIPSE run smoothly. However, trial and error show that by restarting the EnKF for each data update with the ENKF_RERUN keyword, frequent terminal errors is exchanged in a slightly longer simulation time. The ENKF_RERUN keyword has been used in this thesis.

**Separate SCHEDULE file** The SCHEDULE section of the ECLIPSE data file is used to control the temporal progression of the simulation and the ERT depends heavily on the SCHEDULE data. Thus, the ERT requires that the contents of the SCHEDULE sections is in a separate file as the ERT will write an appropriate schedule file to the simulation folder. Naturally, the INCLUDE statement used to source the contents of the SCHEDULE sections should be local.

**Configuration file**

The ERT configuration file serves several purposes, including, but not limited to; defining which ECLIPSE models to use, i.e. supplying paths to a data, grid and schedule file, defining which observation file to use, defining how to run the simulations, defining where to store the results, and creating a parametrization of the given ECLIPSE model (see Section 4.2).

The configuration file is a plain text file, with one statement per line. The first word on each line is a specific keyword, which then is followed by a set of arguments that are unique to the particular keyword. Similarly to ECLIPSE data files, lines starting with "$--$" are treated as comments. The configuration file, with accompanying keywords, used in this thesis can be seen in Section A.0.1, whereas an overview of all existing keywords can be studied in detail at the ERT homepage[3].

**Observation file**

When using the ERT and one of the incorporated algorithms to condition on dynamic data, it is a necessity to specify which data to condition on. Specifically, for a given piece of data/parameter to condition on, the ERT need to to know the actual measured value of the data, the uncertainty of the measured data, the time of measurement, and how to simulate a response of the data given a parametrized ECLIPSE model. This information is provided to the ERT through the observation file, which is a plain text file containing different keywords associated with different observations.

The only keyword used in this thesis is the HISTORY_OBSERVATION keyword which is used for conditioning on observations from the WCONHIST and WCON-INJH keywords in the SCHEDULE section of the ECLIPSE model. A typical entry can look like this;

```
HISTORY_OBSERVATION WOPR:E-1H {ERROR_MODE=RELMIN;ERROR=0.1;ERROR_MIN=1000;};
```

where the name, WOPR:E-1H, must correspond to an ECLIPSE keyword written to the SUMMARY files, the RELMIN is one of three error modes (RELMIN, REL or ABS), the ERROR=0.1 is an estimated 10% error and the ERROR_MIN=1000 is here the lower threshold.

---

[3]URL: http://ert.nr.no/wiki/index.php/Creating_a_configuration_file_for_ERT

```
 /‾‾‾‾‾‾‾‾‾‾‾‾‾‾‾‾‾‾‾‾‾‾‾‾‾‾‾‾\
|                              |
|   __ __   __    ___   ___    |
|  |  _   |  | |  | )  |   |   |
|  | |_|  |  |_/   | |  |   |   |
|  | |    |  | \\    |    |   |
|  |__|   |__| \\_\\  |_|   |
|                              |
|   Ensemble based Reservoir Tool  |
 _____/

Documentation : http://ert.nr.no
git commit    : 9fc94c8472e829ac28847a4688c031f69ebd1864
compile time  : 2013-10-03 11:18:25
site config   : /project/res/etc/ERT/site-config
model config  : /home/danieso/ert/config_MULT_ZFLT.txt


/-----------------------------------------\
|                Main menu                |
|-----------------------------------------|
| c: Manage cases                         |
| r: Run, restart or analyse experiment   |
| u: Quality check                        |
| p: Plot results                         |
| a: Rank results                         |
| e: Export data to other formats         |
| t: Table of results                     |
| m: Miscellanous                         |
| w: Workflows                            |
| h: Help                                 |
| s: Simple menu                          |
| --------------------------------------- |
| q: Quit                                 |
\-----------------------------------------/

==> █
```

FIGURE 3.3: ERT Main Menu and TUI.

# Chapter 4

# History Matching of the Norne Field

## 4.1 Historical data

In this thesis only production rates and pressure data have been used for assimilation. These data have been made available by the IO Center at NTNU through the Norne Benchmark Case (IO Center, 2010). The following data has been included with the WCONHIST and WCONINJ keywords in the SCHEDULE section of the ECLIPSE model; WWPRH, WGPRH, WOPRH, WBHPH and WTHPH for each production well, as well as WGIRH and WWIRH for each injection well, for their respectively active periods. The ERT observation file specifies that the ES and EnKF will assimilate on these data when conditioning the ECLIPSE model, and that all historical data have a relative error of 10 %.

## 4.2 Parametrization

An AHM algorithm like the EnKF and the EnKS needs specific information about the types of reservoir model parameters it can change when assimilating on historical observed data. Thus, a parametrization of the given ECLIPSE reservoir model is required. The ERT has several parametrization keywords, but the ones

used in this thesis is the FIELD and GEN_KW keywords. The following parameters are made available for alteration in the Norne reservoir model, i.e. the EnKF algorithm conditions on these parameters as it seems fit. The FIELD parameters are briefly explained in subsection 4.2.1, while every GEN_KW parameter is explained in detail in the following subsections.

## 4.2.1 FIELD parameters

The FIELD keyword is used to parametrize quantities which have extent over the full grid. The following static FIELD parameters are initialized with the original included or imported file found in the original Norne ECLIPSE data file. When either EnKF or EnKS are utilized for history matching purposes, these parameters are possibly changed for every update. Every FIELD parameter has one value for each active grid block, i.e. approximately 45000 (44431) possible parameters to alter.

**PORO** Specifies every grid block porosity values and is initially upscaled from the geological model.

**PERMX** Specifies every grid block permeability value in the X-direction and is initially upscaled from the geological model. In the Norne reservoir model PERMY is sat equal to PERMX, while PERMZ is also sat equal to PERMX however later altered in certain grid blocks to compensate for stratigraphical barriers and layering.

**NTG** Specifies every grid block net-to-gross thickness ratio. The values specified are used to convert from gross to net thicknesses, and act as multipliers of grid block pore volumes and transmissibilities in the X- and Y-directions, and also on DZ for the calculation of well connection transmissibility factors (Schlumberger, 2009).

**MULTZ** Specifies every grid block transmissibility multiplier in the Z-direction. Is a critical factor for determining vertical fluid flow together with PERMZ.

## 4.2.2 MULTFLT

The MULTFLT keyword is used for modifying the transmissibility and diffusivity across a fault previously defined using the FAULTS keyword (Schlumberger, 2009). Only the transmissibility option has been used in this thesis. When defining a set of faults with the FAULTS keyword fluid flow is not affected, i.e. the transmissibilites are set to 1.0. As previously stated, the Norne Field has a great deal of faults criss-crossing the reservoir, thus correct modelling of the fluid flow across these barriers is a critical factor. Figure 2.14 gives an overview of the interpretations of faults in the reservoir model, while Table 4.1 shows the MULTFLT values used in the original Norne Full-field case. 60 possible parameters to alter.

TABLE 4.1: Original Norne Full-field MULTFLT values, with fault names and their respective transmissibility multiplier.

| | | | |
|---|---|---|---|
| E_01 | 0.01 | C_21_Ti | 0.001 |
| E_01_F3 | 0.01 | C_22 | 0.001 |
| DE_1 | 3.9 | C_23 | 0.1 |
| DE_1_LTo | 0.01 | C_24 | 0.1 |
| DE_B3 | 0.00075 | C_25 | 0.1 |
| DE_2 | 0.015 | C_26 | 0.1 |
| DE_0 | 20 | C_26N | 0.001 |
| BC | 0.1 | C_27 | 0.05 |
| CD | 0.1 | C_28 | 1 |
| CD_To | 0.01 | C_29 | 0.1 |
| CD_B3 | 0.1 | DI | 0.1 |
| CD_0 | 1 | DI_S | 0.1 |
| CD_1 | 0.1 | D_05 | 0.01 |
| C_01 | 0.01 | EF | 1 |
| C_01_Ti | 0.01 | GH | 1 |
| C_08 | 0.01 | G_01 | 0.05 |
| C_08_Ile | 0.1 | G_02 | 0.05 |
| C_08_S | 0.01 | G_03 | 1 |
| C_08_Ti | 1 | G_05 | 0.5 |
| C_08_S_Ti | 1 | G_07 | 0.05 |
| C_09 | 0.1 | G_08 | 0.05 |
| C_02 | 0.01 | G_09 | 0.05 |
| C_04 | 0.05 | G_13 | 0.05 |
| C_05 | 0.1 | H_03 | 1 |
| C_06 | 0.1 | IH | 1 |
| C_10 | 0.01 | m_east | 1 |
| C_12 | 0.1 | m_east_2 | 1 |
| C_20 | 0.5 | m_north | 1 |
| C_20_LTo | 0.5 | m_northe | 1 |
| C_21 | 0.001 | m_west | 1 |

## 4.2.3 MULTREGT

The MULTREGT keyword is used for setting a transmissibility multiplier between regions. The regions in question must previously have been defined using keyword FLUXNUM or MULTNUM in the GRID section (Schlumberger, 2009). In the Norne reservoir model 20 flux regions have been defined with the FLUXNUM keyword. Figure 4.1 shows the the MULTREGT values used in the original Norne Full-field case. 85 possible parameters to alter.

```
############################################################################################################
#     Garn          | Ile            | Tofte          | Tilje_4/3       | Tilje_1/2                   Formation #
#   C   D   E   G   | C   D   E   G  | C   D   E   G  | C    D   E   G  | C     D     E    G    |       Segment      #
#   1   2   3   4   | 5   6   7   8  | 9  10  11  12  | 13  14  15  16  | 17    18    19   20   | Fluxnum            #
#------------------ |------------------------------------------------- |-----------------------|----------------------#
FLUX 1   1   1  0.005| 0   0   0   0  | 0   0   0   0  | 0   0   0   0   | 0     0     0    0    #|  1   C   Garn      #
FLUX     1   1   1  | 0   0   0   0  | 0   0   0   0  | 0   0   0   0   | 0     0     0    0    #|  2   D             #
FLUX         1   1  | 0   0   0   0  | 0   0   0   0  | 0   0   0   0   | 0     0     0    0    #|  3   E             #
FLUX             1  | 0   0   0   0  | 0   0   0   0  | 0   0   0   0   | 0     0     0    0    #|  4   G             #
#------------------ |--------------- |-------------------------------- |-----------------------|----------------------#
FLUX                | 1   1   1 0.01 | 1   1   1   1  | 0.1 0.1 0.1 0.01| 0     0     0    0    #|  5   C   Ile       #
FLUX                |     1 0.05 1   | 1   1   1   1  | 0.1 1   0.1 0.1 | 0     0     0    0    #|  6   D             #
FLUX                |         1   1  | 1   1   1   1  | 0.1 0.1 0.1 0.1 | 0     0     0    0    #|  7   E             #
FLUX                |             1  | 1   1   1   1  | 0.1 0.1 0.1 0.1 | 0     0     0    0    #|  8   G             #
#------------------ |--------------- |--------------- |---------------- |-----------------------|----------------------#
FLUX                |                | 1   1   1 0.01 | 1   1   1   1   | 0.001 0     0    0    #|  9   C   Tofte     #
FLUX                |                |     1   1   1  | 1   1   1   1   | 0     1     0    0    #| 10   D             #
FLUX                |                |         1   1  | 1   1   1   1   | 0     0     0.001 0   #| 11   E             #
FLUX                |                |             1  | 1   1   1   1   | 0     0     0    1    #| 12   G             #
#------------------ |--------------- |--------------- |---------------- |-----------------------|----------------------#
FLUX                |                |                | 1   1   1  0.01 | 0.0008 0    0    0    #| 13   C   Tilje_4/3 #
FLUX                |                |                |     1   1   1   | 0     0.1 0->e-6 0    #| 14   D             #
FLUX                |                |                |         1   1   | 0     0    0.05  0    #| 15   E             #
FLUX                |                |                |             1   | 0     0    0    0.001 #| 16   G             #
#------------------ |--------------- |--------------- |---------------- |-----------------------|----------------------#
FLUX                |                |                |                 | 1     1     1    0.1  #| 17   C   Tilje_1/2 #
FLUX                |                |                |                 |       1     1    1    #| 18   D             #
FLUX                |                |                |                 |             1    1    #| 19   E             #
FLUX                |                |                |                 |                  1    #| 20   G             #
############################################################################################################
```

FIGURE 4.1: Original Norne Full-field MULTREGT values.

## 4.2.4 MULTZ Modifier

The MULTZ keyword is used for specifying every grid block transmissibility multiplier in the Z-direction. However it is not uncommon to further modify this parameter with a script for sensitivity analysis or manual HM procedures. MULTZ is a critical parameter in the modelling of fluid flow in the Norne reservoir model, hence the extra attention. Figure 4.2 shows the the modified MULTZ values used in the original Norne Full-field case. 48 possible parameters to alter.

```
--           Value    i1  i2  j1  j2  k1  k2    Description     |--           Value    i1  i2  j1  j2  k1  k2|  Description
-------------------------------------------------------------   |-------------------------------------------------------------
EQUALS                                                          |-- Layer 15
  'MULTZ'    0.02      6  13  30  50  8   8  /  Layer 8         |EQUALS
/                                                               |  'MULTZ'    0.00003    6  29  11  21  15  15 /  C south
-- Layer 10                                                     |  'MULTZ'    0.00005    6  29  22  39  15  15 /  C middle
EQUALS                                                          |  'MULTZ'    0.000001  19  29  39  49  15  15 /  C-1H
  'MULTZ'    0.005     6  14  11  18  10  10 /  C-3H            |  'MULTZ'    1.0       19  29  38  45  17  17 /  C-1H
  'MULTZ'    0.03     14  29  11  25  10  10 /  C south east    |  'MULTZ'    0.005     16  19  48  61  15  15 /  E-1H/D-3H
  'MULTZ'    0.05     14  25  26  30  10  10 /  C-segm mid/B-2H |  'MULTZ'    0.0008     8  18  40  40  15  15 /  C north
  'MULTZ'    0.25      6  29  11  37  10  10 /  C-segm middle   |  'MULTZ'    0.0008     9  18  41  41  15  15 /
  'MULTZ'    0.5      17  17  42  54  10  10 /  C north west    |  'MULTZ'    0.0008    10  18  42  43  15  15 /
  'MULTZ'    0.5       6  12  38  39  10  10 /  C north west    |  'MULTZ'    0.0008    11  18  44  44  15  15 /
  'MULTZ'    0.5       8  12  40  40  10  10 /  C north west    |  'MULTZ'    0.0008    12  18  45  45  15  15 /
  'MULTZ'    0.5      10  12  41  43  10  10 /  C north west    |  'MULTZ'    0.0008    13  18  46  47  15  15 /
  'MULTZ'    0.5      18  33  38  54  10  10 /  C1, D4 & D3     |  'MULTZ'    0.0008    14  15  48  48  15  15 /
  'MULTZ'    0.5       6  13  44  52  10  10 /  B-4AH           |  'MULTZ'    0.0008    15  15  49  50  15  15 /
  'MULTZ'    0.01     13  13  48  59  10  10 /  D-segm mid (B-4BH)|  'MULTZ'    0.01      12  12  46  56  15  15 /  D-segm
  'MULTZ'    0.01     14  14  49  59  10  10 /  D-segm mid (B-4BH)|  'MULTZ'    0.01      13  13  48  59  15  15 /  D-segm
  'MULTZ'    0.01     15  16  51  59  10  10 /  D-segm mid (B-4BH)|  'MULTZ'    0.01      14  14  49  62  15  15 /  D-segm
  'MULTZ'    0.05     17  19  55  99  10  10 /  E1              |  'MULTZ'    0.01      15  15  51  65  15  15 /  D-segm
  'MULTZ'    0.05     14  14  60  62  10  10 /  E1              |  'MULTZ'    0.01      16  19  62  69  15  15 /  D-segm
  'MULTZ'    0.05     15  15  60  65  10  10 /  E1              |  'MULTZ'    0.01      17  19  70  99  15  15 /  D-segm
  'MULTZ'    0.05     16  16  60  69  10  10 /  E1              |  'MULTZ'    0.0035     6   7  40  60  15  15 /  D, E west
  'MULTZ'    0.005     6   9  52  60  10  10 /  F-3H/E-2H       |  'MULTZ'    0.0035     8   8  41  60  15  15 /
  'MULTZ'    0.005     9   9  53  57  10  10 /  F-3H/E-2H       |  'MULTZ'    0.0035     9   9  42  52  15  15 /
  'MULTZ'    0.005    10  10  54  58  10  10 /  F-3H/E-2H       |  'MULTZ'    0.0035    10  10  44  49  15  15 /
  'MULTZ'    0.005    11  11  55  58  10  10 /  F-3H/E-2H       |/
/
EQUALS
  'MULTZ'    1.0      22  24  21  22  11  11 /  D-1H water
  'MULTZ'    0.1      21  25  17  19  15  15 /  D-1H water
  'MULTZ'    1.0      22  24  17  19  17  17 /  D-1H water
  'MULTZ'    1.0      22  24  15  17  18  18 /  D-1H water
  'MULTZ'    0.1      12  13  34  35  15  15 /  B-1 & B-3 water
  'MULTZ'    0.1      16  19  47  53  18  18 /  D-3H
/
```

FIGURE 4.2: Original Norne Full-field modified MULTZ values.

## 4.2.5 MINPV

The MINPV keyword is used to declare a threshold pore volume that a cell must exceed or it will be made inactive, i.e. this parameter alters how many active grid blocks that are present in the model from realization to realization. Naturally this makes it difficult to specify exactly how many available parameters the EnKF can condition on, as this varies with the active grid blocks. The original Norne Full-field case have a MINPV value of 500.

## 4.2.6 PERMZ Modifier

The PERMZ keyword specifies every grid block permeability in the Z-direction, but is initially only a copy of the PERMX keyword. To account for stratigraphical barriers and layering these values are modified for every grid block in the Z-direction for better modelling the vertical fluid flow. Figure 4.3 shows the the

modified PERMZ values used in the original Norne Full-field case. 21 possible parameters to alter (NOT layer is not active).

```
--           Value    i1 12 j1 j2 k1 k2        Layer
-----------------------------------------------------------------
MULTIPLY
   'PERMZ'    0.2      1 46 1 112  1  1 /       Garn 3
   'PERMZ'    0.04     1 46 1 112  2  2 /       Garn 2
   'PERMZ'    0.25     1 46 1 112  3  3 /       Garn 1
   'PERMZ'    0.0      1 46 1 112  4  4 /       Not  (inactive anyway)
   'PERMZ'    0.13     1 46 1 112  5  5 /       Ile 2.2
   'PERMZ'    0.13     1 46 1 112  6  6 /       Ile 2.1.3
   'PERMZ'    0.13     1 46 1 112  7  7 /       Ile 2.1.2
   'PERMZ'    0.13     1 46 1 112  8  8 /       Ile 2.1.1
   'PERMZ'    0.09     1 46 1 112  9  9 /       Ile 1.3
   'PERMZ'    0.07     1 46 1 112 10 10 /       Ile 1.2
   'PERMZ'    0.19     1 46 1 112 11 11 /       Ile 1.1
   'PERMZ'    0.13     1 46 1 112 12 12 /       Tofte 2.2
   'PERMZ'    0.64     1 46 1 112 13 13 /       Tofte 2.1.3
   'PERMZ'    0.64     1 46 1 112 14 14 /       Tofte 2.1.2
   'PERMZ'    0.64     1 46 1 112 15 15 /       Tofte 2.1.1
   'PERMZ'    0.64     1 46 1 112 16 16 /       Tofte 1.2.2
   'PERMZ'    0.64     1 46 1 112 17 17 /       Tofte 1.2.1
   'PERMZ'    0.016    1 46 1 112 18 18 /       Tofte 1.1
   'PERMZ'    0.004    1 46 1 112 19 19 /       Tilje 4
   'PERMZ'    0.004    1 46 1 112 20 20 /       Tilje 3
   'PERMZ'    1.0      1 46 1 112 21 21 /       Tilje 2
   'PERMZ'    1.0      1 46 1 112 22 22 /       Tilje 1
 /
```

FIGURE 4.3: Original Norne Full-field modified PERMZ values.

### 4.2.7 Relative Permeability Endscaling

The relative permeability of the Norne reservoir model is defined by the two keywords SWOF and SGOF, both consisting of two tables of 4 columns. SWOF; Water saturation, the corresponding water relative permeability, the corresponding oil relative permeability and the corresponding oil-water capillary pressure. SGOF; Gas saturation, the corresponding gas relative permeability, the corresponding oil relative permeability and the corresponding oil-gas capillary pressure. These values are acquired from laboratory work and special core analysis tests (SCAL) performed on core plugs from the Norne Field. However, as with most field parameters, the relative permeability is only evaluated for certain parts of the reservoir (wells), then stochastically estimated for the rest of the reservoir. This makes sizable deviations quite possible.

The ENDSCALE keyword enables the End-Point Scaling option in ECLIPSE which allows one to scale the end-points of the relative permeability curves for each grid block (Schlumberger, 2009). Using this is a convenient way of performing sensitivity analysis on the relative permeability, which again creates effective parameters for history matching. As stated by Cheng; "...end-point values is bearing uncertainty and may be used as tuning parameters in history matching" (Cheng, 2012). The ENDSCALE keyword in the Norne Full-field reservoir model is enabled with the NODIR and REVERS options. NODIR; The saturation table end-point is non-directional, meaning that the same saturation table is used for flow in the X, Y or Z direction. REVERS; The end-point scaling is reversible, meaning that the same table is used whether the flow is from I to I+1 or from I to I-1.

Figure 4.4 shows the the scaling endpoint values used in the original Norne Full-field case. 15 possible parameters to alter (SGU and SGL are not parametrized).

```
--        Value   i1 i2 j1 j2 k1 k2     Layer
------------------------------------------------------------------------------
EQUALS
  SWL     0.04    1 46 1 112 1   1   /
  SWL     0.05    1 46 1 112 2   2   /
  SWL     0.15    1 46 1 112 3   3   /
  SWL     0.15    1 46 1 112 4   4   /
  SWL     0.05    1 46 1 112 5   10  /  Ile 2.2.2, Ile 2.2.1, Ile 2.1.3, Ile 2.1.2,
                                        Ile 2.1.1, Ile 1.3 and Ile 1.2
  SWL     0.16    1 46 1 112 11  12  /  Ile 1.1 and Tofte 2.2
  SWL     0.07    1 46 1 112 13  15  /  Tofte 2.1
  SWL     0.06    1 46 1 112 16  16  /  Tofte 1.2.2
  SWL     0.12    1 46 1 112 17  22  /  Tofte 1.2.1, Tofte 1.2.1, Tofte 1.1 and Tilje
/
ADD
  SWCR    0.08    1 46 1 112 1  22   /
/
MULTIPLY
  SGU     -1      1 46 1 112 1  22   /
/
ADD
  SGU     1       1 46 1 112 1  22   /
/
EQUALS
  SGL     0.0     1 46 1 112 1  22   /
  SGCR    0.03    1 46 1 112 1  22   /
  SOWCR   0.13    1 46 1 112 1  22   /
  SOGCR   0.07    1 46 1 112 1  22   /
  SWU     1.0     1 46 1 112 1  22   /
/
EQUALS
  ISGCR   0.22    1 46 1 112 1  22   /
/
```

FIGURE 4.4: Original Norne Full-field scaling endpoint values. SWL = Connate water saturation, SWCR = Critical water saturation, SGU = Maximum gas saturation, SGL = Connate gas saturation, SGCR = Critical gas saturation, SOWCR = Critical oil-to-water saturation, SOGCR = Critical oil-to-gas saturation, SWU = Maximum water saturation and ISGCR = Critical gas saturation (Imbibition).

## 4.3   Creating the initial ensemble

The construction of an initial, or prior, ensemble is a very important factor when using either EnKF or ES. The EnKF and ES replaces the system state covariance matrix with the sample covariance computed from the ensemble, and as the EnKF assumes that all probability distributions involved in the data assimilation are normal distributions, the ensemble has to be large enough for EnKF to be able to sample it like a normal distribution (Evensen, 2007).

### 4.3.1 Prior distributions

When defining a parametrization of an ECLIPSE model for use with the ERT, a set of prior distributions are available. In this thesis the UNIFORM keyword has been used, i.e. only uniformly distributed parameters. Other prior distributions can be studied in detail at the ERT homepage[1].

**UNIFORM** A stochastic variable is uniformly distributed if it has a constant probability density on a closed interval. Thus, the uniform distribution is completely characterized by its minimum and maximum value. An ERT example, which assigns a uniform distribution between 0 and 1 to a variable, is "<variable_name> UNIFORM 0 1" (Statoil and NCC, 2013).

"It can be shown that among all distributions bounded below by a and above by b, the uniform distribution with parameters a and b has the maximal entropy (contains the least information). Thus, the uniform distribution should be your preferred prior distribution for robust modeling of bounded variables" (Statoil and NCC, 2013).

### 4.3.2 MULTFLT

The initial parametrization of the MULTREGT keyword can be seen in Table 4.2, and the template file the ERT uses to create importable files for ECLIPSE can be seen in Table A.1.

---

[1]URL: http://ert.nr.no/wiki/index.php/Prior_distributions_available_in_enkf

TABLE 4.2: Initial parametrization of the MULTFLT.

| | | | |
|---|---|---|---|
| E_01 | UNIFORM 0.002 0.05 | C_21_Ti | UNIFORM 0.0005 0.01 |
| E_01_F3 | UNIFORM 0.002 0.05 | C_22 | UNIFORM 0.0005 0.01 |
| DE_1 | UNIFORM 1 12 | C_23 | UNIFORM 0.02 0.5 |
| DE_1_LTo | UNIFORM 0.003 0.05 | C_24 | UNIFORM 0.02 0.5 |
| DE_B3 | UNIFORM 0.0001 0.005 | C_25 | UNIFORM 0.02 0.5 |
| DE_2 | UNIFORM 0.003 0.7 | C_26 | UNIFORM 0.02 0.5 |
| DE_0 | UNIFORM 5 60 | C_26N | UNIFORM 0.0005 0.01 |
| BC | UNIFORM 0.02 0.5 | C_27 | UNIFORM 0.05 0.3 |
| CD | UNIFORM 0.02 0.5 | C_28 | UNIFORM 0.3 3 |
| CD_To | UNIFORM 0.002 0.05 | C_29 | UNIFORM 0.01 0.5 |
| CD_B3 | UNIFORM 0.02 0.5 | DI | UNIFORM 0.01 0.5 |
| CD_0 | UNIFORM 0.3 3 | DI_S | UNIFORM 0.01 0.5 |
| CD_1 | UNIFORM 0.02 0.5 | D_05 | UNIFORM 0.001 0.05 |
| C_01 | UNIFORM 0.001 1.5 | EF | UNIFORM 0.3 3 |
| C_01_Ti | UNIFORM 0.002 0.05 | GH | UNIFORM 0.3 3 |
| C_08 | UNIFORM 0.002 0.05 | G_01 | UNIFORM 0.05 0.3 |
| C_08_Ile | UNIFORM 0.02 0.5 | G_02 | UNIFORM 0.05 0.3 |
| C_08_S | UNIFORM 0.002 0.05 | G_03 | UNIFORM 0.3 3 |
| C_08_Ti | UNIFORM 0.3 3 | G_05 | UNIFORM 0.1 1.5 |
| C_08_S_Ti | UNIFORM 0.3 3 | G_07 | UNIFORM 0.05 0.3 |
| C_09 | UNIFORM 0.02 0.5 | G_08 | UNIFORM 0.05 0.3 |
| C_02 | UNIFORM 0.003 0.1 | G_09 | UNIFORM 0.05 0.3 |
| C_04 | UNIFORM 0.01 0.3 | G_13 | UNIFORM 0.05 0.3 |
| C_05 | UNIFORM 0.002 0.5 | H_03 | UNIFORM 0.3 3 |
| C_06 | UNIFORM 0.002 0.5 | IH | UNIFORM 0.3 3 |
| C_10 | UNIFORM 0.002 0.1 | m_east | UNIFORM 0.3 3 |
| C_12 | UNIFORM 0.02 0.5 | m_east_2 | UNIFORM 0.3 3 |
| C_20 | UNIFORM 0.05 1.5 | m_north | UNIFORM 0.3 3 |
| C_20_LTo | UNIFORM 0.1 1.5 | m_northe | UNIFORM 0.3 3 |
| C_21 | UNIFORM 0.0005 0.01 | m_west | UNIFORM 0.3 3 |

### 4.3.3 MULTREGT

The initial parametrization of the MULTREGT keyword can be seen in Table 4.3, and the template file the ERT uses to create importable files for ECLIPSE can be seen in Table A.2.

TABLE 4.3: Initial parametrization of the MULTREGT.

| | | | |
|---|---|---|---|
| **MULTREGT0** | UNIFORM 0.1 10 | **MULTREGT83** | UNIFORM 0.1 10 |
| **MULTREGT1** | UNIFORM 0.1 10 | **MULTREGT84** | UNIFORM 0.01 1 |
| **MULTREGT2** | UNIFORM 0.1 10 | **MULTREGT85** | UNIFORM 0.01 1 |
| **MULTREGT3** | UNIFORM 0.0005 0.05 | **MULTREGT86** | UNIFORM 0.1 10 |
| **MULTREGT4** | UNIFORM 0.1 10 | **MULTREGT87** | UNIFORM 10 1000 |
| **MULTREGT5** | UNIFORM 0.1 10 | **MULTREGT88** | UNIFORM 0.1 10 |
| **MULTREGT14** | UNIFORM 0.1 10 | **MULTREGT89** | UNIFORM 0.1 10 |
| **MULTREGT19** | UNIFORM 0.1 10 | **MULTREGT90** | UNIFORM 0.1 10 |
| **MULTREGT20** | UNIFORM 0.005 0.5 | **MULTREGT95** | UNIFORM 0.01 1 |
| **MULTREGT25** | UNIFORM 0.001 0.1 | **MULTREGT96** | UNIFORM 0.01 1 |
| **MULTREGT26** | UNIFORM 0.1 10 | **MULTREGT97** | UNIFORM 0.01 1 |
| **MULTREGT27** | UNIFORM 0.1 10 | **MULTREGT98** | UNIFORM 0.01 1 |
| **MULTREGT32** | UNIFORM 0.1 10 | **MULTREGT99** | UNIFORM 0.1 10 |
| **MULTREGT33** | UNIFORM 0.1 10 | **MULTREGT100** | UNIFORM 0.1 10 |
| **MULTREGT34** | UNIFORM 0.1 10 | **MULTREGT101** | UNIFORM 0.1 10 |
| **MULTREGT35** | UNIFORM 0.1 10 | **MULTREGT102** | UNIFORM 0.1 10 |
| **MULTREGT40** | UNIFORM 0.1 10 | **MULTREGT103** | UNIFORM 0.1 10 |
| **MULTREGT41** | UNIFORM 0.1 10 | **MULTREGT104** | UNIFORM 0.1 10 |
| **MULTREGT42** | UNIFORM 0.1 10 | **MULTREGT109** | UNIFORM 0.001 0.1 |
| **MULTREGT43** | UNIFORM 0.1 10 | **MULTREGT110** | UNIFORM 0.01 1 |
| **MULTREGT44** | UNIFORM 0.1 10 | **MULTREGT111** | UNIFORM 0.01 1 |
| **MULTREGT49** | UNIFORM 0.1 10 | **MULTREGT112** | UNIFORM 0.01 1 |
| **MULTREGT50** | UNIFORM 0.1 10 | **MULTREGT113** | UNIFORM 0.1 10 |
| **MULTREGT51** | UNIFORM 0.1 10 | **MULTREGT114** | UNIFORM 0.1 10 |
| **MULTREGT52** | UNIFORM 0.1 10 | **MULTREGT115** | UNIFORM 0.1 10 |
| **MULTREGT53** | UNIFORM 0.1 10 | **MULTREGT116** | UNIFORM 0.1 10 |
| **MULTREGT54** | UNIFORM 0.1 10 | **MULTREGT117** | UNIFORM 0.001 0.1 |
| **MULTREGT59** | UNIFORM 0.1 10 | **MULTREGT118** | UNIFORM 0.1 10 |
| **MULTREGT60** | UNIFORM 0.1 10 | **MULTREGT119** | UNIFORM 0.1 10 |
| **MULTREGT61** | UNIFORM 0.1 10 | **MULTREGT128** | UNIFORM 0.0001 0.01 |
| **MULTREGT62** | UNIFORM 0.1 10 | **MULTREGT132** | UNIFORM 0.0008 0.008 |
| **MULTREGT63** | UNIFORM 0.001 0.1 | **MULTREGT145** | UNIFORM 0.1 10 |
| **MULTREGT64** | UNIFORM 0.1 10 | **MULTREGT149** | UNIFORM 0.01 1 |
| **MULTREGT65** | UNIFORM 0.1 10 | **MULTREGT152** | UNIFORM 0.1 10 |
| **MULTREGT70** | UNIFORM 0.01 1 | **MULTREGT163** | UNIFORM 0.0001 0.01 |
| **MULTREGT71** | UNIFORM 0.01 1 | **MULTREGT167** | UNIFORM 0.005 0.5 |
| **MULTREGT72** | UNIFORM 0.01 1 | **MULTREGT169** | UNIFORM 0.1 10 |
| **MULTREGT73** | UNIFORM 0.01 1 | **MULTREGT170** | UNIFORM 0.1 10 |
| **MULTREGT74** | UNIFORM 0.1 10 | **MULTREGT182** | UNIFORM 0.1 10 |
| **MULTREGT75** | UNIFORM 0.1 10 | **MULTREGT186** | UNIFORM 0.0001 0.01 |
| **MULTREGT76** | UNIFORM 0.1 10 | **MULTREGT187** | UNIFORM 0.01 1 |
| **MULTREGT77** | UNIFORM 0.1 10 | **MULTREGT188** | UNIFORM 0.1 10 |
| **MULTREGT82** | UNIFORM 0.01 1 | **MULTREGT189** | UNIFORM 0.1 10 |

### 4.3.4 MULTZ Modifier

The initial parametrization of the MULTZ keyword can be seen in Table 4.4 for the E-segment and in Table 4.5. The template file the ERT uses to create importable files for ECLIPSE can be seen in section A.0.4.

TABLE 4.4: Initial parametrization of the MULTZ Modifier, Norne E-segment model.

| | | | |
|---|---|---|---|
| **MULTZ1** | UNIFORM 0.04 0.01 | **MULTZ28** | UNIFORM 0.0004 0.0015 |
| **MULTZ2** | UNIFORM 0.002 0.01 | **MULTZ29** | UNIFORM 0.0004 0.0015 |
| **MULTZ3** | UNIFORM 0.01 0.06 | **MULTZ30** | UNIFORM 0.0004 0.0015 |
| **MULTZ4** | UNIFORM 0.02 0.1 | **MULTZ31** | UNIFORM 0.0004 0.0015 |
| **MULTZ5** | UNIFORM 0.1 0.5 | **MULTZ32** | UNIFORM 0.0004 0.0015 |
| **MULTZ6** | UNIFORM 0.1 0.9 | **MULTZ33** | UNIFORM 0.0004 0.0015 |
| **MULTZ7** | UNIFORM 0.1 0.9 | **MULTZ34** | UNIFORM 0.0004 0.0015 |
| **MULTZ8** | UNIFORM 0.1 0.9 | **MULTZ35** | UNIFORM 0.0004 0.0012 |
| **MULTZ9** | UNIFORM 0.1 0.9 | **MULTZ36** | UNIFORM 0.005 0.03 |
| **MULTZ10** | UNIFORM 0.1 0.9 | **MULTZ37** | UNIFORM 0.005 0.03 |
| **MULTZ11** | UNIFORM 0.1 0.9 | **MULTZ38** | UNIFORM 0.005 0.03 |
| **MULTZ12** | UNIFORM 0.005 0.02 | **MULTZ39** | UNIFORM 0.005 0.03 |
| **MULTZ13** | UNIFORM 0.005 0.02 | **MULTZ40** | UNIFORM 0.005 0.03 |
| **MULTZ14** | UNIFORM 0.005 0.02 | **MULTZ41** | UNIFORM 0.005 0.03 |
| **MULTZ15** | UNIFORM 0.01 0.5 | **MULTZ42** | UNIFORM 0.001 0.005 |
| **MULTZ16** | UNIFORM 0.01 0.5 | **MULTZ43** | UNIFORM 0.0015 0.006 |
| **MULTZ17** | UNIFORM 0.01 0.5 | **MULTZ44** | UNIFORM 0.0015 0.006 |
| **MULTZ18** | UNIFORM 0.01 0.5 | **MULTZ45** | UNIFORM 0.0015 0.006 |
| **MULTZ19** | UNIFORM 0.001 0.01 | **MULTZ46** | UNIFORM 0.7 1.2 |
| **MULTZ20** | UNIFORM 0.001 0.01 | **MULTZ47** | UNIFORM 0.05 0.2 |
| **MULTZ21** | UNIFORM 0.001 0.01 | **MULTZ48** | UNIFORM 0.7 1.2 |
| **MULTZ22** | UNIFORM 0.001 0.01 | **MULTZ49** | UNIFORM 0.7 1.2 |
| **MULTZ26** | UNIFORM 0.7 1.2 | **MULTZ50** | UNIFORM 0.05 0.2 |
| **MULTZ27** | UNIFORM 0.001 0.05 | **MULTZ51** | UNIFORM 0.05 0.2 |

T ABLE 4.5: Initial parametrization of the MULTZ Modifier, Norne Full-field model.

| MULTZ1 | UNIFORM 0.04 0.01 | MULTZ28 | UNIFORM 0.0004 0.0015 |
|---|---|---|---|
| MULTZ2 | UNIFORM 0.002 0.01 | MULTZ29 | UNIFORM 0.0004 0.0015 |
| MULTZ3 | UNIFORM 0.01 0.06 | MULTZ30 | UNIFORM 0.0004 0.0015 |
| MULTZ4 | UNIFORM 0.02 0.1 | MULTZ31 | UNIFORM 0.0004 0.0015 |
| MULTZ5 | UNIFORM 0.1 0.5 | MULTZ32 | UNIFORM 0.0004 0.0015 |
| MULTZ6 | UNIFORM 0.2 1 | MULTZ33 | UNIFORM 0.0004 0.0015 |
| MULTZ7 | UNIFORM 0.2 1 | MULTZ34 | UNIFORM 0.0004 0.0015 |
| MULTZ8 | UNIFORM 0.2 1 | MULTZ35 | UNIFORM 0.0004 0.0012 |
| MULTZ9 | UNIFORM 0.2 1 | MULTZ36 | UNIFORM 0.005 0.03 |
| MULTZ10 | UNIFORM 0.2 1 | MULTZ37 | UNIFORM 0.005 0.03 |
| MULTZ11 | UNIFORM 0.2 1 | MULTZ38 | UNIFORM 0.005 0.03 |
| MULTZ12 | UNIFORM 0.005 0.02 | MULTZ39 | UNIFORM 0.005 0.03 |
| MULTZ13 | UNIFORM 0.005 0.02 | MULTZ40 | UNIFORM 0.005 0.03 |
| MULTZ14 | UNIFORM 0.005 0.02 | MULTZ41 | UNIFORM 0.005 0.03 |
| MULTZ15 | UNIFORM 0.02 0.1 | MULTZ42 | UNIFORM 0.0015 0.006 |
| MULTZ16 | UNIFORM 0.02 0.1 | MULTZ43 | UNIFORM 0.0015 0.006 |
| MULTZ17 | UNIFORM 0.02 0.1 | MULTZ44 | UNIFORM 0.0015 0.006 |
| MULTZ18 | UNIFORM 0.02 0.1 | MULTZ45 | UNIFORM 0.0015 0.006 |
| MULTZ19 | UNIFORM 0.002 0.01 | MULTZ46 | UNIFORM 0.7 1.2 |
| MULTZ20 | UNIFORM 0.002 0.01 | MULTZ47 | UNIFORM 0.05 0.2 |
| MULTZ21 | UNIFORM 0.002 0.01 | MULTZ48 | UNIFORM 0.7 1.2 |
| MULTZ22 | UNIFORM 0.002 0.01 | MULTZ49 | UNIFORM 0.7 1.2 |
| MULTZ26 | UNIFORM 0.7 1.2 | MULTZ50 | UNIFORM 0.05 0.2 |
| MULTZ27 | UNIFORM 0.002 0.01 | MULTZ51 | UNIFORM 0.05 0.2 |

## 4.3.5 MINPV

The initial parametrization of the MINPV keyword is defined as MIN_PV_GEN UNIFORM 400 600, and the template file the ERT uses to create importable files for ECLIPSE then look like this;

MINPV

<MIN_PV_GEN> /

## 4.3.6   PERMX Modifier

The initial parametrization of the PERMZ keyword can be seen in Table 4.6 for the E-segment and in Table 4.7. The template file the ERT uses to create importable files for ECLIPSE can be seen in section A.0.5.

TABLE 4.6: Initial parametrization of the PERMZ Modifier, Norne E-segment model.

| | |
|---|---|
| **PERMZ1** | UNIFORM 0.02 0.5 |
| **PERMZ2** | UNIFORM 0.005 0.1 |
| **PERMZ3** | UNIFORM 0.02 0.7 |
| **PERMZ5** | UNIFORM 0.01 0.4 |
| **PERMZ6** | UNIFORM 0.01 0.4 |
| **PERMZ7** | UNIFORM 0.01 0.4 |
| **PERMZ8** | UNIFORM 0.01 0.4 |
| **PERMZ9** | UNIFORM 0.01 0.3 |
| **PERMZ10** | UNIFORM 0.001 0.25 |
| **PERMZ11** | UNIFORM 0.002 0.5 |
| **PERMZ12** | UNIFORM 0.002 0.3 |
| **PERMZ13** | UNIFORM 0.1 2 |
| **PERMZ14** | UNIFORM 0.1 2 |
| **PERMZ15** | UNIFORM 0.1 2 |
| **PERMZ16** | UNIFORM 0.1 2 |
| **PERMZ17** | UNIFORM 0.1 2 |
| **PERMZ18** | UNIFORM 0.002 0.05 |
| **PERMZ19** | UNIFORM 0.0005 0.01 |
| **PERMZ20** | UNIFORM 0.0005 0.01 |
| **PERMZ21** | UNIFORM 0.2 2 |
| **PERMZ22** | UNIFORM 0.2 2 |

Table 4.7: Initial parametrization of the PERMZ Modifier, Norne Full-field model.

| | |
|---|---|
| **PERMZ1** | UNIFORM 0.02 0.7 |
| **PERMZ2** | UNIFORM 0.005 0.2 |
| **PERMZ3** | UNIFORM 0.02 0.8 |
| **PERMZ5** | UNIFORM 0.02 0.6 |
| **PERMZ6** | UNIFORM 0.02 0.6 |
| **PERMZ7** | UNIFORM 0.02 0.6 |
| **PERMZ8** | UNIFORM 0.02 0.6 |
| **PERMZ9** | UNIFORM 0.01 0.4 |
| **PERMZ10** | UNIFORM 0.001 0.35 |
| **PERMZ11** | UNIFORM 0.002 0.6 |
| **PERMZ12** | UNIFORM 0.002 0.4 |
| **PERMZ13** | UNIFORM 0.1 2.5 |
| **PERMZ14** | UNIFORM 0.1 2.5 |
| **PERMZ15** | UNIFORM 0.1 2.5 |
| **PERMZ16** | UNIFORM 0.1 2.5 |
| **PERMZ17** | UNIFORM 0.1 2.5 |
| **PERMZ18** | UNIFORM 0.002 0.07 |
| **PERMZ19** | UNIFORM 0.0005 0.02 |
| **PERMZ20** | UNIFORM 0.0005 0.02 |
| **PERMZ21** | UNIFORM 0.2 2.5 |
| **PERMZ22** | UNIFORM 0.2 2.5 |

## 4.3.7   Relative Permeability Endscaling

The initial parametrization of the keywords available with the ENDSCALE option can be seen in Table 4.8 , and the template file the ERT uses to create importable files for ECLIPSE can be seen in section A.0.6.

TABLE 4.8: Initial parametrization of the keywords available with the END-SCALE option.

| endpoint1 | UNIFORM 0.01 0.1 |
|---|---|
| endpoint2 | UNIFORM 0.01 0.1 |
| endpoint3 | UNIFORM 0.05 0.25 |
| endpoint4 | UNIFORM 0.05 0.25 |
| endpoint5 | UNIFORM 0.01 0.1 |
| endpoint6 | UNIFORM 0.05 0.25 |
| endpoint7 | UNIFORM 0.12 0.03 |
| endpoint8 | UNIFORM 0.01 0.1 |
| endpoint9 | UNIFORM 0.05 0.25 |
| endpoint10 | UNIFORM 0.03 0.15 |
| endpoint13 | UNIFORM 0.01 0.08 |
| endpoint14 | UNIFORM 0.05 0.25 |
| endpoint15 | UNIFORM 0.01 0.1 |
| endpoint17 | UNIFORM 0.15 0.3 |

# Chapter 5

# Results

## 5.1 E-segment

The E-segment ES- and EnkF-assimilation was performed with an ensemble consisting of 120 ECLIPSE realizations, with ES- and EnKF-updates for every $25^{th}$ report step [258 in total]. An ensemble size with a lower bound of approximately 100 members ensure a non-biased sampling by the ES- and EnKF-algorithm (Natvik and Evensen, 2003). The reference case and the historical data records begins at the $14^{th}$ of November 1997 and ends at the $1^{st}$ of December 2004, while the ensemble and ES- and EnKF-assimilation simulates and predicts for 4 more years until the $1^{st}$ of November 2008. With 120 realization members the execution runtime was ~4 hours for the initial ensemble and the ES, and ~20 hours for the EnKF[1]. ~55GB of data was generated for each set of realizations (initial ensemble, analyzed ensemble (ES) and analyzed ensemble (EnKF)).

---

[1]Note: The bigmem queue on the Kongull cluster was utilized, running maximum 40 realizations simultaneously. 1 node (2 AMD Opteron model 2431 6-core (Istanbul) processors, 2400 GHz core speed and 667 MHz bus frequency) per realization.

FIGURE 5.1: Oil production rate for well E-1H with mismatch plot. X-axis = Time. Y-axis = STB/DAY.
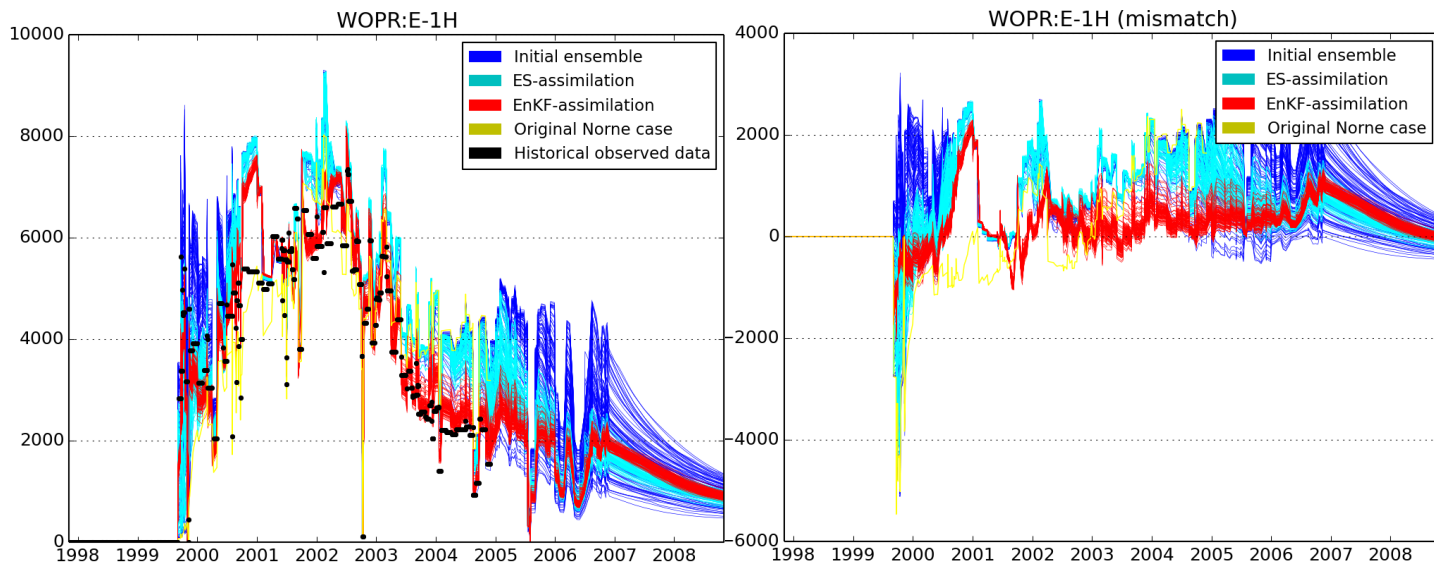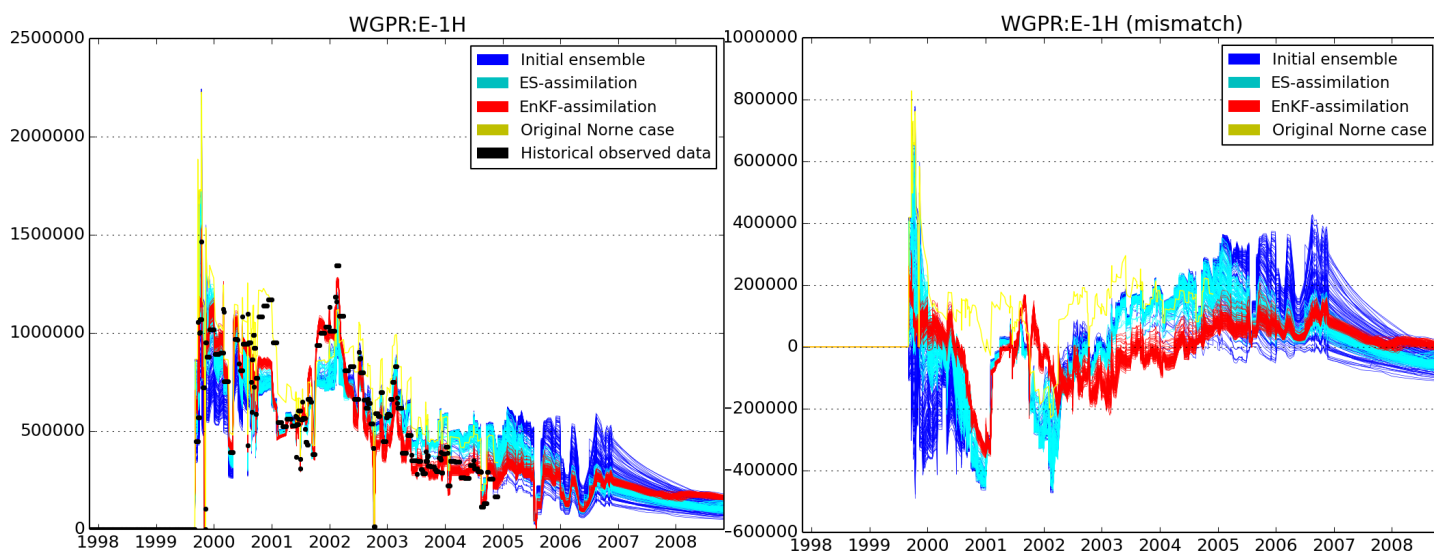


FIGURE 5.2: Gas production rate for well E-1H with mismatch plot. X-axis = Time. Y-axis = MSCF/DAY.
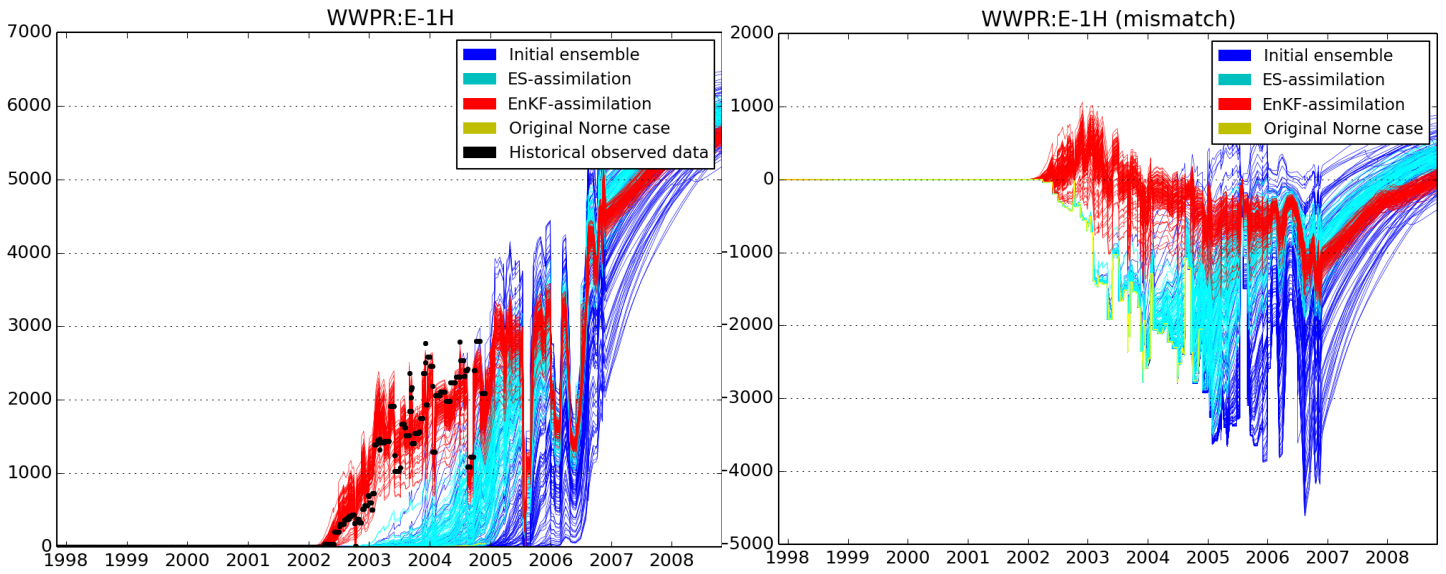
FIGURE 5.3: Water production rate for well E-1H with mismatch plot. X-axis = Time. Y-axis = STB/DAY.
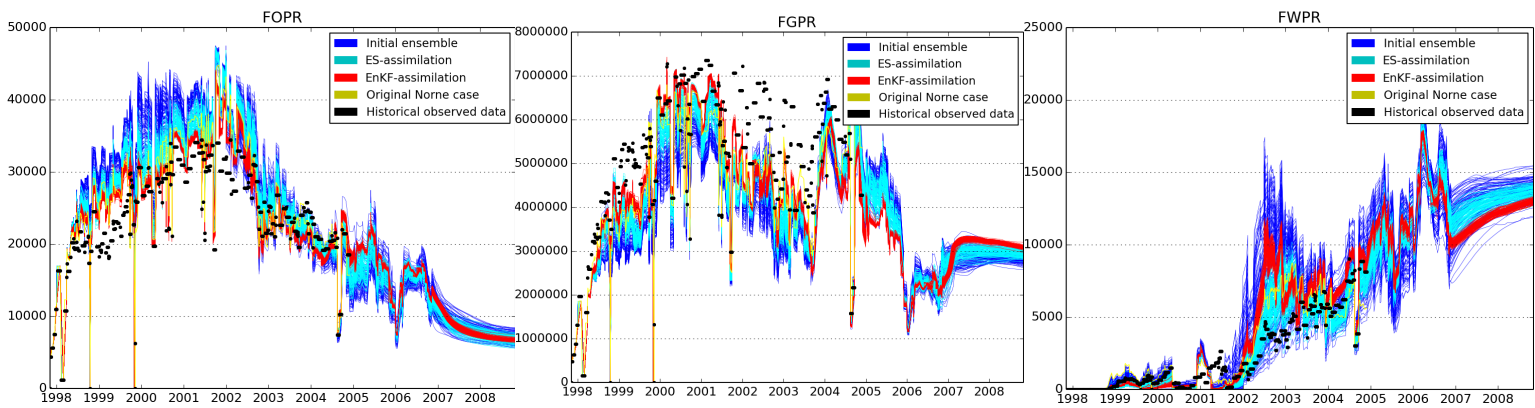


FIGURE 5.4: Plots for the FIELD rates, based on the coarsened E-segment model. X-axis = Time. Y-axis = STB/DAY, MSCF/DAY, STB/DAY, respectively.
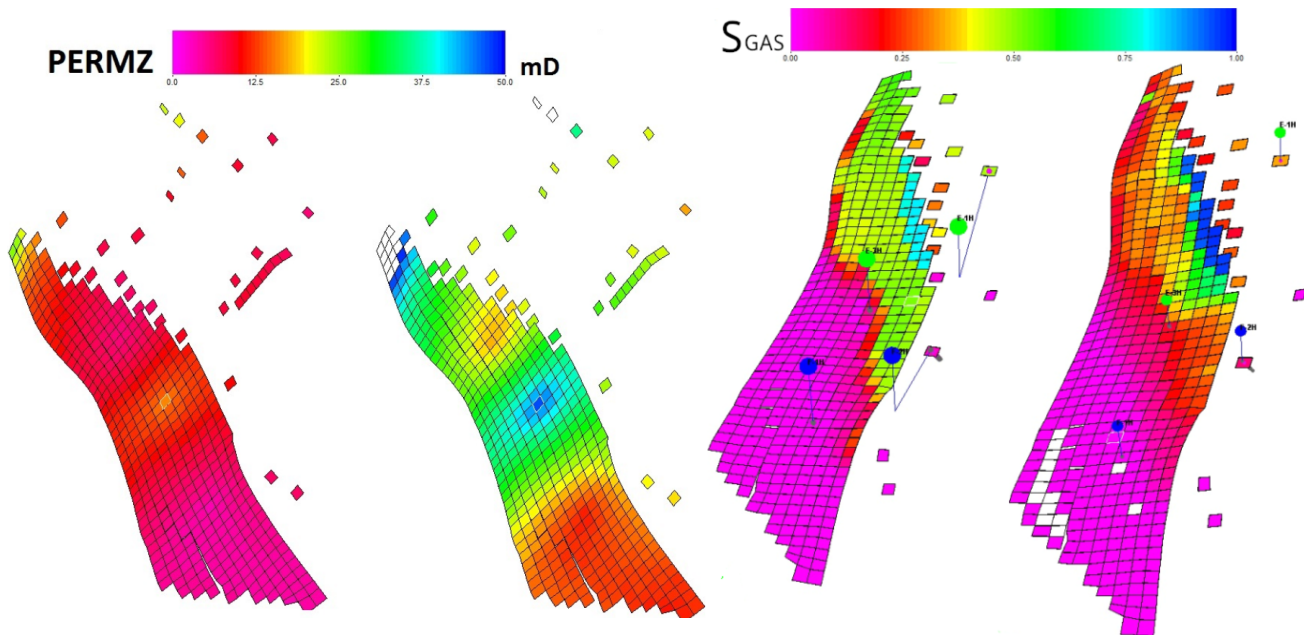
FIGURE 5.5: PERMZ, E-segment. Left: Original Norne case. Right: EnKF-analyzed ensemble member #60. Well E-3H perforated in indicated cell (12, 72, 5).

FIGURE 5.6: Gas saturation $1^{st}$ of May 2000, E-segment. Left: Original Norne case. Right: EnKF-analyzed ensemble member #60.

In the included EnKF_analyzed_models.zip the EnKF-analyzed ensemble member #60 (ECLIPSE.DATA-file with importable files) may be studied in further depth.

## 5.2 Full-field

The Full-field ES- and EnkF-assimilation was performed with an ensemble consisting of 80 ECLIPSE realizations, with ES- and EnKF-updates for every $50^{th}$ report step [266 in total]. The low number of ensemble members and fairly large update step are due to the size of the Full-field model. A single simulation run of the original Full-field Norne model has a runtime of ~1.5 hrs. However, certain ensemble members initialized with abnormal parameters made the model very dense, thus resulting in longer convergence time for ECLIPSE. The consequence of this was runtimes of more than 6 hrs. The time limit on this thesis, available computational capacity and a consistent ensemble collapse while assimilating, made it

necessary with preliminary measures like smaller ensemble size and larger EnKF update step.

The reference case and the historical data records begins at the 14th of November 1997 and ends at the 1st of December 2006, while the ensemble and ES- and EnKF-assimilation simulates and predicts for 1.25 years more until the 1st of March 2008 (the EnKF-assimilation had to be cut half a year early due to a technical mishap). With 80 realization members the execution runtime was ~25 hours for the initial ensemble and the ES, and approximately 1 week for the EnKF[2]. ~140GB of data was generated for each set of realizations (initial ensemble, analyzed ensemble (ES) and analyzed ensemble (EnKF)).
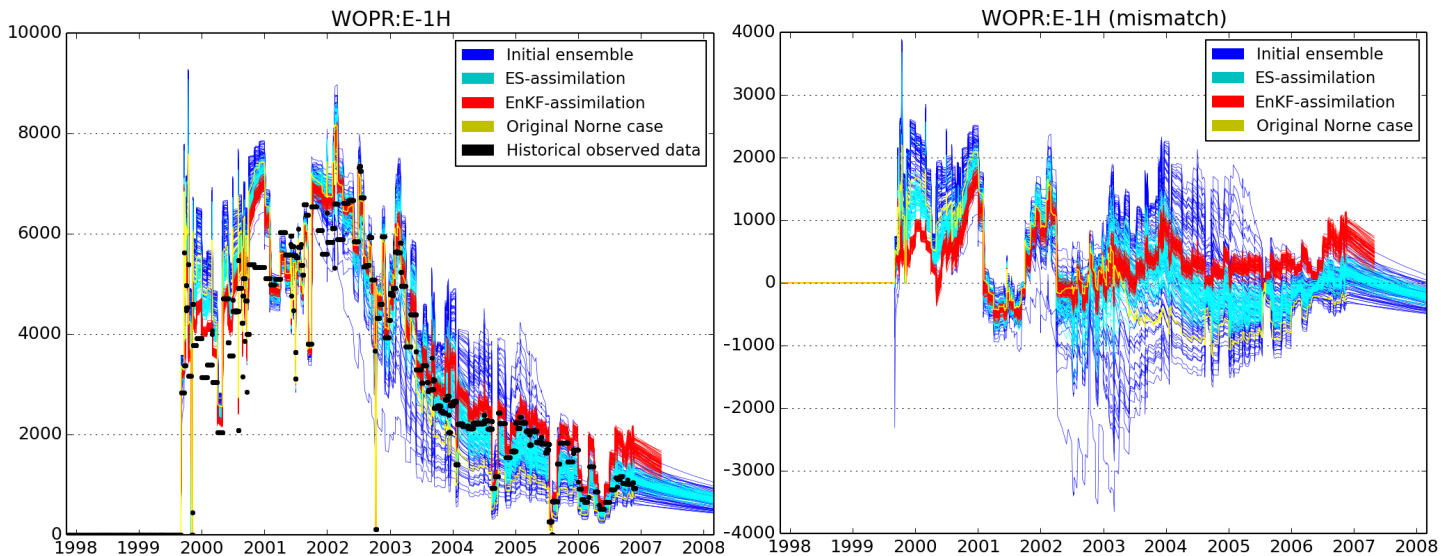


FIGURE 5.7: Oil production rate for well E-1H with mismatch plot. X-axis = Time. Y-axis = STB/DAY.

---

[2]Note: The bigmem queue on the Kongull cluster was utilized, running maximum 30 realizations simultaneously. 1 node (2 AMD Opteron model 2431 6-core (Istanbul) processors, 2400 GHz core speed and 667 MHz bus frequency) per realization.
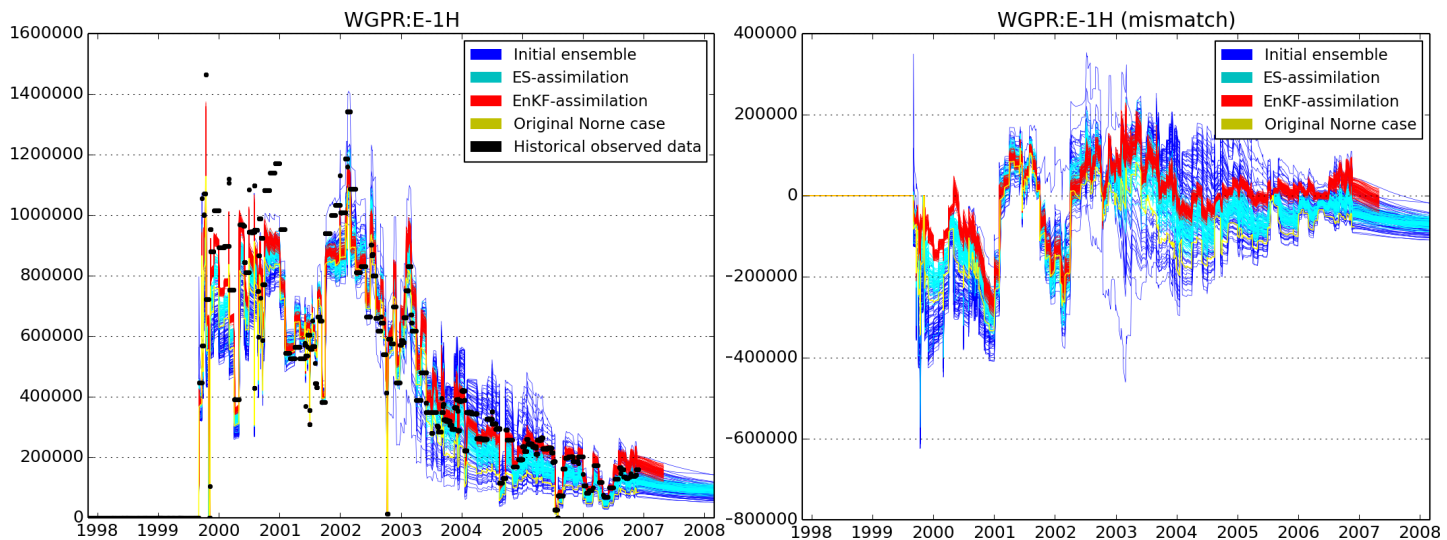
FIGURE 5.8: Gas production rate for well E-1H with mismatch plot. X-axis = Time. Y-axis = MSCF/DAY.
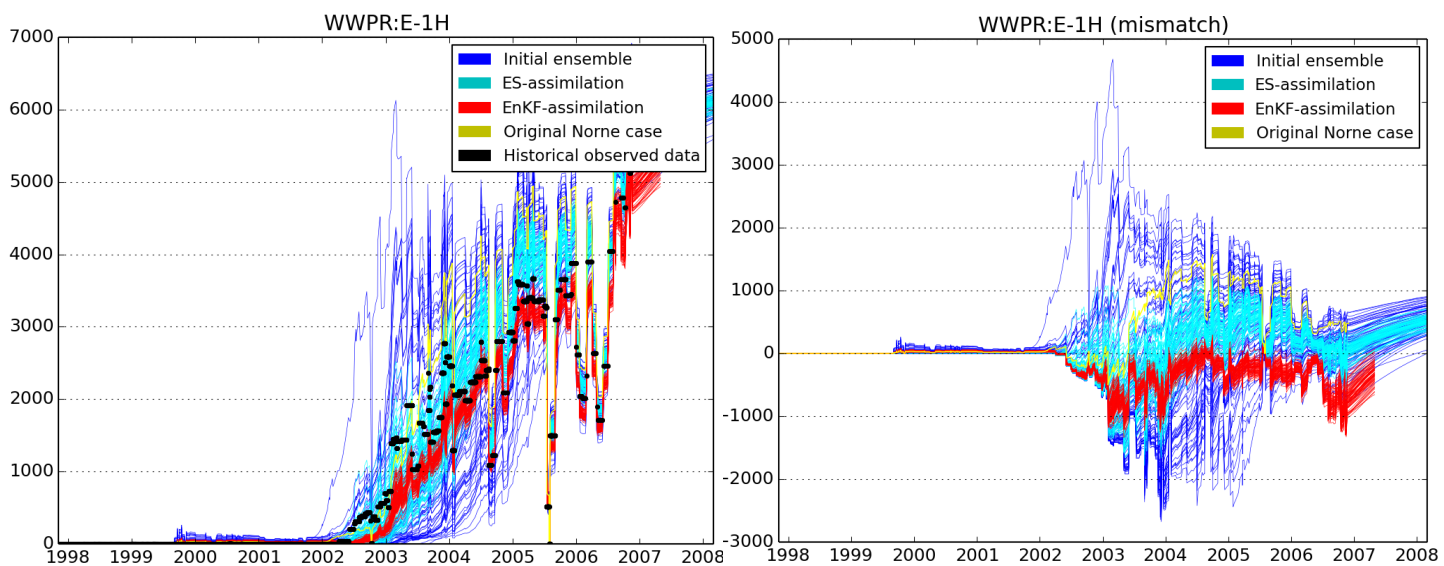


FIGURE 5.9: Water production rate for well E-1H with mismatch plot. X-axis = Time. Y-axis = STB/DAY.
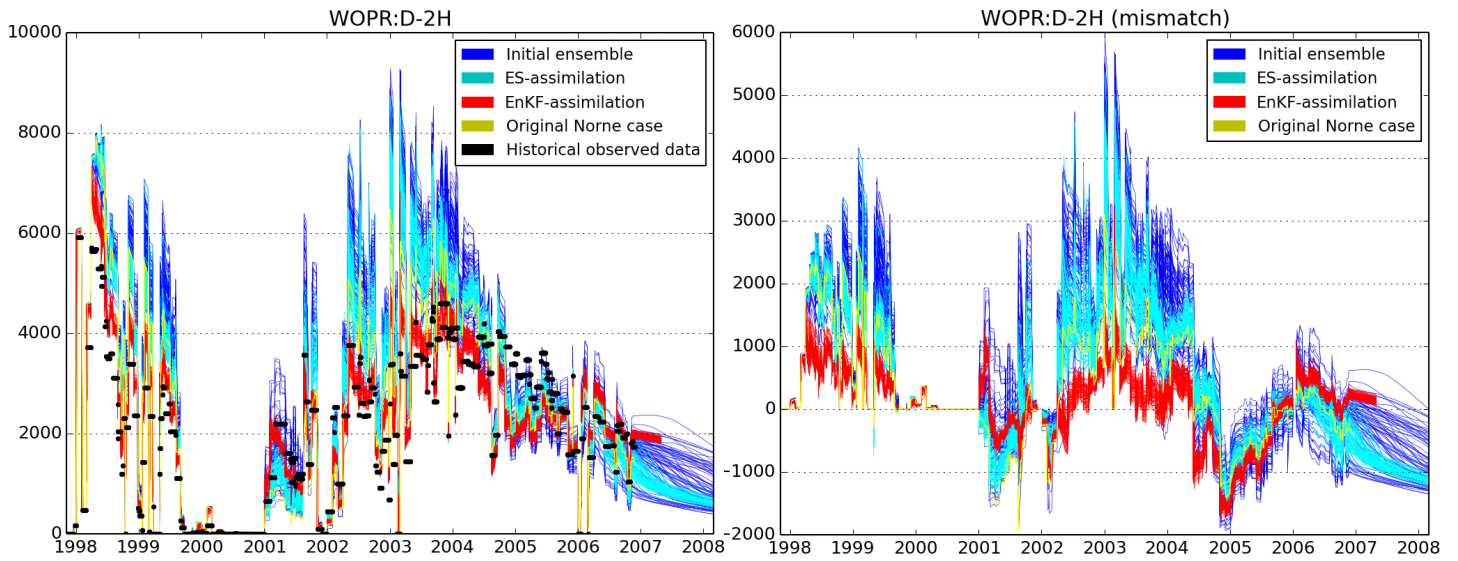
FIGURE 5.10: Oil production rate for well D-2H with mismatch plot. X-axis = Time. Y-axis = STB/DAY.
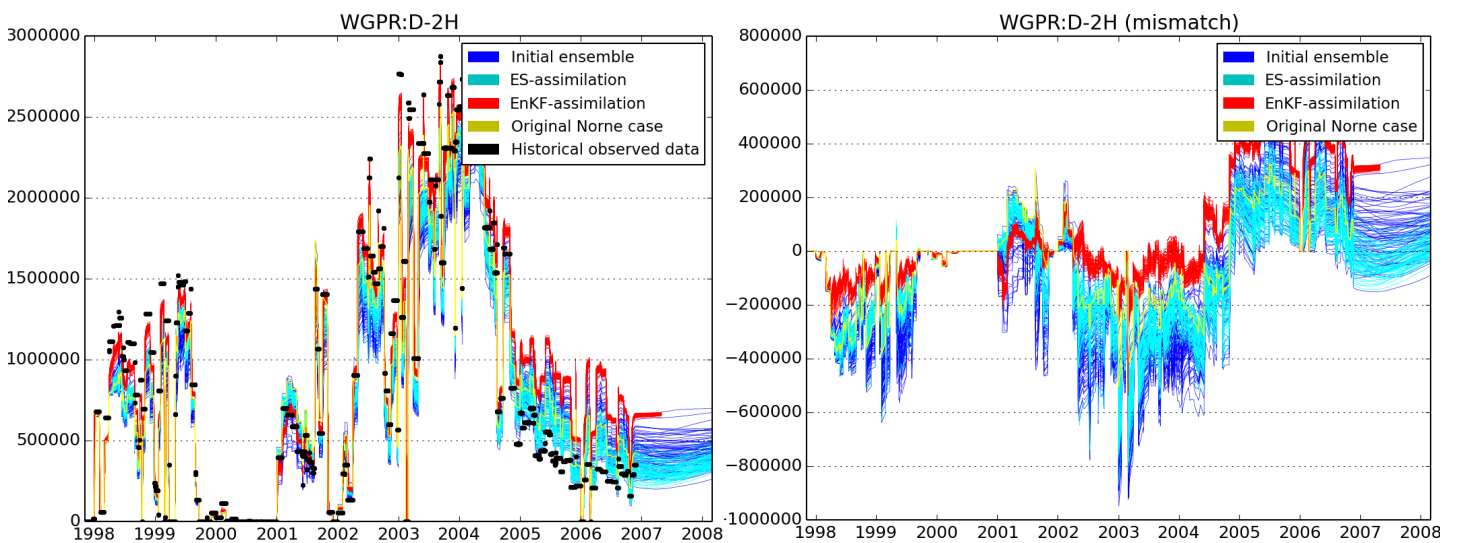


FIGURE 5.11: Gas production rate for well D-2H with mismatch plot. X-axis = Time. Y-axis = MSCF/DAY.
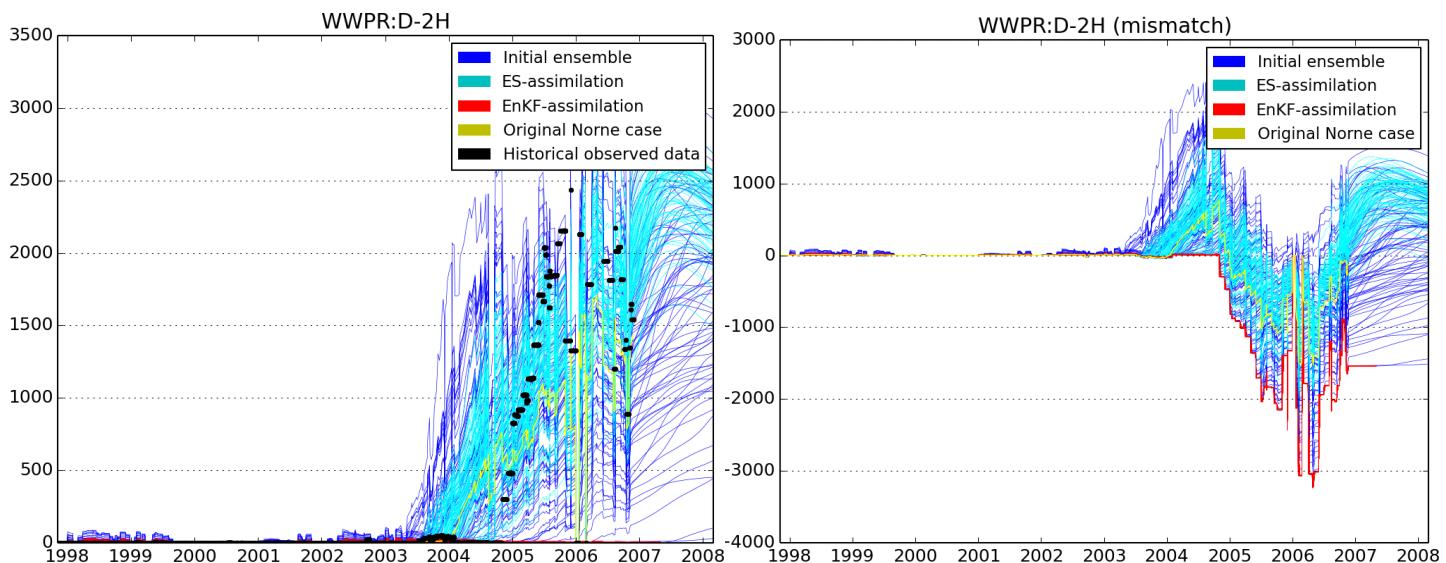
FIGURE 5.12: Water production rate for well D-2H with mismatch plot. X-axis = Time. Y-axis = STB/DAY.
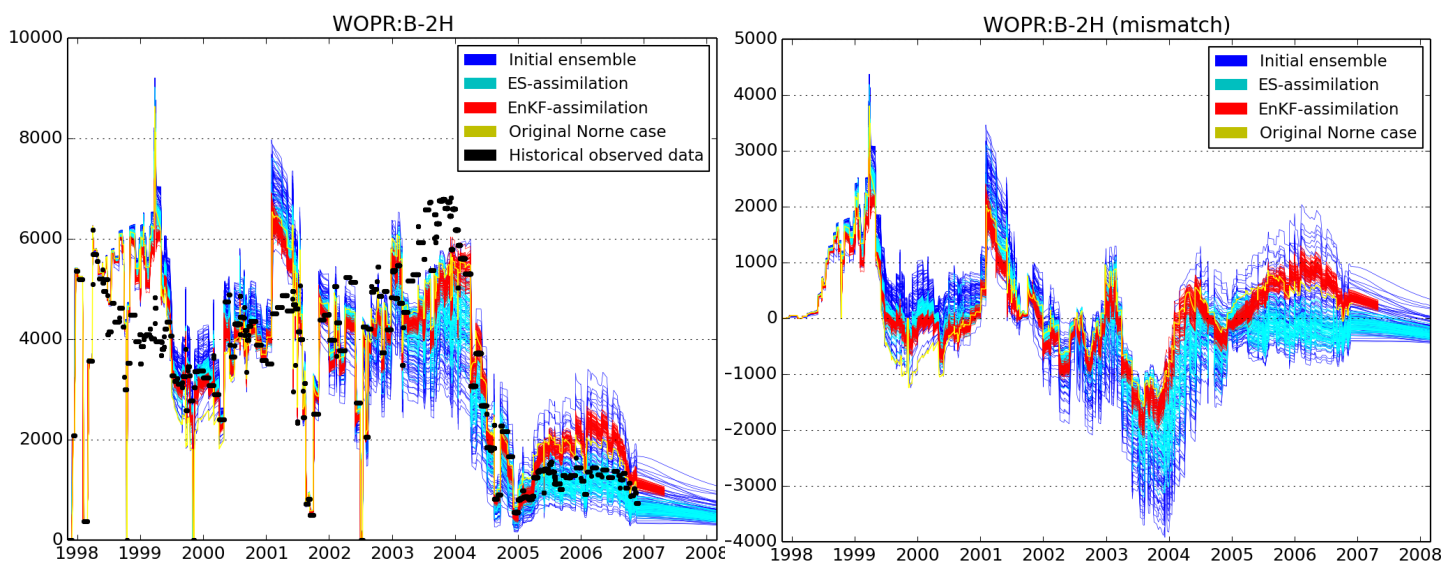


FIGURE 5.13: Oil production rate for well B-2H with mismatch plot. X-axis = Time. Y-axis = STB/DAY.
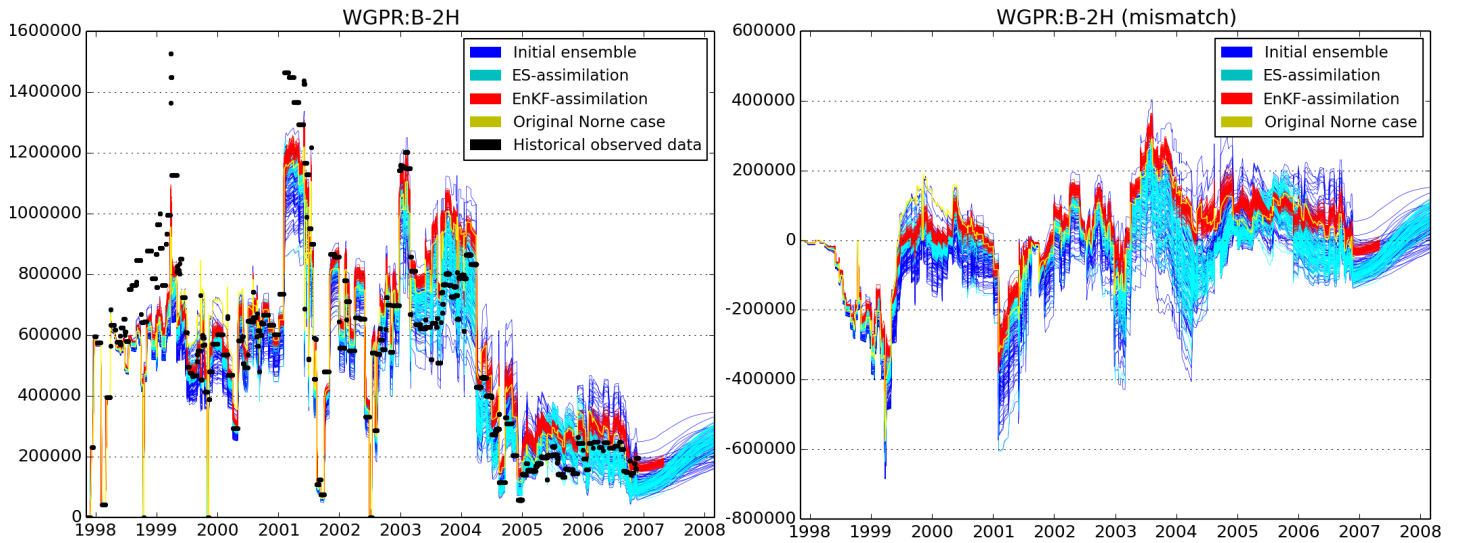
FIGURE 5.14: Gas production rate for well B-2H with mismatch plot. X-axis = Time. Y-axis = MSCF/DAY.
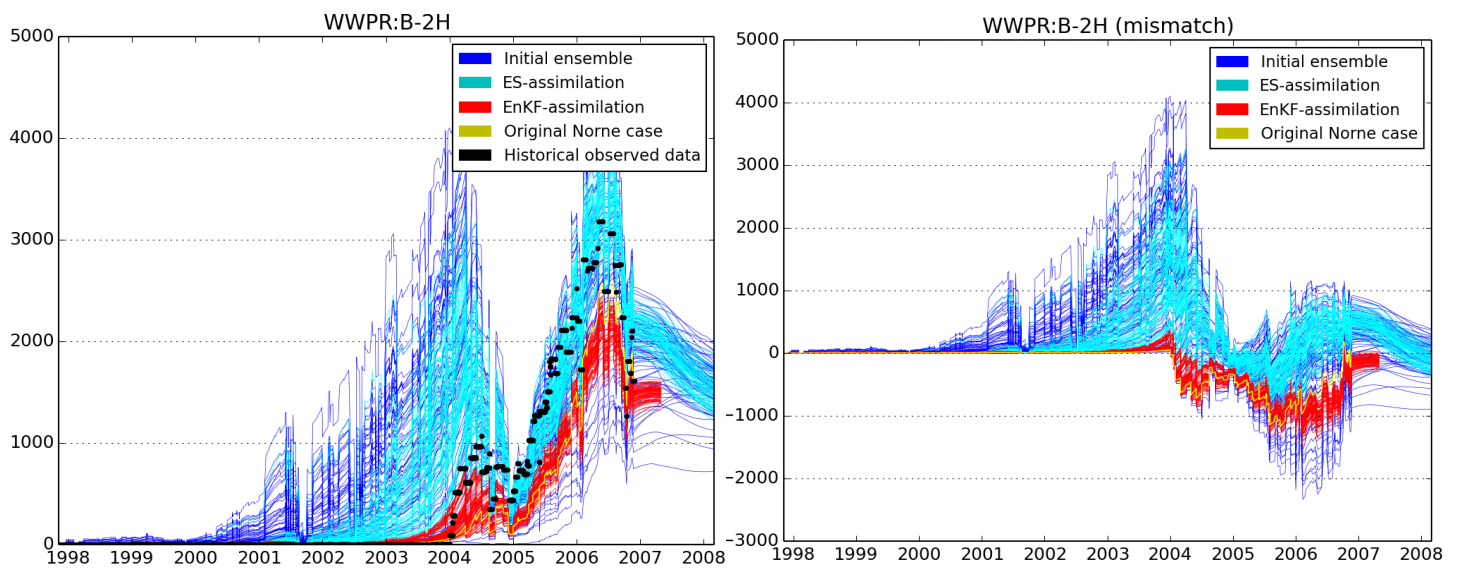


FIGURE 5.15: Water production rate for well B-2H with mismatch plot. X-axis = Time. Y-axis = STB/DAY.
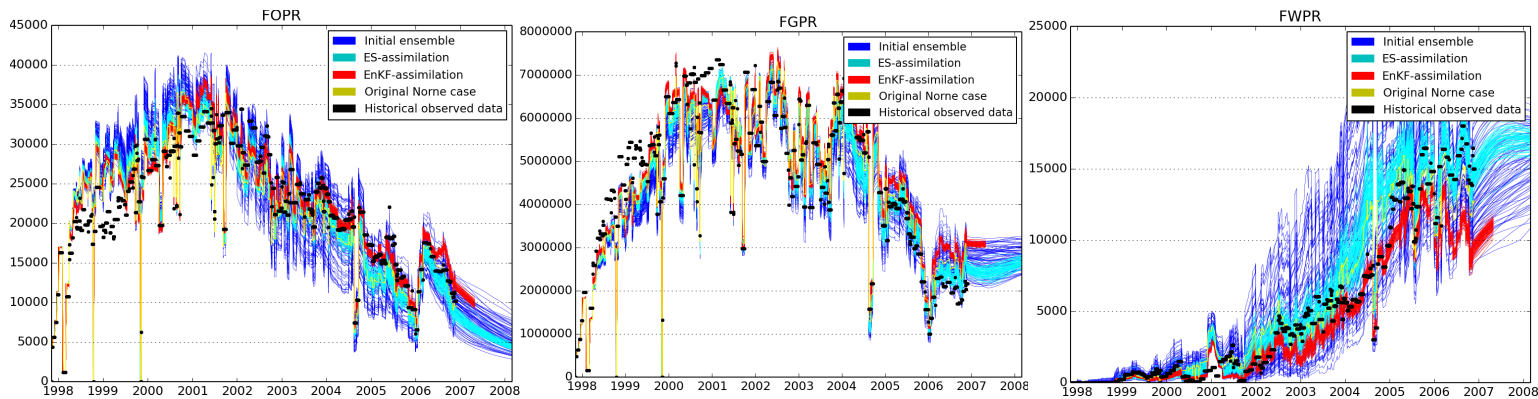
FIGURE 5.16: Plots for the FIELD rates, based on Full-field model. X-axis =
Time. Y-axis = STB/DAY, MSCF/DAY, STB/DAY, respectively.

In the included EnKF_analyzed_models.zip the EnKF-analyzed ensemble member #40 (ECLIPSE.DATA-file with importable files) may be studied in further depth.

## 5.3   E-segment vs. Full-field

The Norne E-segment model consists, as earlier stated, of a fine-gridded E-segment and coarsened, large grid blocks for the rest of the field. Nevertheless, the coarsened E-segment model is, as the Norne Full-field model, meant to resemble the actual Norne reservoir model, and should produce reasonable matched estimates compared to the Full-field model. Comparison of these two is therefore of high interest.
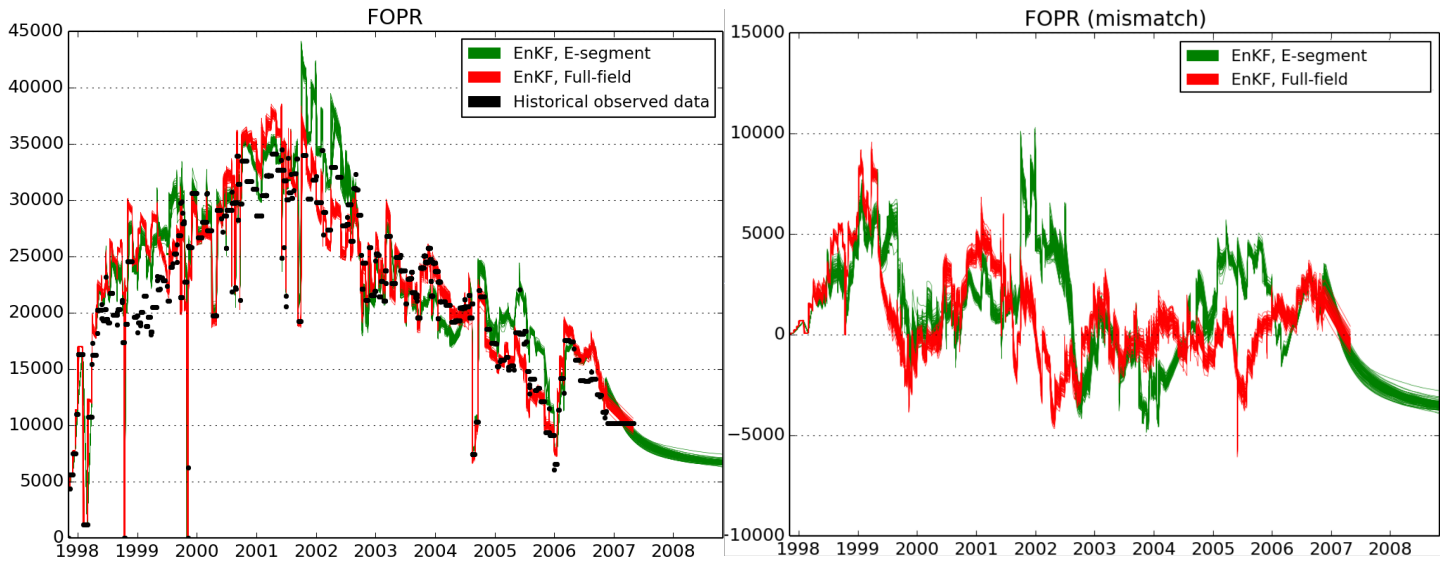
FIGURE 5.17: Oil production FIELD rates with mismatch plot, E-segment EnKF-assimilation vs. Full-field EnKF-assimilation. X-axis = Time. Y-axis = STB/DAY.
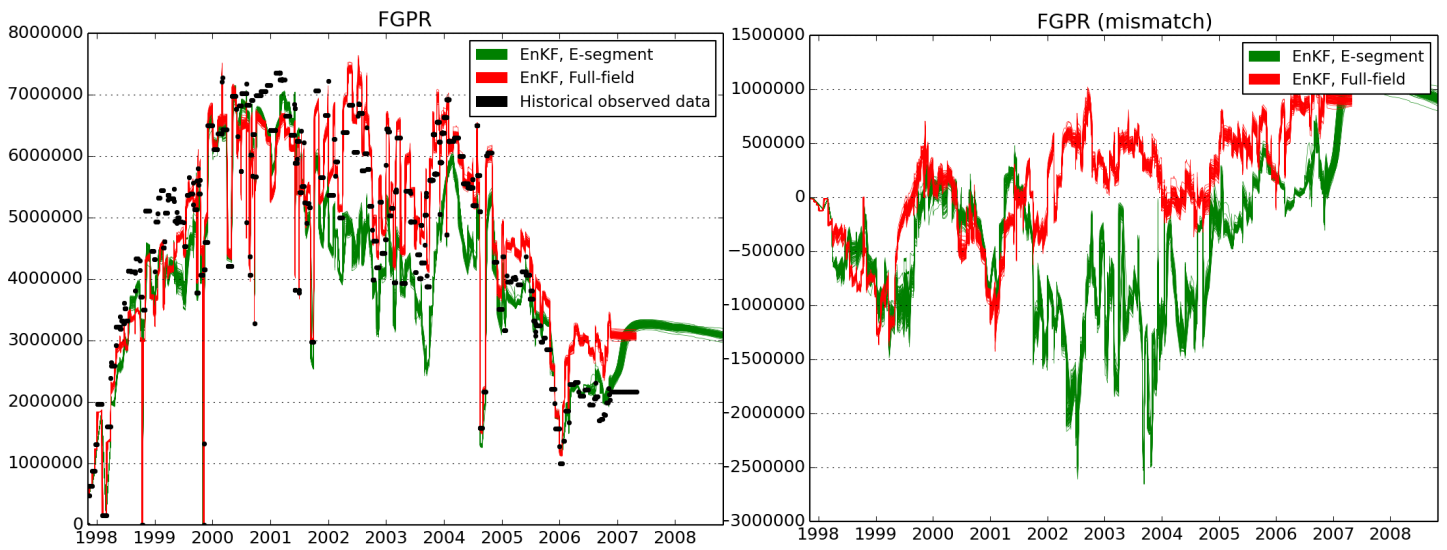


FIGURE 5.18: Gas production FIELD rates with mismatch plot, E-segment EnKF-assimilation vs. Full-field EnKF-assimilation. X-axis = Time. Y-axis = MSCF/DAY.
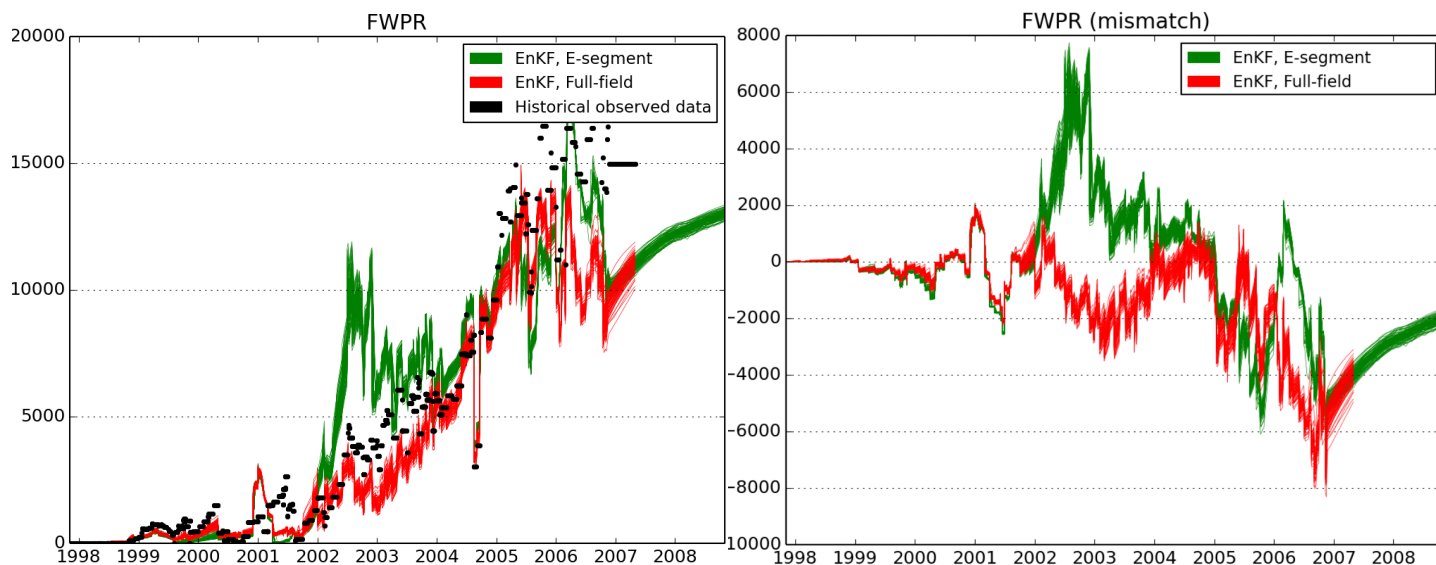
FIGURE 5.19: Water production FIELD rates with mismatch plot, E-segment EnKF-assimilation vs. Full-field EnKF-assimilation. X-axis = Time. Y-axis = STB/DAY.

# Chapter 6

# Discussion & Conclusion

## 6.1 Discussions

The results from the ES and EnKF history matching of the Norne E-segment model and the Norne Full-field model are shown in Figures 5.1-5.16. Production rate plots for oil, gas and water per well and FIELD are created. Mismatch plots are plots where the curves' distance from zero denotes mismatch. The wells B-2H, D-2H and E-1H are the longest producing wells in their respective segment, hence the results from these three wells can be assumed representative for the rest of the wells in the field. The location of these wells can be seen in Figure 2.13. The blue curves represent the 120/80 (E-segment/Full-field) realizations of the initial ensemble, the cyan curves are the 120/80 ES-analyzed ensemble members, while the red curves represent the 120/80 EnKF-analyzed ensemble members. The historical observations are represented by the black dots and the Norne reference case from 2013 is represented by the yellow line.

The initial uncertainty in the parametrization of model parameters leads to a significant uncertainty in the simulated production. This is illustrated by the initial ensemble spread in the oil, gas and water production rates. Ideally the spread should cover the historical observations at all points in time, which is more or less achieved for all production rates. If one chooses to look at the ES and EnKF

update as a linear regression problem, the importance of initial ensemble, or prior, coverage is evident; with coverage the update problem becomes linear interpolation, without coverage it becomes linear extrapolation. Without prior coverage it is therefore much harder for the ES- and EnKF-algorithm to perform a successful update analysis of the ensemble and better condition the model. However, if the historical observed data and the unknown conditioning parameters are highly correlated, extrapolation may be as successful as interpolation. This exception can be seen in Figure 5.3.

The difference in correctness (and performance) of the Ensemble Smoother versus the Ensemble Kalman Filter is clearly seen in the results. The ES does one pass of the ensemble and incorporates all observed historical values into this pass, hence a significant amount of time and computational power is saved compared to the EnKF which restarts the simulation for every $25^{th}$ (E-Segment) and $50^{th}$ (Full-field) report step. However, the large amount of time and computational power required by the EnKF is made up for in much better results in terms of higher correlation with the historical observed data. This is unquestionable for both the E-segment and Full-field results.

Looking at the actual history matching, the first impression is that the model matching can be ordered from water rates, best match, to gas rates, worst match. The oil rates are situated mostly somewhere in between these. This is highly evident for the E-segment, but not so much for the Full-field model. The results for the Full-field model suggest that the highest uncertainty is found in the water production rates (see Figure 5.9, 5.12 and 5.15), including a most probably biased EnKF-analyzed ensemble result in Figure 5.12. The exact reason for the biased result is hard to explain without a thorough numerical analysis of the data assimilation for the D-segment, but a probable cause could be a filter divergence. The ensemble size used for the Full-field model is unfortunately in the lower threshold, and an insufficient ensemble size can typically cause an underestimation of the error variances. This may ultimately lead to a filter divergence when the filter trusts its own forecast and ignores the information provided by the observations. This is caused by ensemble members aligning with the most unstable parameter

directions and is exacerbated by large observational noise (Gottwald and Majda, 2013). A more technical analysis of the biased result can be provided with the help of an equation from (Sætrom and Omre, 2013):

Let $\mathbf{x}^{(i)}$ and $\mathbf{x}^{(j)}$ represent two realizations in my posteriori ensemble. The covariance between these two realizations (the underlying linear dependency between the two) are, under Gaussian assumptions, given as

$$\text{Cov}(\mathbf{x}^{(i)}, \mathbf{x}^{(j)}) = \frac{\text{Tr}[\text{Var}(\mathbf{d})^{-1}(\mathbf{d^o} - \text{E}[\mathbf{d}])(\mathbf{d^o} - \text{E}[\mathbf{d}])^T]}{n_e - n_d - 2}\text{Var}(\mathbf{x}|\mathbf{d}) \tag{6.1}$$

where Tr denotes the trace value, Var denotes the variance, the $\mathbf{d}$ denotes the true historical observations, the $\mathbf{d^o}$ denotes the measured historical observations ($\mathbf{d^o} = \mathbf{d} + \epsilon_d$), E[$\mathbf{d}$] denotes the expected historical observations, the $\mathbf{x}$ denotes the ensemble members, the $n_e$ denotes the ensemble size and the $n_d$ denotes the number of historical observations.

Looking at equation 6.1, the covariance will increase:

1. If the true historical observations are co-linear, i.e. many Var($\mathbf{d}$) are nearly singular which leads to high values in the Var($\mathbf{d}$)$^{-1}$

2. With a large mismatch between measured historical observations, $\mathbf{d^o}$, and the expected historical observations, E[$\mathbf{d}$]

3. With a large number of historical observations, $n_d$

4. With a small ensemble size, $n_e$, relative to the $n_d$

5. With a large Var($\mathbf{x}|\mathbf{d}$), which implies high-dimensional $\mathbf{x}$ with true observations $\mathbf{d}$, that carry little information about $\mathbf{x}$

Since the expectation value of the empirical covariance matrix is given as E[$\sigma_{\hat{x}}$] = Cov($\mathbf{x}^{(i)}$) − Cov($\mathbf{x}^{(i)}, \mathbf{x}^{(j)}$), an ensemble collapse is inevitable if one of the factors described above increases too much. In the case of the biased result in Figure 5.12, factor number two comes into play. The prior ensemble is very "skewed" compared

to the historical observed data, hence more "dependency" (bigger $\text{Cov}(\mathbf{x}^{(i)}, \mathbf{x}^{(j)})$) is introduced after each and every EnKF-update. In the end, this results in an ensemble collapse and an EnKF-analyzed ensemble "off the chart".

Out of all the wells plotted in the Full-field model, E-1H has the overall best match, suggesting that the E-segment is the best matched part of the reservoir. This is not an illogical result, as the E-segment is the part of the Norne Field given the most attention with regards to data gathered and model detail. Figures 5.7 and 5.9 however, showing the oil and water production rate for well E-1H for the Full-field model, are the only plots where the ES-analyzed ensemble may be interpreted with a slightly better match than the EnKF. Although, looking at the spread, or the uncertainty, of the two analyzed ensembles, the EnKF is a lot more certain than the ES. The mean value of the ES-analyzed ensemble could be close or even worse than the mean value of the EnKF, even though the results seems to show otherwise. Nonetheless, these results are more coincidental than a tendency, as it is not seen in the rest of the results.

A fairly large error for both the ES- and EnKF-analysed realizations can be seen around November 2000 to February 2001. This error is most significant for well E-1H, but can be detected in nearly all the plots for both models. It is clearly seen in Figures 5.1, 5.2, 5.7 and 5.8. The original Norne case does not seem to have this error, and the question is what happens with the ensemble initialization and analysis in this period to cause this inaccuracy. The $22^{\text{nd}}$ of September 2000 the injection well F-3H starts injecting water for the first time. This well is located in close proximity to the well E-1H (see Figure 2.13), hence an undesirable incorporation of the historical observed data from well F-3H may be a reason. Another reason may be the closing and plugging of well E-3H the $1^{\text{st}}$ of April 2000, located right in the middle of the gas displacement front. An abrupt change in data at this point may have lead to numerical difficulties for the ES- and EnKF-algorithm. Figure 5.6 shows the gas saturation in layer five in the E-segment model the $1^{\text{st}}$ of May 2000. Large differences can be seen for swept area, and more specifically, the transition area of the gas sweeping in the EnKF-analyzed model is much less

than in the original model. This implies a higher mobility ratio for the gas in the EnKF-analyzed model, at least for layer five.

Comparing the FIELD rates of the E-segment versus the Full-field model the results are generally as expected. As of Figure 5.17, 5.18 and 5.19 none of the models are able to get a perfect fit. In addition, the uncertainty of the EnKF-analyzed ensemble is not insignificant for either case. A slight uncertainty in the EnKF-analyzed ensemble means that the assimilation could have been better and that the algorithms are still sampling Gaussian distributed parameters within a smaller bounded interval than for the initial ensemble. There is no doubt that with only 80 ensemble members updated every $50^{\text{th}}$ report step for the Full-field EnKF-assimilation the match could have been better for the Full-field model. Nonetheless, an overall slightly better match are acquired for the FIELD rates with the Full-field EnKF-assimilation, which is according to theory and expectations.

As seen in Figure 5.5 the EnKF algorithm has done rather large modifications to the static PERMZ parameter of the E-segment. Similar changes are seen in the other static parameters, also the Full-field model, hence proving that the EnKF has conditioned on the parameters chosen. The fact that the ES- and EnKF-algorithms get to have complete control of the large amount of parameter chosen to condition on, is positive with regards to correctness and correlation of parameters in the model. Although, it can also be a negative thing. When performing manual HM a reservoir engineer needs to acquire in depth knowledge of every aspect of the model - down to cell level. He or she can then begin to history match by altering each and every parameter in question. This is time-consuming and initially seldom successful. However, after some initial work the increasing knowledge of the reservoir should provide an experienced reservoir engineer the necessary feedback to be able to pin-point certain critical parameters. With AHM it is easy to lose control and blindly trust the mathematics behind the algorithms. If the results end up being illogical it is not easy to troubleshoot and find errors in an algorithm not fully understood or in a reservoir model of only basic knowledge.

The EnKF is an efficient AHM algorithm, but it has some drawbacks. The ensemble and ensemble size in the EnKF needs to be selected carefully such that uncertainty is sufficiently captured. To avoid high computational costs, a relatively small ensemble size may be necessary (as for the Full-field model) which is small compared to the number of unknown parameters (in this thesis; in the number of model grid blocks). The assimilation of large amounts of data with relatively small ensembles can lead to spurious correlations and/or filter divergence, which may lead to unphysical updates of model parameters (see especially Figure 5.12). However, in spite of some illogical results most of the EnKF-analysed production rates show a slightly better match than the reference case, as well as a lot less uncertainty than the initial ensemble. This should lead to the conclusion that both the ES-assimilation and especially the EnKF-assimilation are in fact performing well.

## 6.2 Conclusions & Recommendations

In this thesis two stochastic algorithms, the Ensemble Smoother (ES) and the Ensemble Kalman filter (EnKS), has been utilized as automatic history matching methods through the Statoil developed program the Ensemble based Reservoir Tool. Real historical production and pressure data, provided by Statoil through IO Center NTNU, has been used to condition on a parametrized ECLIPSE reservoir model of the Norne Field. Parameters conditioned on includes the field parameters porosity, i-permeability, net-to-gross, and z-direction transmissibility multiplier, as well as fault multipliers, region transmissibility multipliers, minimum pore volumes and relative permeability endscaling options. The stand-alone E-segment model and the Full-field model were both studied.

With an ensemble size of 120 realizations for the E-Segment model and 80 realizations for the Full-field model both algorithms performed well. In most of the results an initial high uncertainty in the prior provided the necessary coverage of the historical observed data. Overall the EnKF performed better than the ES,

which is natural comparing time and computational power required. Some spurious correlations and one particular ensemble collapse were experienced. The EnKF-analysed ensemble production rates provides a lot less uncertainty than the initial ensemble, and for most plots a slightly better match than the reference case. The EnKF-algorithm is shown to be vulnerable of small ensemble sizes versus large amounts of conditioning parameters, as well as highly correlated historical observations.

In the last years 4D seismic data has become a valuable tool for reservoir engineers. The higher resolution and more frequently shot seismic gathers provide them with another view of the fluid movement inside the reservoir. Where pressure and production data give detailed, but localized, information, 4D seismic data provides coarse, but global information. The research on 4D seismic data has naturally become a large part of the literature, and several articles have been published dealing with the subject of EnKF-assimilation and 4D seismic data, e.g. (Fahimuddin et al., 2010) and (Han et al., 2013). The general consensus of these articles is that the quantitative 4D seismic data complements the qualitative production- and pressure data very well, resulting in significantly better history matching of reservoir models. EnKF is especially suited for history matching with 4D seismic data due to the efficient incorporation of the large amount of assimilation data in such cases. As a proposal for further research on the Norne Field, automatic history matching using EnKF and incorporating both the available 4D seismic data and the pressure- and production data would be the next natural step.

# Appendix A

# The ERT specific files

### A.0.1 Configuration file

```
-- ============================================================================
--
--
-- N O R N E  F U L L - F I E L D  M O D E L   2 0 1 4  -  ERT CONFIG FILE
--
--
-- ============================================================================
--
-- Ensemble Reservoir Tool (ERT) configuration for the Norne full-field model
-- Daniel A. Solheim - 2014 - danieso@stud.ntnu.no

-- Documentation:
-- See the README file.  Keywords used in this file are documented at:
--
--     http://sdp.statoil.no/wiki/index.php/res:enkf
--     http://ert.nr.no
-- ============================================================================

-- Using the DEFINE keyword to avoid overwriting simulations
DEFINE <USER>     $USER
DEFINE <SCRATCH> /work/danieso/Scratch
DEFINE <CASE>     TEST2_FULLF_FULLPARA
DEFINE <PWD>      $PWD
```

```
-- Do some magic to set ECLBASE and RUNPATH

ECLBASE           FIRST_GEN_NORNE-<CASE>-%d

RUNPATH           <SCRATCH>/<CASE>/realization-%d

ENSPATH           <SCRATCH>/Storage/<CASE>


-- Make sure ECLIPSE gets the right path to the include files like the relperm
etc.
DEFINE <ECLPATH> /work/danieso/norne/Norne_ATW2013/


-- Name of .SCH file we are using in the current setup

DEFINE <SCHEDULE_FILE_NAME> BC0407_HIST01122006_NEW2.SCH


-- Use the record storage system

DBASE_TYPE BLOCK_FS


-- Set the number of realizations to run

NUM_REALIZATIONS 80


--Use the TORQUE queue system for running simulation on Kongull

QUEUE_SYSTEM TORQUE

QUEUE_OPTION TORQUE QSUB_CMD /home/danieso/ert/Scripts/myqsub.sh

QUEUE_OPTION TORQUE NUM_NODES 1

QUEUE_OPTION TORQUE NUM_CPUS_PER_NODE 1

QUEUE_OPTION TORQUE MAX_RUNNING 40

QUEUE_OPTION TORQUE KEEP_QSUB_OUTPUT 1

QUEUE_OPTION TORQUE ASSUME_MISSING_COMPLETE TRUE


-- Set image type for the plots generated

IMAGE_TYPE png


-- Load the .EGRID file

GRID              /work/danieso/norne/Norne_ATW_2013/NORNE_ATW2013.GRID


-- Location of the ECLIPSE .DATA

DATA_FILE /work/danieso/norne/Norne_ATW_2013/NORNE_ATW2013_CORRECT_MOD.DATA


--Alltid starte EnFK fra tidssteg 0 etter oppdatering

ENKF_RERUN TRUE

ENKF_MERGE_OBSERVATIONS TRUE


--Only do updates on report steps specified in schedule file

ENKF_SCHED_FILE /home/danieso/etc/EnKF_update_setup.txt
```

```
ENKF_LOCAL_CV TRUE

ENKF_CV_FOLDS 7

KEEP_RUNPATH 0-79


-- Parametrization:

-- Uncertainty in MULTFLT

GEN_KW MULTFLT templates/MULTFLT.tmpl MULTFLT.INC  parameters/MULTFLT.txt


--UNcertainty for MULTZ Equals stuff

GEN_KW MULTZ_KW templates/MULTZ.tmpl MULTZ_KW.INC  parameters/MULTZ2.txt


-- Uncertainty in MULTREGT

GEN_KW MULTREGT templates/MULTREGT.tmpl MULTREGT.INC  parameters/MULTREGT.txt


-- Testing sensitivity of MINPV (UNIFORM 400-600)

GEN_KW MINPV templates/minpv.temp MINPV.INC parameters/minpv_params.txt


--Testing sensitiviy of PERMZ

GEN_KW PERMZ templates/multiply_permz.temp PERMZ.INC  parameters/PERMZ4.txt


--Testing sensitivty of RELPERM through ENDPOINTS

GEN_KW ENDPOINTS  templates/ENDPOINTS.tmpl  ENDPOINTS.INC

parameters/ENDPOINTS.txt


--Adding a porosity field (unbounded)

FIELD PORO PARAMETER   PORO.INC

INIT_FILES:/work/danieso/norne/Norne_ATW_2013/INCLUDE/PETRO/PORO_0704.prop


--Adding a permeability field

FIELD PERMX PARAMETER   PERM.INC

INIT_FILES:/work/danieso/norne/Norne_ATW_2013/INCLUDE/PETRO/PERM_0704.prop


--Adding a net-to-gross field

FIELD NTG PARAMETER   NTG.INC

INIT_FILES:/work/danieso/norne/Norne_ATW_2013/INCLUDE/PETRO/NTG_0704.prop


--Adding a MULTZ field

FIELD MULTZ PARAMETER   MULTZ.INC

INIT_FILES:/work/danieso/norne/Norne_ATW_2013/INCLUDE/PETRO/MULTZ_HM_1.INC


-- Load historic data from a reference case.  This is needed to get the
```

historic accumulated production, as ERT is not able to compute it from
the schedule file.
HISTORY_SOURCE    REFCASE_HISTORY

REFCASE           /work/danieso/norne/Norne_ATW_2013/NORNE_ATW2013.DATA


--Need observations to be able to plot and assimilate the historic data.
OBS_CONFIG        /home/danieso/etc/observations2.txt


-- Collect non-observed summary variables for monitoring
SUMMARY FOIP
SUMMARY TCPU
SUMMARY FPR

SUMMARY FOPT
SUMMARY FGPT
SUMMARY FWPT

SUMMARY FOPR
SUMMARY FGPR
SUMMARY FWPR

PLOT_REFCASE   FALSE
REFCASE_LIST   /work/danieso/norne/Norne_ATW_2013/NORNE_ATW2013.DATA


IMAGE_VIEWER /d/proj/bg/enkf/bin/noplot.sh


--Plot error bar
PLOT_ERRORBAR_MAX 100


--Location of the SCHEDULE file
SCHEDULE_FILE
/work/danieso/norne/Norne_ATW_2013/INCLUDE/BC0407_HIST01122006_NEW2.SCH


-- Install the custom jobs
--INSTALL_JOB MULTIPLY_PERMZ_DOE jobs/MULTIPLY_PERMZ_DOE


-- Definition of the forward models.
-- 1.0 Replace the ECLPATH data in the generated ECLIPSE DATA file (not necessary)
-- 4.0 If necessary, copy runpath folder
-- 7.0 Perform a so-called Design Of Engineering matrix sensitivity run
 on XXXX (not in final AHM)
-- 10 Run Eclipse in parallel/single mode

```
-- 1.0
--FORWARD_MODEL REPLACE(<FROM>=__ECLPATH__ , <TO>=<ECLPATH> , <FILE>=<ECLBASE>.DATA)


-- 4.0
--FORWARD_MODEL COPY_FOLDER(<copyfrom> = <CONFIG_PATH>
/../rms/rmsIMPORT/ipl_lib, <copyto> = <RUNPATH>/rms/rmsIMPORT/)


-- 7.0
--Do DOE sensitivity on the PERMZ multiplyer
--FORWARD_MODEL MULTIPLY_PERMZ_DOE(<TEMPLATE> =
/home/danieso/ert/templates/multiply_permz.temp,<PARAMETERS> =
/home/danieso/ert/parameters/multiply_permz.txt, <IENS> = <IENS>)


-- 10
FORWARD_MODEL ECLIPSE100_2011.1(<ECLBASE>=<ECLBASE>,<NUM_CPU>=1)
```

## A.0.2 MULTFLT

TABLE A.1: The MULTFLT template file.

```
MULTFLT
 'E_01'         <E_01>         /
 'E_01_F3'      <E_01_F3>      /
 'DE_1'         <DE_1>         /
 'DE_1_LTo'     <DE_1_LTo>     /
 'DE_B3'        <DE_B3>        /
 'DE_2'         <DE_2>         /
 'DE_0'         <DE_0>         /
 'BC'           <BC>           /
 'CD'           <CD>           /
 'CD_To'        <CD_To>        /
 'CD_B3'        <CD_B3>        /
 'CD_0'         <CD_0>         /
 'CD_1'         <CD_1>         /
 'C_01'         <C_01>         /
 'C_01_Ti'      <C_01_Ti>      /
 'C_08'         <C_08>         /
 'C_08_Ile'     <C_08_Ile>     /
 'C_08_S'       <C_08_S>       /
 'C_08_Ti'      <C_08_Ti>      /
 'C_08_S_Ti'    <C_08_S_Ti>    /
 'C_09'         <C_09>         /
 'C_02'         <C_02>         /
 'C_04'         <C_04>         /
 'C_05'         <C_05>         /
 'C_06'         <C_06>         /
```

```
'C_10'        <C_10>         /
'C_12'        <C_12>         /
'C_20'        <C_20>         /
'C_20_LTo'    <C_20_LTo>     /
'C_21'        <C_21>         /
'C_21_Ti'     <C_21_Ti>      /
'C_22'        <C_22>         /
'C_23'        <C_23>         /
'C_24'        <C_24>         /
'C_25'        <C_25>         /
'C_26'        <C_26>         /
'C_26N'       <C_26N>        /
'C_27'        <C_27>         /
'C_28'        <C_28>         /
'C_29'        <C_29>         /
'DI'          <DI>           /
'DI_S'        <DI_S>         /
'D_05'        <D_05>         /
'EF'          <EF>           /
'GH'          <GH>           /
'G_01'        <G_01>         /
'G_02'        <G_02>         /
'G_03'        <G_03>         /
'G_05'        <G_05>         /
'G_07'        <G_07>         /
'G_08'        <G_08>         /
'G_09'        <G_09>         /
'G_13'        <G_13>         /
'H_03'        <H_03>         /
'IH'          <IH>           /
'm_east'      <m_east>       /
'm_east_2'    <m_east_2>     /
'm_north'     <m_north>      /
'm_northe'    <m_northe>     /
'm_west'      <m_west>       /
/
```

## A.0.3  MULTREGT

TABLE A.2: The MULTREGT template file.

```
MULTREGT
    2      1    <MULTREGT0>      /
    3      1    <MULTREGT1>      /
    3      2    <MULTREGT2>      /
    4      1    <MULTREGT3>      /
    4      2    <MULTREGT4>      /
    4      3    <MULTREGT5>      /
    5      1    0.0              /
```

| | | | |
|---|---|---|---|
| 5 | 2 | 0.0 | / |
| 5 | 3 | 0.0 | / |
| 5 | 4 | 0.0 | / |
| 6 | 1 | 0.0 | / |
| 6 | 2 | 0.0 | / |
| 6 | 3 | 0.0 | / |
| 6 | 4 | 0.0 | / |
| 6 | 5 | <MULTREGT14> | / |
| 7 | 1 | 0.0 | / |
| 7 | 2 | 0.0 | / |
| 7 | 3 | 0.0 | / |
| 7 | 4 | 0.0 | / |
| 7 | 5 | <MULTREGT19> | / |
| 7 | 6 | <MULTREGT20> | / |
| 8 | 1 | 0.0 | / |
| 8 | 2 | 0.0 | / |
| 8 | 3 | 0.0 | / |
| 8 | 4 | 0.0 | / |
| 8 | 5 | <MULTREGT25> | / |
| 8 | 6 | <MULTREGT26> | / |
| 8 | 7 | <MULTREGT27> | / |
| 9 | 1 | 0.0 | / |
| 9 | 2 | 0.0 | / |
| 9 | 3 | 0.0 | / |
| 9 | 4 | 0.0 | / |
| 9 | 5 | <MULTREGT32> | / |
| 9 | 6 | <MULTREGT33> | / |
| 9 | 7 | <MULTREGT34> | / |
| 9 | 8 | <MULTREGT35> | / |
| 10 | 1 | 0.0 | / |
| 10 | 2 | 0.0 | / |
| 10 | 3 | 0.0 | / |
| 10 | 4 | 0.0 | / |
| 10 | 5 | <MULTREGT40> | / |
| 10 | 6 | <MULTREGT41> | / |
| 10 | 7 | <MULTREGT42> | / |
| 10 | 8 | <MULTREGT43> | / |
| 10 | 9 | <MULTREGT44> | / |
| 11 | 1 | 0.0 | / |
| 11 | 2 | 0.0 | / |
| 11 | 3 | 0.0 | / |
| 11 | 4 | 0.0 | / |
| 11 | 5 | <MULTREGT49> | / |
| 11 | 6 | <MULTREGT50> | / |
| 11 | 7 | <MULTREGT51> | / |
| 11 | 8 | <MULTREGT52> | / |
| 11 | 9 | <MULTREGT53> | / |
| 11 | 10 | <MULTREGT54> | / |
| 12 | 1 | 0.0 | / |
| 12 | 2 | 0.0 | / |

| | | | |
|----|----|------------------|---|
| 12 | 3  | 0.0              | / |
| 12 | 4  | 0.0              | / |
| 12 | 5  | <MULTREGT59>     | / |
| 12 | 6  | <MULTREGT60>     | / |
| 12 | 7  | <MULTREGT61>     | / |
| 12 | 8  | <MULTREGT62>     | / |
| 12 | 9  | <MULTREGT63>     | / |
| 12 | 10 | <MULTREGT64>     | / |
| 12 | 11 | <MULTREGT65>     | / |
| 13 | 1  | 0.0              | / |
| 13 | 2  | 0.0              | / |
| 13 | 3  | 0.0              | / |
| 13 | 4  | 0.0              | / |
| 13 | 5  | <MULTREGT70>     | / |
| 13 | 6  | <MULTREGT71>     | / |
| 13 | 7  | <MULTREGT72>     | / |
| 13 | 8  | <MULTREGT73>     | / |
| 13 | 9  | <MULTREGT74>     | / |
| 13 | 10 | <MULTREGT75>     | / |
| 13 | 11 | <MULTREGT76>     | / |
| 13 | 12 | <MULTREGT77>     | / |
| 14 | 1  | 0.0              | / |
| 14 | 2  | 0.0              | / |
| 14 | 3  | 0.0              | / |
| 14 | 4  | 0.0              | / |
| 14 | 5  | <MULTREGT82>     | / |
| 14 | 6  | <MULTREGT83>     | / |
| 14 | 7  | <MULTREGT84>     | / |
| 14 | 8  | <MULTREGT85>     | / |
| 14 | 9  | <MULTREGT86>     | / |
| 14 | 10 | <MULTREGT87>     | / |
| 14 | 11 | <MULTREGT88>     | / |
| 14 | 12 | <MULTREGT89>     | / |
| 14 | 13 | <MULTREGT90>     | / |
| 15 | 1  | 0.0              | / |
| 15 | 2  | 0.0              | / |
| 15 | 3  | 0.0              | / |
| 15 | 4  | 0.0              | / |
| 15 | 5  | <MULTREGT95>     | / |
| 15 | 6  | <MULTREGT96>     | / |
| 15 | 7  | <MULTREGT97>     | / |
| 15 | 8  | <MULTREGT98>     | / |
| 15 | 9  | <MULTREGT99>     | / |
| 15 | 10 | <MULTREGT100>    | / |
| 15 | 11 | <MULTREGT101>    | / |
| 15 | 12 | <MULTREGT102>    | / |
| 15 | 13 | <MULTREGT103>    | / |
| 15 | 14 | <MULTREGT104>    | / |
| 16 | 1  | 0.0              | / |
| 16 | 2  | 0.0              | / |

| | | | |
|---|---|---|---|
| 16 | 3 | 0.0 | / |
| 16 | 4 | 0.0 | / |
| 16 | 5 | <MULTREGT109> | / |
| 16 | 6 | <MULTREGT110> | / |
| 16 | 7 | <MULTREGT111> | / |
| 16 | 8 | <MULTREGT112> | / |
| 16 | 9 | <MULTREGT113> | / |
| 16 | 10 | <MULTREGT114> | / |
| 16 | 11 | <MULTREGT115> | / |
| 16 | 12 | <MULTREGT116> | / |
| 16 | 13 | <MULTREGT117> | / |
| 16 | 14 | <MULTREGT118> | / |
| 16 | 15 | <MULTREGT119> | / |
| 17 | 1 | 0.0 | / |
| 17 | 2 | 0.0 | / |
| 17 | 3 | 0.0 | / |
| 17 | 4 | 0.0 | / |
| 17 | 5 | 0.0 | / |
| 17 | 6 | 0.0 | / |
| 17 | 7 | 0.0 | / |
| 17 | 8 | 0.0 | / |
| 17 | 9 | <MULTREGT128> | / |
| 17 | 10 | 0.0 | / |
| 17 | 11 | 0.0 | / |
| 17 | 12 | 0.0 | / |
| 17 | 13 | <MULTREGT132> | / |
| 17 | 14 | 0.0 | / |
| 17 | 15 | 0.0 | / |
| 17 | 16 | 0.0 | / |
| 18 | 1 | 0.0 | / |
| 18 | 2 | 0.0 | / |
| 18 | 3 | 0.0 | / |
| 18 | 4 | 0.0 | / |
| 18 | 5 | 0.0 | / |
| 18 | 6 | 0.0 | / |
| 18 | 7 | 0.0 | / |
| 18 | 8 | 0.0 | / |
| 18 | 9 | 0.0 | / |
| 18 | 10 | <MULTREGT145> | / |
| 18 | 11 | 0.0 | / |
| 18 | 12 | 0.0 | / |
| 18 | 13 | 0.0 | / |
| 18 | 14 | <MULTREGT149> | / |
| 18 | 15 | 0.0 | / |
| 18 | 16 | 0.0 | / |
| 18 | 17 | <MULTREGT152> | / |
| 19 | 1 | 0.0 | / |
| 19 | 2 | 0.0 | / |
| 19 | 3 | 0.0 | / |
| 19 | 4 | 0.0 | / |

```
19       5   0.0                    /
19       6   0.0                    /
19       7   0.0                    /
19       8   0.0                    /
19       9   0.0                    /
19      10   0.0                    /
19      11   <MULTREGT163>          /
19      12   0.0                    /
19      13   0.0                    /
19      14   0.0000001              /
19      15   <MULTREGT167>          /
19      16   0.0                    /
19      17   <MULTREGT169>          /
19      18   <MULTREGT170>          /
20       1   0.0                    /
20       2   0.0                    /
20       3   0.0                    /
20       4   0.0                    /
20       5   0.0                    /
20       6   0.0                    /
20       7   0.0                    /
20       8   0.0                    /
20       9   0.0                    /
20      10   0.0                    /
20      11   0.0                    /
20      12   <MULTREGT182>          /
20      13   0.0                    /
20      14   0.0                    /
20      15   0.0                    /
20      16   <MULTREGT186>          /
20      17   <MULTREGT187>          /
20      18   <MULTREGT188>          /
20      19   <MULTREGT189>          /
 /
```

## A.0.4  MULTZ Modifier

```
-- Layer 8
EQUALS
 'MULTZ' <MULTZ1> 6 13 30 50 8 8 /
/

-- MZ layer 10
EQUALS
 'MULTZ' <MULTZ2> 6 14 11 18 10 10 /   C-3H
 'MULTZ' <MULTZ3> 14 29 11 25 10 10 /   C south east
```

```
'MULTZ' <MULTZ4> 14 25 26 30 10 10 /   C-segm mid/B-2H
'MULTZ' <MULTZ5> 6 29 11 37 10 10 /   C-segm middle
'MULTZ' <MULTZ6> 17 17 42 54 10 10 /   C north west
'MULTZ' <MULTZ7> 6 12 38 39 10 10 /   C north west
'MULTZ' <MULTZ8> 8 12 40 40 10 10 /   C north west
'MULTZ' <MULTZ9> 10 12 41 43 10 10 /   C north west
'MULTZ' <MULTZ10> 18 33 38 54 10 10 /   C1, D4 & D3
'MULTZ' <MULTZ11> 6 13 44 52 10 10 /   B-4AH
'MULTZ' <MULTZ12> 13 13 48 59 10 10 /   D-segm mid (B-4BH)
'MULTZ' <MULTZ13> 14 14 49 59 10 10 /   D-segm mid (B-4BH)
'MULTZ' <MULTZ14> 15 16 51 59 10 10 /   D-segm mid (B-4BH)
'MULTZ' <MULTZ15> 17 19 55 99 10 10 /   E1
'MULTZ' <MULTZ16> 14 14 60 62 10 10 /   E1
'MULTZ' <MULTZ17> 15 15 60 65 10 10 /   E1
'MULTZ' <MULTZ18> 16 16 60 69 10 10 /   E1
'MULTZ' <MULTZ19> 6 9 52 60 10 10 /   F-3H/E-2H
'MULTZ' <MULTZ20> 9 9 53 57 10 10 /   F-3H/E-2H
'MULTZ' <MULTZ21> 10 10 54 58 10 10 /   F-3H/E-2H
'MULTZ' <MULTZ22> 11 11 55 58 10 10 /   F-3H/E-2H
/

-- MZ layer 15
EQUALS
 'MULTZ' 0.00003 6 29 11 21 15 15 /   C south
 'MULTZ' 0.00005 6 29 22 39 15 15 /   C middle
 'MULTZ' 0.000001 19 29 39 49 15 15 /   C-1H
 'MULTZ' <MULTZ26> 19 29 38 45 17 17 /   C-1H
 'MULTZ' <MULTZ27> 16 19 48 61 15 15 /   E-1H/D-3H
 'MULTZ' <MULTZ28> 8 18 40 40 15 15 /   C north
 'MULTZ' <MULTZ29> 9 18 41 41 15 15 /
 'MULTZ' <MULTZ30> 10 18 42 43 15 15 /
 'MULTZ' <MULTZ31> 11 18 44 44 15 15 /
 'MULTZ' <MULTZ32> 12 18 45 45 15 15 /
 'MULTZ' <MULTZ33> 13 18 46 47 15 15 /
 'MULTZ' <MULTZ34> 14 15 48 48 15 15 /
 'MULTZ' <MULTZ35> 15 15 49 50 15 15 /

 'MULTZ' <MULTZ36> 12 12 46 56 15 15 /   D-segm
```

```
'MULTZ' <MULTZ37> 13 13 48 59 15 15 /   D-segm

'MULTZ' <MULTZ38> 14 14 49 62 15 15 /   D-segm

'MULTZ' <MULTZ39> 15 15 51 65 15 15 /   D-segm

'MULTZ' <MULTZ40> 16 19 62 69 15 15 /   D-segm

'MULTZ' <MULTZ41> 17 19 70 99 15 15 /   D-segm

'MULTZ' <MULTZ42> 6 7 40 60 15 15 /   D, E west

'MULTZ' <MULTZ43> 8 8 41 60 15 15 /

'MULTZ' <MULTZ44> 9 9 42 52 15 15 /

'MULTZ' <MULTZ45> 10 10 44 49 15 15 /
/

-- D-1H water
EQUALS
'MULTZ' <MULTZ46> 22 24 21 22 11 11 /

'MULTZ' <MULTZ47> 21 25 17 19 15 15 /

'MULTZ' <MULTZ48> 22 24 17 19 17 17 /

'MULTZ' <MULTZ49> 22 24 15 17 18 18 /
/

-- B-1 & B-3 water
EQUALS
'MULTZ' <MULTZ50> 12 13 34 35 15 15 /
/

-- RFT D_-H
EQUALS
'MULTZ' <MULTZ51> 16 19 47 53 18 18 /   D-3H
/
```

## A.0.5   PERMZ Modifier

```
MULTIPLY
   'PERMZ' <PERMZ1>     1 46 1 112  1  1 /  Garn 3
   'PERMZ' <PERMZ2>     1 46 1 112  2  2 /  Garn 2
   'PERMZ' <PERMZ3>     1 46 1 112  3  3 /  Garn 1
   'PERMZ' 0            1 46 1 112  4  4 /  Not (inactive anyway)
   'PERMZ' <PERMZ5>     1 46 1 112  5  5 /  Ile 2.2
   'PERMZ' <PERMZ6>     1 46 1 112  6  6 /  Ile 2.1.3
```

```
   'PERMZ' <PERMZ7>      1 46 1 112  7  7 /  Ile 2.1.2

   'PERMZ' <PERMZ8>      1 46 1 112  8  8 /  Ile 2.1.1

   'PERMZ' <PERMZ9>      1 46 1 112  9  9 /  Ile 1.3

   'PERMZ' <PERMZ10>     1 46 1 112 10 10 /  Ile 1.2

   'PERMZ' <PERMZ11>     1 46 1 112 11 11 /  Ile 1.1

   'PERMZ' <PERMZ12>     1 46 1 112 12 12 /  Tofte 2.2

   'PERMZ' <PERMZ13>     1 46 1 112 13 13 /  Tofte 2.1.3

   'PERMZ' <PERMZ14>     1 46 1 112 14 14 /  Tofte 2.1.2

   'PERMZ' <PERMZ15>     1 46 1 112 15 15 /  Tofte 2.1.1

   'PERMZ' <PERMZ16>     1 46 1 112 16 16 /  Tofte 1.2.2

   'PERMZ' <PERMZ17>     1 46 1 112 17 17 /  Tofte 1.2.1

   'PERMZ' <PERMZ18>     1 46 1 112 18 18 /  Tofte 1.1

   'PERMZ' <PERMZ19>     1 46 1 112 19 19 /  Tilje 4

   'PERMZ' <PERMZ20>     1 46 1 112 20 20 /  Tilje 3

   'PERMZ' <PERMZ21>     1 46 1 112 21 21 /  Tilje 2

   'PERMZ' <PERMZ22>     1 46 1 112 22 22 /  Tilje 1
/
```

## A.0.6   Relative Permeability Endscaling

```
EQUALS
   SWL <endpoint1>    1 46 1 112 1  1   /

   SWL <endpoint2>    1 46 1 112 2  2   /

   SWL <endpoint3>    1 46 1 112 3  3   /

   SWL <endpoint4>    1 46 1 112 4  4   /

   SWL <endpoint5>    1 46 1 112 5  10  / Ile 2.2.2 and Ile 2.2.1,
   Ile 2.1.3, Ile 2.1.2, and Ile 2.1.1, Ile 1.3 and Ile 1.2

   SWL <endpoint6>    1 46 1 112 11 12  / Ile 1.1 and Tofte 2.2

   SWL <endpoint7>    1 46 1 112 13 15  / Tofte 2.1

   SWL <endpoint8>    1 46 1 112 16 16  / Tofte 1.2.2

   SWL <endpoint9>    1 46 1 112 17 22  / Tofte 1.2.1,
   Tofte 1.2.1, Tofte 1.1, Tilje
/
COPY
  SWL SWCR /
  SWL SGU  /
```

```
/
ADD
   SWCR   <endpoint10>  1 46 1 112 1 22  /
/
--SGU = 1 - SWL
MULTIPLY
   SGU  -1        1 46 1 112 1 22  /
/
ADD
   SGU   1.0        1 46 1 112 1 22  /
/
EQUALS
   SGL   0.0        1 46 1 112 1 22  /
   SGCR  <endpoint13>   1 46 1 112 1 22  /
   SOWCR <endpoint14>   1 46 1 112 1 22  /
   SOGCR <endpoint15>   1 46 1 112 1 22  /
   SWU   1.0        1 46 1 112 1 22  /
/
--Hysteresis input
EHYSTR
   0.1  0  0.1  0.3  BOTH /

COPY
   'SWCR'  'ISWCR'    1 46 1 112  5  22 /
   'SGU'   'ISGU'     1 46 1 112  5  22 /
   'SWL'   'ISWL'     1 46 1 112  5  22 /
   'SWU'   'ISWU'     1 46 1 112  5  22 /
   'SGL'   'ISGL'     1 46 1 112  5  22 /
   'SOGCR' 'ISOGCR'   1 46 1 112  5  22 /
   'SOWCR' 'ISOWCR'  1 46 1 112  5  22 /
 /
EQUALS
  ISGCR <endpoint17> 1 46 1 112  1  22 /
/
```

# Bibliography

Norne. Technical report, Norwegian Petroleum Directorate, April 2012. URL
`http://www.npd.no/en/Publications/Facts/Facts-2012/Chapter-10/`
`Norne/`.

Andreas Antoniou and Wu-Sheng Lu. *Practical Optimization: Algorithms and Engineering Applications.* Springer, 2007.

G. Chavent, M. Dupuy, and P. Lemonnier. History Matching by Use of Optimal Theory. *The Society of Petroleum Engineers (SPE4627)*, 1975.

Wen H. Chen and John H. Seinfeld. Estimation of the Location of the Boundary of a Petroleum Reservoir. *The Society of Petroleum Engineers (SPE4814)*, 1975.

Nan Cheng. Update on Norne Full Field Simulation Model for IO Center, NTNU. Microsoft Office Powerpoint Presentation, June 2012.

K.H Coats. *Petroleum Engineering Handbook.* Society of Petroleum Engineers, 1987.

Mohsen Dadashpour. *Reservoir Characterization Using Production Data and Time-Lapse Seismic Data.* PhD thesis, Norwegian University of Science and Technology, 2009.

Geir Evensen. Sequential data Assimilation with a nonlinear quasi-geostrophic model using Monte Carlo methods to forecast error statistics. *Journal of Geophysical Research*, 99(C5):143–162, May 1994.

Geir Evensen. *Data Assimilation; The Ensemble Kalman Filter.* Springer, 2007.

Abul Fahimuddin, Sigurd Ivar Aanonsen, and Jan-Arild Skjervheim. 4D Seismic History Matching of a Real Field Case with EnKF: Use of Local Analysis of

Modul Updating. *The Society of Petroleum Engineers (SPE134894)*, September 2010.

Guohua Gao, Mohammad Zafari, and Albert C. Reynolds. Quantifying Uncertainty for the PUNQ-S3 Problem in a Bayesian Setting With RML and EnKF. *The Society of Petroleum Engineers (SPE93324)*, pages 506–516, December 2006.

Josiah Willard Gibbs. *Elementary Principles in Statistical Mechanics*. Charles Scribner's Sons, New York, 1902.

G. A. Gottwald and A. J. Majda. A mechanism for catastrophic filter divergence in data assimilation for sparse observation networks. *Nonlinear Processes in Geophysics*, (20):705–712, September 2013.

Yasin Hajizadeh, Mike Christie, and Vasily Demyanov. Comparative Study of Novel Population-Based Optimization Algorithms for History Matching and Uncertainty Quantification: PUNQ-S3 Revisited. *The Society of Petroleum Engineering (SPE136861)*, 2010.

Mei Han, Gaoming Li, and Jingyi Chen. Assimilating Microseismic and Welltest Data Using EnKF for Accurate Reservoir Characterisation. *International Petroleum Technology Conference, Beijing*, March 2013.

NTNU IO Center, IPT. Norne Benchmark Case, 2010. URL `http://www.ipt.ntnu.no/~norne/wiki/doku.php`. Accessed: 10.11.2013.

S. Kahrobaei, G.M. van Essen, J.F.M. Van Doren, P.M.J. Van den Hof, and J.D. Jansen. Adjoint-Based History Matching of Structural Models Using Production and Time-Lapse Seismic Data. *The Society of Petroleoum Engineers (SPE163586)*, 2013.

R.E. Kalman. A New Approach to Linear Filtering and Prediction Problems. *Journal of Basic Engineering*, page 35–45, 1960.

W.D. Kruger. Determining Areal Permeability Distribution by Calculations. *The Society of Petroleoum Engineers (SPE1580-G)*, July 1961.

Gaoming Li and A. C. Reynolds. An Iterative Ensemble Kalman Filter for Data Assimilation. *The Society of Petroleum Engineers (SPE109808)*, November 2007.

R. Li, A.C. Reynolds, and D.S. Oliver. Sensitivity Coefficients for Three-Phase Flow History Matching. *The Journal of Canadian Petroleum Technology*, 42(4): 70–77, 2003.

A. Lorenc. Analysis methods for numerical weather prediction. *Quarterly Journal of the Royal Meteorological Society*, 112(474):1177–1194, October 1986.

L. Mohamed, M. Christie, and V. Demyanov. Comparison of Stochastic Sampling Algorithms for Uncertainty Quantification. *The Society of Petroleoum Engineers (SPE119139)*, 2009.

Eirik Morell. History matching of the Norne field. Master's thesis, Norwegian University of Science and Technology, September 2010.

L.-J. Natvik and G. Evensen. Assimilation of ocean colour data into a biochemical model of the North Atlantic. Part 1: Data assimilation experiments. *Journal of Marine Systems*, (40-41):127–153, 2003.

Jorge Nocedal and Stephen J. Wright. *Numerical Optimization*. Springer, 2nd edition, 2006.

Ahmed Ouenes and Naji Saad. A New, Fast Parallel Simulated Annealing Algorithm for Reservoir Characterization. *The Society of Petroleum Engineers (SPE26419)*, October 1993.

C.E. Romero, J.N. Carter, R.W. Zimmerman, and A.C. Gringarten. Improved Reservoir Characterization through Evolutionary Computation. *The Society of Petroleum Engineers (SPE62942)*, January 2000.

R. Rwechungura, E. Suwartadi, M. Dadashpour, J. Kleppe, and B. Foss. The Norne Field Case - A Unique Comparative Case Study. *The Society of Petroleum Engineers (SPE127538)*, 2010.

Richard Rwechungura. *Fast Reservoir Characterization and Development of a Field Case Study with Real Production and 4D Seismic Data*. PhD thesis, Norwegian University of Science and Technology, 2012.

Schlumberger. *ECLIPSE Reference Manual*, 2009.2 edition, 2009.

R.W. Schulze-Riegert, J.K. Axmann, O. Haase, D.T. Rian, and Y.-L. You. Evolutionary Algorithms Applied to History Matching of Complex Reservoirs. *SPE, Reservoir Evaluation and Engineering*, 2002.

Mrinal K. Sen, Akhil Datta-Gupta, P.L. Stoffa, L.W. Lake, and G.A. Pope. Stochastic Reservoir Modeling Using Simulated Annealing and Genetic Algorithms. *The Society of Petroleum Engineers (SPE24754)*, March 1995.

Statoil. PL128-Norne Field Reservoir Management Plan. Technical report, 2001.

Statoil. Annual reservoir development plans Norne Field, 2006.

Statoil and Norwegian Computing Center NCC. The Ensemble based Reservoir Tool, 2013. URL `http://ert.nr.no/wiki/index.php/Main_Page`. Accessed: 10.11.2013.

Ivar Steffensen and Per Ivar Karstad. Norne Field Development: Fast Track From Discovery to Production. *The Society of Petroleum Engineers, Statoil*, April 1996.

Streamsim Technologies, Inc. Classical Approaches to History Matching, 2011. URL `http://streamsim.com/technology/history-matching-using-evolutionary-algorithms`. Accessed: 26.02.2014.

Jon Sætrom and Henning Omre. Uncertainty Quantification in the Ensemble Kalman Filter. *Scandinavian Journal of Statistics*, 40(4):868–885, December 2013.

Albert Tarantola. *Inverse Problem Theory and Methods for Model Parameter Estimation*. Society for Industrial and Applied Mathematics, 2005.

Z. Tavassoli, Jonathan N. Carter, and Peter R. King. Errors in History Matching. *The Society of Petroleum Engineers (SPE86883)*, September 2004.

Sebastian Thrun. Particle Filters in Robotics. In *Proceedings of the 17th Annual Conference on Uncertainty in AI (UAI)*, 2002.

Erlend H. Vefring, Gerhard Nygaard, Rolf Johan Lorentzen, Geir Nævdal, and
Kjell Kåre Fjelde. Reservoir Characterization during UBD: Methodology and
Active Tests. *The Society of Petroleum Engineers (SPE81634)*, March 2003.

Signe Berg Verlo and Mari Hetland. Development of a field case with real produc-
tion and 4D data from the Norne Field as a benchmark case for future reservoir
simulation model testing. Master's thesis, Norwegian University of Science and
Technology, June 2008.